2022

Mining Marine Environments for Novel Antimicrobial Biologics

Koch, Matthew James

UNIVERSITY OF
PLYMOUTH

Mining marine environments for novel antimicrobial biologics

by

MATTHEW JAMES KOCH

A thesis submitted to the University of Plymouth

in partial fulfilment for the degree of

DOCTOR OF PHILOSOPHY

School of Biomedical Sciences

October 2021

Acknowledgements

Biggest thank you to Marigold, I love you. Thanks to Mat, Kerry and Phil for all the guidance and support. Thanks to all the people in the lab and at DRF who made the experience bearable! Special mention to Poppy for being my best friend through the whole thing. Lastly, thanks to SfAM for the funding.

Author's declaration

At no time during the registration for the degree of *Doctor of Philosophy* has the author been registered for any other University award without prior agreement of the Doctoral College Quality Sub-Committee.

This thesis has been proofread by a third party; no factual changes or additions or amendments to the argument were made as a result of this process. A copy of the thesis prior to proofreading will be made available to the examiners upon request.

Work submitted for this research degree at the University of Plymouth has not formed part of any other degree either at the University of Plymouth or at another establishment.

This study was financed with the aid of a studentship form the *Society for Applied Microbiology* and carried out in collaboration with *University of Plymouth*.

The following external institutions were visited for research and consultation purposes:

University of Bristol

Publications (or public presentation of creative research outputs):

Koch, MJ., Hesketh-Best, PJ., Smerdon, G., Warburton, PJ., Howell, K., Upton, M. (2021). Impact of growth media and pressure on the diversity and antimicrobial activity

of isolates from two species of Hexactinellid Sponge (Koch et al., 2021. *Microbiology* (Reading). 2021; 167(12): 001123).

Presentations at conferences:

Poster Presentations:

SfAM ECS Symposium – 22-26 March 2021 (Online, London, UK)

IMAP – 38-30 August 2019 (Utrecht, Netherlands)

ABX network Inaugural Meeting – 11-12 July 2019 (St. Austell, UK)

Bristol AMR Symposium – 13-14 November 2019 (Bristol, UK)

3rd International Symposium on Sponge Microbiology – 25-29 October 2018 (Shanghai, China)

SfAM ECS Symposium – 28 March 2018 (London, UK) (**Poster Prize Winner**)

Plymouth University Annual Research Event 22-26 January 2018 (Plymouth, UK)

Postgraduate Society Research Showcase – 4 December 2017 (Plymouth, UK) (**Poster Prize Winner**)

Oral Presentations:

Antimicrobial potential of the deep-sea sponge microbiome, presented at:

Plymouth University Annual Research Event – 13 March 2019 (Plymouth, UK)

3rd International Symposium on Sponge Microbiology – 25-29 October 2018 (Shanghai, China)

Word count of main body of thesis: 28,616

Signed  .....

Date 29/11/2021

Title: Mining Marine Environments for Novel Antimicrobial Biologics

Author: Matthew James Koch

Abstract

Deaths attributable to antimicrobial resistance (AMR) are predicted to rise from 700,000 per year now to 10 million by 2050. There is an urgent need for new antibiotics to meet the threat posed by AMR; the WHO recently reported that there are not enough antibiotics in development to meet this need. The sponge microbiota has emerged as one of the most prolific sources of novel antimicrobial candidates from marine environments in recent decades. The majority of work on sponge microbiology, however, has been carried out on shallow-water sponges of the Demosponge Class. This work explores the cultivable diversity and antimicrobial potential of bacteria from two species of Hexactinellid sponge (*Pheronema carpenteri* and *Hertwigia* sp.). Bacteria were cultured using a variety of methods including the novel use of pressurised environments, revealing bacteria belonging to the Proteobacteria, Actinobacteria and Firmicutes. Bacteria were screened for antimicrobial activity, revealing a higher proportion of active isolates from *Pheronema carpenteri*, leading to the purification of an antimicrobial with protease inhibitory activity, and further genomic characterisation of a potentially novel species of *Streptomyces* displaying inhibitory activity against Gram-positive and Gram-negative organisms. Culture-independent methods were used in order to provide the first characterisation of the microbiota of the deep-sea Hexactinellid sponge *Pheronema carpenteri*, as well as supporting a comparison of its microbiota to that of the surrounding sediment and seawater. Taxonomic classification of the microbiota of these samples revealed the following: that *P. carpenteri* has a microbiota that is generally congruent with that of the global sponge and Hexactinellid microbiota; it contains a smaller core microbiota; has a

smaller sample-specific microbiota; and is comprised of distinct phyla when compared to sediment samples. Differences were also observed in *P. carpenteri* replicates that were collected from two separate sampling sites. The presence of cultivated isolates within the *P. carpenteri* metagenome was also demonstrated, indicating that culture-dependent studies are to some extent successful in obtaining sponge-associated bacteria for the purposes of natural product discovery. Overall, this work displays that the Hexactinellid sponges investigated are a promising source for the discovery of novel bacterial species and antimicrobial candidates.

Table of Contents

List of Tables and Figures

carpenteri, respectively (dots represent individual growth media). Bars represent Standard Deviation. All media were inoculated in triplicate. Number in parentheses in individual graph title represents sponge replicate ID. Abbreviations: OM, Oatmeal Agar; SYP-SW, Starch-Yeast-Peptone Seawater Agar; ABC, 'ABC' Agar; LC, LB + Carnitine Hydrochloride; RC, R2a + Carnitine Hydrochloride; LB, LB Agar; MA, Marine Agar; MC, Marine Agar + Carnitine.

Figure 2.4 –Venn diagram of shared diversity between *Hertwigia* sp. replicates (in green) and *Pheronema carpenteri* replicates (in yellow). The number on the outer edges of the ellipses denote the number of morphotypes for each individual replicate. The percentage number in the corresponding colour denotes the shared morphotypes between replicates of the same type. The central figure denotes the number of shared morphotypes between all *Hertwigia* sp. and *Pheronema carpenteri* replicates as a whole.

Figure 2.5 – A) Growth statistics for bacteria grown in different media using the dilution to extinction method. **B)** Table displays statistics for number of bacteria recovered from each treatment. Single, Double and Triple refers to the number of wells from which 1, 2 or 3 different morphotypes, respectively, were recovered when liquid from wells was plated onto solid media.

Figure 2.6 – Abundance and diversity measurements for bacteria recovered from *P. carpenteri* and cultured under altered atmospheric conditions. **A)** abundance counts. **B)** Diversity counts. Bars: Standard Deviation across 3 technical replicates.

Figure 2.7 – Neighbour-joining tree of 16S rDNA sequences obtained from bacterial isolates cultured from *P. carpenteri*. Taxonomic ID's represent the top BLASTn hit for each sequence. Colours represent treatment at which isolate was recovered. Green: 21% O_2/1.01 bar, Blue: 21% O_2/5 bar, Red: 4% O_2/5 bar.

Figure 2.8 – A) Phylum- and **B)** Genus-level distribution of all *P. carpenteri* isolates sequenced. **C)** Phylum- and **D)** Genus-level distribution of isolates recovered, split by sample treatment.

Figure 3.1 – Number of bacterial sequences deposited to NCBI for cultivated Actinobacteria from sponge samples. Search criteria: (((sponge* or porifera*) and (cultured* or cultivated*) NOT (uncultured* or uncultivated*))) AND "actinobacteria". **Inset:** Number of Sponge Actinobacteria-derived antibacterial compounds reported by Indraningrat, Schmidt & Sipkema (1).

Figure 3.2 – Factors regulating the formation of aerial hyphae development in *Streptomyces* sp. (5). Text in rectangular boxes represent genes involved in the signalling pathways indicated in the regulation of the formation of aerial hyphae, and signalling factors involved in the same process

Figure 3.3 – Graphical representation of the apparatus used to create wells in agar diffusion plates

Figure 3.4 – Diagram (produced by the author) to represent the set-up of microtitre-plate protease inhibition testing. B refers to Buffer. T refers to Trypsin.

Figure 3.5 – Picture (left): Isolate A11 grown on Oatmeal Agar. Table: Top 3 BLASTn hits obtained using the draft genome sequence. 'QC' refers to Query Cover of top BLASTn hit. 'Identity' refers to identical nucleotide site match with highest BLASTn hit. 'Max Score' refers to highest alignment score of a particular genome segment. Total score refers to the sum of the alignment scores of all segments. E-Score refers to number of hits expected at that level of identity (score) by chance.

Figure 3.6 – Mauve alignment of A11 with *Streptomyces sp.* 3211. Upper alignment displays contigs for A11. Lower alignment displays contigs for *Streptomyces sp.* 3211. Lines show position of each region in each genome.

Figure 3.7 – antiSMASH output displaying hits present in the A11 hybrid assembly. Colours in the left-hand column are generated by antiSMASH and are related to the 'type' of BGC, as listed in the second column.

Figure 3.8 – Growth curve of isolate A11 in LB broth. Detection of antimicrobial activity against *Escherichia coli* NCTC 10418 in liquid culture indicated by coloured squares. Red: no activity detected. Green: activity detected.

Figure 3.9 – Subsequent rounds of injection of the strain A11 active fractions into the Akta pure system for size exclusion chromatography. Highlighted blue section represents the antimicrobial containing fraction as confirmed by well diffusion assays, measured at a UV wavelength of 220 nm.

Figure 3.10 – LC/MS absorbance spectra for **C-A11**. Numbers above peaks represent *m/z* values.

Figure 3.11 – A) Graphs displaying OD_{600} of cultures treated with C-A11. MIC and MBC indicated on graph**. B)** Table of C-A11 MIC/MBC figures. Bars represent Standard Error. Significance determined by t-test. GC refers to Growth Control (no inhibition). NC refers to Negative Control (no cells).

Figure 3.12 – *In vivo* toxicity assay for **C-A11**.

Figure 3.13 – Genomic regions in the deimino-antipain cluster (*S. albulus* NRRL B-3066) with the clusters from the 2 most similar genomes to A11. In each panel, the coloured sections represent the deimino-antipain cluster regions/proteins identified by antiSMASH that are also present in those clusters. Colouring of regions is arbitrary and does not represent function/identity. The identity of regions in the deimino-antipain cluster (top panel) are scaled separately and are taken from the original research article detailing functional assignment (6).

Figure 3.14 – A) Skim milk agar assay. **B)** Measurement of trypsination of BAPNA over time. **C)** Endpoints for BAPNA assay. Values indicate the percentage inhibition relative to control (Trypsin + BAPNA). **D)** Endpoints for BAPNA assay over further concentrations Bars: Standard Error. Significance measured by t-test. '*****' represents p-value of <0.05, '******' represents p-value of <0.01, '*******' represents p-value of <0.001.

Figure 4.1 – Sampling sites of sponge, seawater and sediment samples used in this study.

Figure 4.2 – Comparison of taxonomic classification for samples sequenced across two separate MinION runs. Sample ID denotes library, run and barcode information i.e. L3B1 denotes library 3, barcode 1. L32B1 denotes library 3, run 2, barcode 1.

Figure 4.3 – Comparison of taxonomic classification for samples sequenced after one or two amplification steps. Numbers above bars denote number of PCR amplification steps used in library preparation. Sample ID denotes library, run and barcode information i.e. L2B4 denotes library 3, barcode 4. L32B4 denotes library 3, run 2, barcode 4.

Figure 4.4 – Range in relative abundance of each phylum, in sponge samples (009 and 010) that were sequenced after one or two amplification steps. Bars represent mean abundance. Lines represent range (minimum to maximum).

Figure 4.5 – Overview of OTUs that had a change in relative abundance of ≥1% after a second amplification step. **A)** OTUs that were changed by ≥1% after a second amplification in Sponge_009, compared to the amount by which they were altered in Sponge_010. **B)** OTUs that were changed by ≥1% after a second amplification in Sponge_010, compared to the amount by which they were altered in Sponge_009.

Figure 4.6 – Graphical representation of the combination of reads from samples determined to be sufficiently similar.

Figure 4.7 – Taxonomic composition of all sponge and sediment samples at phylum level. Phyla for which the relative abundance in at least one sample was ≥1% are displayed in the legend in bold font.

Figure 4.8 – Relative abundance of all phyla in sponge and sediment samples. Left panel: Phylum level abundance in each sample. Right panel: Average phylum abundance in sponge and sediment microbiota as a whole. Phyla which have a higher relative abundance appear towards the green end of the spectrum.

Figure 4.9 – A) Principal Co-Ordinate Analysis Plot based on the relative abundance of all OTUs in each sponge and sediment sample community. Numbers on graph refer to the ID for each sample. Colour depicts sample type (sponge; sediment). Shape depicts sample site (T07; T52). **B)** Alpha Diversity (Chao1; Shannon; Inverse-Simpson) indices based on true (non-relative) abundance values of each sample. All plots were constructed using in R using the phyloseq package.

Figure 4.10 – The *Pheronema carpenteri* core microbiota. **A)** Number of phyla in the core microbiota that were represented by OTUs at various relative abundance thresholds. **B)** Number of OTUs in the core microbiota that had relative abundances above various thresholds. Abundance thresholds represent average abundance for each OTU across all samples.

Figure 4.11 – The *Pheronema carpenteri* (sponge)-specific microbiota. No phyla were observed to be sponge-specific. **A)** Number of phyla that were represented by sponge-specific OTUs at various relative abundance thresholds. **B)** Number of sponge-specific OTUs that had relative abundances above various thresholds. Abundance thresholds represent average abundance for each OTU across all samples.

Figure 4.12 – Sediment core microbiota. **A)** Number of phyla in the core microbiota that were represented by OTUs at various relative abundance thresholds. **B)** Number

of OTUs in the core microbiota that had relative abundances above various thresholds. Abundance thresholds represent average abundance for each OTU across all samples.

Figure 4.13 – The Sediment-specific microbiota. **A)** Number of phyla that were represented by sediment-specific OTUs at various relative abundance thresholds. **B)** Number of sediment-specific OTUs that had relative abundances above various thresholds. Abundance thresholds represent average abundance for each OTU across all samples.

Figure 4.14 – Histogram to display the relative abundance distribution of OTUs in samples subsets (Total, Core, Specific). Box limits represent upper and lower quartiles. Middle line represents mean. Lines represent minimum and maximum. Core microbiota is given at a 100% replicate threshold.

Figure 4.15 – Relative abundance of isolates cultured from *Pheronema carpenteri* within the sediment and sponge metagenome determined microbiota.

Table 2.1 – Samples collection metadata for sponges used in this study.

Table 2.2 – Isolates obtained from Hexactinellid sponges that displayed antimicrobial activity in a simultaneous antagonism assay.

Table 3.1 – Genome statistics for reads obtained from each sequencing platform. N50 refers to average read length as opposed to median.

Table 3.2 – Cross-referencing antiSMASH analysis for stain A11 vs. literature-derived information for similarly sized compounds.

Table 3.3 – BGCs present in the genomes of both A11 and *S. albulus* NRRL B-3066, detected by AntiSMASH.

Table 3.4 – Annotated regions the Biosynthetic Gene Cluster (BGC) responsible for deimino-antipain production in the A11 genome. QC: Query Cover (%) score from BLASTp result. Identity: identical base matches from BLASTp result.

Table 4.2 – Sample information for sponge, sediment and seawater samples collected in this study.

Table 4.3 – Sample and library information for MinION runs performed in this study.

Table 4.4 – Sequence read information for all samples sequenced in this study.

Table 4.5 – Sample information for classified reads obtained from samples over two separate MinION runs. Sample ID denotes library, run and barcode information i.e. L3B1 denotes library 3, barcode 1. L32B1 denotes library 3, run 2, barcode 1.

Chapter 1

Introduction - Culturing deep-sea sponge-associated bacteria and exploring their antimicrobial potential

1.1 Antimicrobial Resistance & The Role of Sponges

The worldwide threat to public health posed by drug-resistant bacteria has become increasingly apparent over the last decade, with the seminal report from Lord O'Neill predicting that deaths attributable to multi-drug resistant (MDR) bacteria will rise from 700,000 per year currently to 10 million by 2050 (7). An analysis of this much quoted statistic, performed by de Kraker, Stewardson and Harbarth (8), suggested it to perhaps be an overestimation, yet they did not provide a more up do date estimation based on their objections to the statistical modelling used in the original AMR report. Therefore, the initial figure of '10 million deaths a year' currently still stands as a working axiom, moving forward in the design and instigation of antimicrobial stewardship and discovery programs for the future.

Classified as one of the biggest threats to global human health by the World Health Organisation (9), antibiotic resistance poses one of the greatest challenges to clinical practice as well as drug discovery. Problems posed by resistant organisms include the emergence and spread of mechanisms of resistance, with a particular risk attributed to β-Lactam (especially Carbapenem) resistance (**Figure 1.1**).

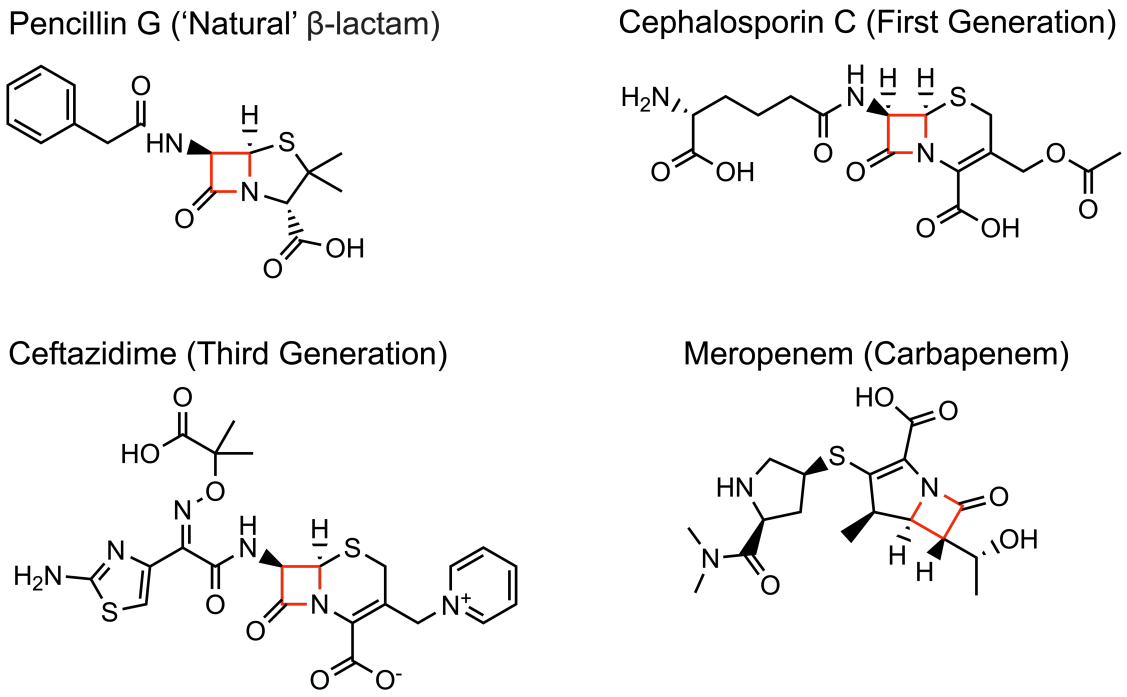

Figure 1.1 – Chemical structure of several iterations of β-lactam antibiotics. β-lactam rings are highlighted in red (produced by M. Koch using ChemDraw 21.0.0).

The discovery and spread of the NDM-1 Carbapenemase, first characterised in 2009 (10) exists as a major example of the growing threat posed by MDR organisms over the last decade. In late 2015, the discovery of the resistance gene *mcr-1* (11) that confers plasmid-mediated resistance to the 'last-resort' antibiotic colistin heralded major concerns over the imminent danger of 'pan-resistance' in clinical isolates (12). Shortly after, the widespread presence, and human infection with pan-resistant bacteria was highlighted by the death of a woman in the USA as a result of a *Klebsiella pneumoniae* infection, resistant to all available antibiotics (13). The spread of antimicrobial resistance, as outlined above highlights not only need to discover new antimicrobials, but especially those of novel class.

Additionally, issues in the supply chain of new antibiotics has become a major contributor to the inability to treat microbial infections (14,15). However, platforms for

the discovery of novel compounds have begun to re-emerge in recent years with the reduction in cost and rise in accessibility of next-generation sequencing techniques (16), and the ability to culture certain organisms previously considered ‘uncultivable’, often referred to as ‘microbial dark matter’ (17). Prior to the recent discovery of Teixobactin via the employ of highly novel culture techniques (18), no novel classes of antibiotics had been discovered in several decades (14). The revival of natural product (NP) screening in this manner, combined with deep-sequencing methodologies has not only reinvigorated the search for new antimicrobial treatments, but also facilitated interest into the microbiomes of hitherto unexplored natural environments, in an attempt to capitalise on the potentially vast and novel array of bioactive compounds harboured within them (19). A growing body of literature has detailed the emergence of sponges in recent years as a major source of new antimicrobials, revealing them as the most prolific source of novel bioactive compounds over the last decade (1,20,21).

Due in part to the re-discovery of similar compounds across different sponge species, it is now apparent that many compounds once thought to be of sponge origin are in fact produced by their symbiotic bacteria (22). This realisation provided an interesting avenue of discovery for novel antibacterial compounds, as well as a need for the classification of the major producers of antimicrobial compounds from sponges and investigation of their distribution across both shallow and deep-waters. A systematic review compiling sponge-derived antibacterial compound discoveries (1) reveals that species of *Actinobacteria* have thus far comprised the most prolific producers (48.8%), with *Streptomyces* responsible for 30% of compounds and *Kocuria* responsible for 20% (Fig. 1). The Proteobacteria comprise the second highest proportion of producers

of sponge-derived compounds (36.6%), specifically the *Alphaproteobacteria* and in particular the *Pseudovibrio* (9%) (1).

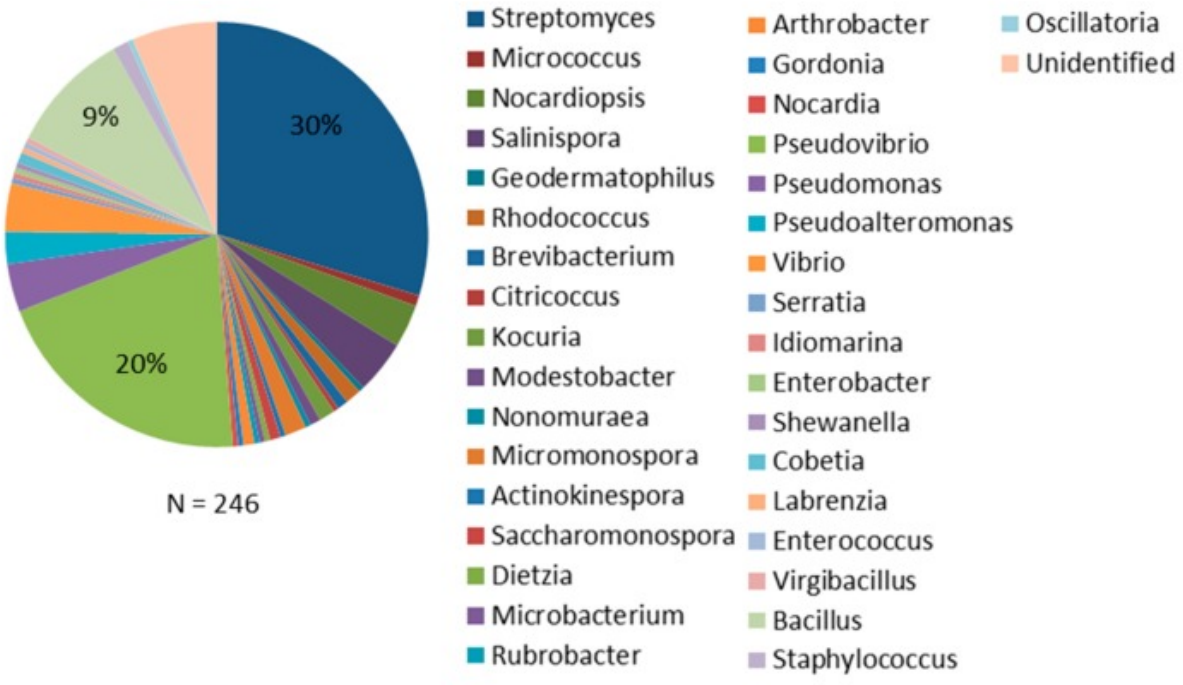

Figure 1.2 – Antimicrobial agents derived from sponge bacteria reported (reproduced from (1). 30%: *Streptomyces*; 20%: *Pseudovibrio*; 9%: *Bacillus*.

The discovery of novel antimicrobials for sponge-derived Actinobacteria [reviewed by Abdelmohsen, Bayer and Hentschel (23)] has produced an array of compounds predominantly active against Gram-positive bacteria, however several instances of anti-Gram-negative activity have also been reported. The discovery of Kocurin from *Kocuria* and *Micrococcus* spp. (24) represents one of the most potent antimicrobial compound derived from sponge Actinobacteria to date. Kocurin was shown to exhibit notable activity against methicillin resistant *Staphylococcus aureus* (MRSA; MIC 0.25 µg/mL as well as activity against several Gram-negative organisms. At the time of discovery, the biosynthetic gene clusters identified in *Kocuria* isolates were shown to not be responsible for the production of Kocurin. However, subsequent genome mining

and bioinformatic analysis has allowed the identification of the responsible biosynthetic pathways (25). Kocurin is also a thiopeptide, and is categorised as a thiazolyl peptide (26). Thiopeptides have emerged in recent years as promising candidates for novel drug discovery, particularly where marine sponges are concerned. The thiopeptide antibiotics YM-266183 and YM-266184, produced by *Bacillus cereus* QN03323 isolates (27) both exhibited notable activity against *S. aureus* and *Enterococcus faecium* with an observed MIC of 0.025 μg/mL. YM-266184 also produced the same MIC when tested against *E. faecalis*, however both were inactive when tested against Gram-negative organisms.

A further sponge Actinobacteria-derived compound of note is Mayamycin, produced by a *Streptomyces* sp. strain (28). Mayamycin is a polyketide that exhibits both anti-Gram-positive and -negative activity, outperforming the standard treatment used as a control when tested *in vitro* in the primary study, perhaps most notably against *Pseudomonas aeruginosa*.

As a result of isolating Actinobacteria from sponge samples, several obligate marine species have been identified. Abdelmohsen, Bayer and Hentschel (23) remark upon the fact that although a degree of correlation between some sponge species and the occurrence of certain Actinobacteria species has been observed, a large scale, directed study has not yet been undertaken (29–38). Several studies have characterised antimicrobial agents from Actinobacteria associated with individual sponges, however, a large-scale review has not yet been carried out.

1.2 Sponge Microbiota Overview

Sponges (Porifera) are sessile metazoan organisms thought to have emerged around 600 million years ago (39,40). Representing the most widely sampled marine phyla in the hunt for novel bioactives over the last 45 years, the Porifera comprise the most prolific source of such agents from the marine environment in recent years (21,41). As filter-feeding organisms, certain species have been predicted to filter up to 50,000L of seawater per litre of sponge per day (42), bringing them into contact with large quantities of marine debris, nutrients and planktonic bacteria. Both culture-dependent and culture-independent studies have been used to reveal the inter and intraspecific differences between the microbiota of different sponge species.

Broad-scale metagenomic studies have revealed that the sponge microbiota is generally conserved, with a shared, convergent evolution (43). Studies detailing the relative bacterial species percentage of marine sponges have revealed a general pattern of microbial inhabitants across 52 different bacterial phyla (43,44). Major bacterial sponge-symbionts include *Proteobacteria* (particularly *Alpha*- and *Gammaproteobacteria*), along with Actinobacteria, Chloroflexi, Cyanobacteria and Acidobacteria. Two candidate phyla, Poribacteria (45) and Entotheonella (46) are proposed to be sponge-specific bacterial phyla. The Poribacteria have been shown to contain a diverse range of phylotypes, and to be widely distributed amongst sponge species (47).

Despite trends observed in the global sponge microbiota, host identity in conjunction with environmental factors such as geographic location and temperature have been suggested to have the greatest impact on the composition of the sponge microbiota (48–51). This is due not only to the conservation of certain microbial constituents

across species, but also to the stability of the microbiota over time compared to the high turnover of planktonic bacteria in the surrounding environment (48,52). Whilst a lack of studies incorporating a high number of replicates for individual sponges limits definite conclusions, it does provide a basis for the culture-dependent investigation of each sponge microbiota. The impact of host and environmental factors provides a rationale for performing culture-dependent studies in a species-dependent manner. This is particularly relevant for studies seeking to characterise the biochemical and physiological profiles of sponge-associated bacteria.

1.3 Culture-Dependent vs. Culture-Independent Studies

Culture-dependent approaches have been used to investigate a variety of functions of sponge-associated microbes. Previous studies have characterised bacteria involved in quorum sensing (53), surfactant production (54), sponge disease (55), as well as the effect of long-term mariculture on the sponge microbiota (56). Numerous studies have used a culture-dependent approach to complement culture-independent approaches, in an attempt to reveal what portion of the sponge microbiota as a whole is capable of being cultivated under laboratory conditions (57–62). As a result, culture-dependent studies have included the discovery and characterisation of several novel species (36,46,59,63–66) in addition to species that have been identified via metagenome-assembled genomes (MAGs) (67). Numerous studies focusing on antimicrobial screening and the characterisation of drug candidates (3,30,46,68,69).

Many culture-dependent studies have focused on *Actinobacteria* (23,29–36,38,54,70), which are currently the most prolific source of antibacterial compounds isolated from sponge-bacteria (1).

As with culture-independent studies, trends are also apparent in the types of bacteria that have been cultured from different sponge species. The largest portion of 16S rRNA gene sequences submitted to NCBI that pertain to cultured sponge isolates (Fig.1) belong to the *Proteobacteria* (307/685; 45.01%) - which is congruent with the most dominant members of the sponge microbiota (43). A large portion of 16S rDNA sequences submitted to the NCBI is comprised of the Actinobacteria (28.59%), which is likely a reflection of the focus of culture-dependent studies on identifying novel antimicrobial compounds. Other common members include the Firmicutes (21.56%) and the Bacteroidetes (4.84%). At the genus level however, the most frequently submitted sequences pertain to *Bacillus* isolates (16.9%), followed by the *Streptomyces* (11%) and *Pseudovibrio* (8.2%). Again, this appears to be a reflection of the bacterial genera responsible for the production of antibacterial agents in the literature (1,21,41). In reviewing the sources of antibacterial agents derived from 'sponge-associated bacteria', it was demonstrated that 9% of agents characterised have been derived from members of the *Bacillus* genus, representing the third most prolific genus after *Streptomyces* and *Pseudovibrio* (1). The repeated recovery of isolates of the *Bacillus* genus from marine and freshwater sponges presents an interesting point of discussion that will be covered in more detail later.

Bacteria isolated from sponges are often referred to as 'sponge-associated microbes', a term coined by Taylor et al. (71). Often apparent in cultivation studies is the question as to whether such isolates are indeed associated with the parent sponge and whether they can be regarded as true symbionts. In accordance with molecular studies detailing the overall composition of the sponge microbiota, the majority of the cultivable fraction is often comprised of members of the *Proteobacteria* (58,64,72–74). Reports of cultivated isolates have also however included the presence of 'terrestrial' species,

members of the *Bacillus* genus, or those that have been previously associated with non-marine environments (75–77).

It has been suggested that the recovery of such isolates from sponge samples can be attributed to contamination associated with the sampling process (64) and such isolates are often overlooked. Phelan et al. (77) however, have explored the presence of spore-forming *Bacillus* within the sponge microbiota in light of their 'productive' nature and variable presence within sponge microbiotas in general (78). The failure of culture-independent approaches to detect *Bacillus* spp. in the *Haliclona simulans* microbiota led Phelan et al. (77) to suggest that such species may be present in its microenvironment predominantly in the form of spores. This assumption brings with it questions about the role of *Bacillus* spp. within the sponge microbiota and whether they exist as adapted, metabolically active members or simply terrestrial contaminants that have become localised within sponge tissue. The continued 're-discovery' of such isolates in marine environments, and in particular their variable presence within sponge microbiota provides at least a suggestion however that they may indeed be 'sponge-', or 'marine-associated' bacteria. It should be noted that the biochemical and molecular differences between *Bacillus* isolates recovered from marine samples has been previously explored (79). Differences in biochemical profiles as well as phylogenetic distance to reference strains was shown to vary with regard to depth and geographic location, providing a suggestion that the divergence of *Bacillus* isolates within the marine/sponge environment is a phenomenon that merits further investigation.

More recently, Liu et al. (80) have demonstrated the divergence of marine ecotypes of members of the *Bacillus* genus once thought to be uniquely terrestrial. Strains of *B. pumilus*, *B. lichenoformis*, *B. safensis* and *B. altitudinis* that were inseparable on the

basis of 16S rRNA sequences were differentiated on the basis of 7 housekeeping genes. Isolates obtained from marine environments were found to cluster into 3 distinct phylogenetic groups, largely separate from terrestrial isolates of the same species. Such evidence points towards a genuine divergence of species of *Bacillus* once thought to be uniquely terrestrial. Further investigation into the metabolic adaptation to the marine environment and to the sponge micro-environment in particular will be of benefit in shedding some light on the lifestyles of such organisms.

Several reports of bacteria isolated from sponge samples have documented the presence of certain isolates not being detected when the same sponge samples are subjected to culture-independent, molecular characterisation (60,62,74,81). This may either be attributed to variable sequencing depth, or the result of contamination during sampling, as discussed above (64). The possibility that cultured isolates represent members of the 'rare biosphere', as well as the impact of PCR bias have also been explored (60,62,74,81–83). Noticeable in culture-dependent reports is also a variation in the overall percentage of species (between 0-14%) present in the microbiota (as confirmed by molecular characterisation) that were capable of being cultured under the conditions applied (57,60,81). It is interesting to consider how the composition of the sponge microbiota may have a part to play in determining the types of bacteria that can be isolated in culture-dependent studies. For instance, there have been several instances where the most abundant organisms in the microbiota have not been cultivable under laboratory conditions (58,60,69). In addition, rare taxa (those that have a relative abundance of ≤0.01%) were found to comprise 90% of the cultivable microbiota of several species of the deep sea *Hexadella* sponges (83). The wealth of antimicrobial compounds elicited from sponge-associated microbes is perhaps

promising given that they have been obtained from species comprising only a small minority of the microbiota in general (1).

1.4 Bacteria from Hexactinellid (Glass) Sponges

Sponges are typically classified using the Systema Porifera devised by Hooper and Van Soest (84). Traditional classification is based on categorising sponges according to the shape and size of their spicules, while molecular methods are becoming more widely employed (85). The vast majority of studies to date have focused not only on sponges from shallow waters, but also on those of the Demosponge population. Hexactinellid, or 'Glass' sponges represent an extremely under-explored class of the Porifera with regard to both their microbiota and bioactive potential (3,4,86–88). Occurring almost exclusively below 200m, Hexactinellid sponges are characterised by having a basket-like skeleton comprised of siliceous spicules (89), which in some cases comprises up to 90% of their mass (90). The outer dermal membrane of the sponge tissue is connected to an inner chamber via trabecular strands (**Figure 1.2**) (2).

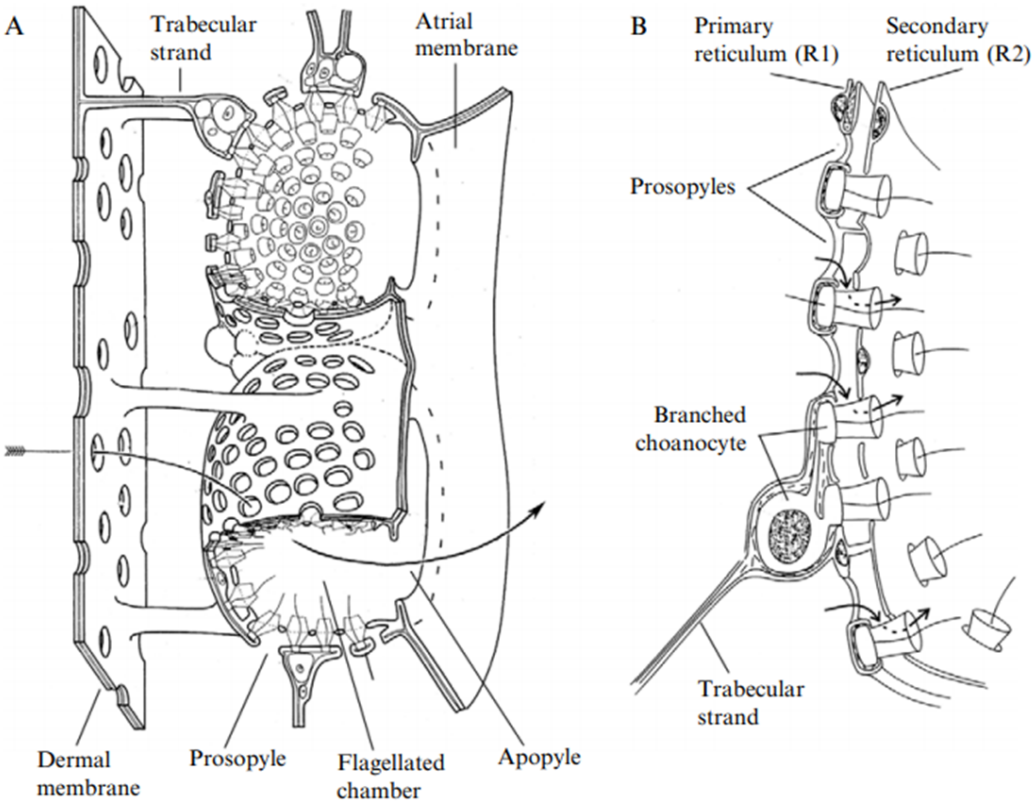

Figure 1.3 – A) Cross-section of Hexactinellid soft tissue organisation. **B)** Cross-section of the flagellated chamber wall. Arrows display flow of water (2).

The composition of the Hexactinellid microbiota has been explored in depth by relatively few studies, with only a small number of Hexactinellid species having been characterised (86–88). The Hexactinellid microbiota however does appear to be distinct from that of Demosponges. In terms of composition, the microbiota of 7 species of Hexactinellid sponge have been shown to share more bacterial operational taxonomic units (OTUs) with each other and with seawater, than with Demosponges that were collected from a similar geographic location (87). The Hexactinellid microbiota also showed lower diversity and evenness scores than Demosponges. The uncultured Hexactinellid microbiota were dominated by Proteobacteria (specifically Gammaproteobacteria), which is in general similar to Demosponges (43). Whilst there

were no Hexactinellid-specific phyla, Patescibacteria and Nitrospinae were more likely to be found in Hexactinellids. The microbiota of the glass sponge *Vazella pourtalesii* has been shown to possess a higher intra-species dissimilarity than sediment and seawater collected form the same site, as well as differences in the microbial community at two different sites (88). Similarly to Hexactinellid sponges analysed by Steinert et al. (87), the microbiota of *V. pourtalesii* was dominated by Proteobacteria. Other abundant phyla were the Patescibacteria, Bacteroidetes, Spirochaetes, and Planctomycetes.

With regards to the high microbial abundance-low microbial abundance (HMA-LMA) dichotomy that has become apparent in sponge taxonomy (91–93), it has been proposed that all deep-sea sponges may in fact be LMA sponges ($1x10^{5-6}$ bacterial cells/g wet-weight of sponge tissue) in contrast to HMA sponges with $1x10^{8-10}$ bacterial cells/g wet-weight of tissue (94). Steinert et al. (87) reported the microbiota of 7 Hexactinellid sponges that were consistent with those of LMA sponges. Evidence for a deep-sea specific sponge microbiota has been put forward (94), however the characterisation of the Hexactinellid microbiota from currently unexplored species will inform discussion regarding the Hexactinellid-specific microbiota. It may be difficult to determine whether differences between Hexactinellid and Demosponge microbiota are due to host-associated factors or to the increase in depth. This is owing to the fact that Hexactinellid sponges occur almost exclusively in deeper waters (2). The lack of significance of the impact of depth on the composition of seawater microbiota (95), as well as the impact of host identity in determining Demosponge microbiota (48) potentially suggest that differences are more likely to be host-driven. The change in all environmental factors that accompany the increase in depth must also be taken

into account when assessing the impact of depth on driving microbiota composition (95).

Mangano et al. in 2009 (3) first reported the recovery of bacterial isolates from a deep-sea Hexactinellid sponge (*Anoxycalyx joubini*). Similar to studies characterising sponges from shallow waters, cultivable isolates consisted of *Alphaproteobacteria* (41.2%), *Gammaproteobacteria* (35.3%), *Bacteroidetes* (17.6%) and *Actinobacteria* (5.9%). Xin et al. (4) have also reported the cultivation of bacterial isolates from two species of Hexactinellid sponges (*Rossella nuda*, *Rossella racovitzae*). Bioactivity screening revealed that 88% of all tested isolates displayed antimicrobial activity against at least one bacterial plant pathogen. Clinically-relevant strains associated with human disease were not screened against however. Interestingly, all isolates were determined to be Gram-positive (Actinobacteria, 52.2%%; Firmicutes, 47.8%), none of which required seawater for their growth (4).

Whilst similarities are observed between the types of bacteria isolated from Hexactinellid sponges and the Porifera in general, there appear to be slight differences in the relative percentages of the specific bacterial groups. In order to explore this, a literature review was carried out in order to identify papers that have cultured bacteria from Hexactinellida, and was combined with sequences obtained from the NCBI database (**Figure 1.3**). Cultured isolates from both Classes of sponge are comprised largely of Proteobacteria, Actinobacteria, Firmicutes and Bacteroides. The biggest difference currently observable is that a higher percentage of the isolates obtained from Hexactinellid sponges belong to the Bacteroidetes, which may be a reflection of their relatively high abundance within the Hexactinellid microbiota (88). The small number of representative isolates from Hexactinellid sponges (n=53) however

prevents a more meaningful analysis. Whilst such a comparison helps to provide an early insight into the Hexactinellid-specific cultivable community, the limited number of glass-sponge specific studies represents a knowledge-gap in the current literature.

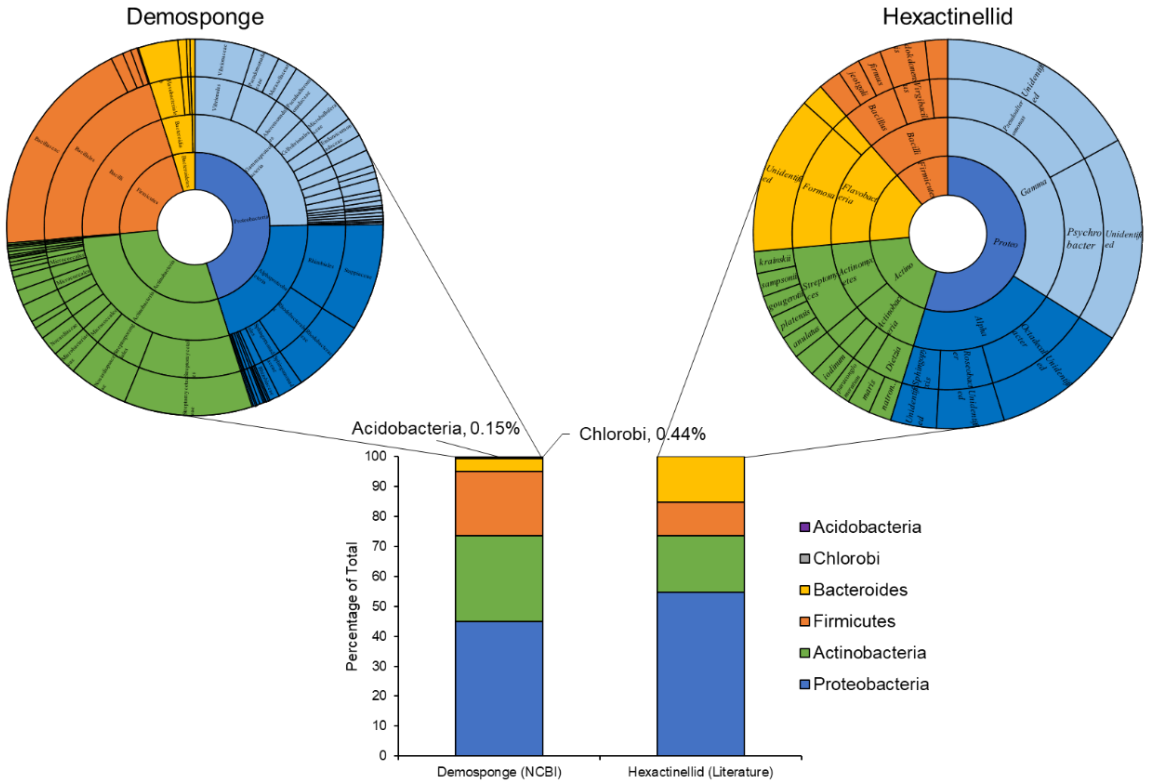

Figure 1.4 – Phylum-level comparison of isolates recovered from Demosponges and Hexactinellid sponges. Representative Demosponge isolate information obtained from entries submitted to NCBI using search criteria: [(sponge* or porifera*) and (16S* or ssu* or rRNA*) and (cultured*) NOT (18S* or lsu* or large subunit* or mitochondria* or 23S* or 5S* or 5.8S* or 28S* or crab* or alga* or mussel* or bivalve* or crustacea* or uncultured*)]. Hexactinellid isolate information obtained from a literature search of studies that have cultured bacteria from Hexactinellid sponges (3,4).

1.5 Antimicrobials from the Deep-Sea Sponge Microbiota

Examples of the elucidation of compounds from deep-water sponges are noticeably less common than from shallow-water sponges. The systematic review published by Indraningrat, Smidt and Sipkema (1), compiling instances of sponge-derived antimicrobial compounds did not contain any published literature concerning sponges recovered from deeper than 40m. Turk and colleagues (96) have reported the antibacterial activity of sponge-derived extracts from 33 deep-sea arctic sponges (200-900m). The extracts exhibited relatively weak antibacterial activity, with a slightly better activity against isolates also obtained from arctic waters. The results are perhaps slightly incomparable to those from studies looking directly at sponge-derived microorganisms, as the extracts were obtained directly from sponge samples rather than their microbial constituents and may therefore be a combination of compounds, at different concentrations than may be obtained from direct bacterial culture.

Wright et al. (97) recently reported the activity of the novel compound Dragmacidin G, obtained by ethanolic extraction of a sponge from 630m depth, obtained from Long Island, Bahamas. Antimicrobial activity against *S. aureus* and MRSA was observed (MIC 0.62 µg/mL), as well as against *Mycobacterium tuberculosis* (MIC 21µM).

An investigation into the capability of sponge-derived *Pseudovibrio* spp. to produce bioactive compounds has been carried out by researchers at the University of Cork (75,98). The genomic analysis of various strains revealed the presence of numerous biosynthetic gene clusters (BGCs) encoding Non-Ribosomal Peptide Synthases (NRPSs) and Polyketide Synthases (PKS) (99), providing potential leads for subsequent NP discovery. It has also been remarked upon that sponge bacteria isolated from the deep-sea environment are likely to harbour a range of both known

and unknown gene clusters responsible for the biosynthesis of antimicrobial compounds (100). A recent landmark study (95) showed that whilst taxonomic abundance decreased with depth, the taxonomic diversity increased. In addition, the abundance of functional genes increased in relation to the depth at which host bacteria were collected (5m-600m). Whilst marine sponges were not included in this analysis, it does pose interesting questions concerning the potential for novel natural product discovery. A total of 90% of the functional genes observed within the sample collected at 600m were not found in known databases, which provides a promising outlook for discovery of deep-sea sponge-specific compounds. The discovery of genetic elements associated with shallow-water sponges in deep-sea sponges suggests transfer between the shallow and deep-sea environments (100). The microbiota of shallow and deep-water sponges however are suspected to be generally distinct (94).

1.6 Aims & Objectives

The information presented in this introduction reveals the relative lack of available information regarding the microbiota of deep-sea Hexactinellid sponges. It also suggests that the Hexactinellid microbiota may contain novel bacterial species with the ability to produce novel antimicrobial candidates. In order to address these gaps in the field of sponge microbiology, work in subsequent chapters will address these themes via the following objectives. Culture-dependent methods will be employed to culture and identify bacterial antimicrobial producers from two species of Hexactinellid sponge. Bacterial culture will consist of the use of solid and liquid growth media, with the manipulation of environmental parameters including nutrient availability and temperature. Bacterial culture will also include the use of a novel technique, which by manipulating atmospheric pressure will aim to broaden the cultivable diversity of

microbial isolates. Cultured bacterial isolates will be screened *in vitro* for antimicrobial activity against clinically-relevant Gram-positive and Gram-negative strains using traditional, plate-based techniques. The production of antimicrobial agents via fermentation will be optimised via the manipulation of nutrient availability, temperature and other culture parameters, and purified using a combination of reverse-phase affinity and size exclusion chromatography. Isolates that display antimicrobial activity will be further characterised *in vitro* as well as *in silico*. Whole-genome sequencing will be used to provide strain-level resolution as well as determine the presence of known BGCs with the use of publicly available software. Information obtained from BGC classification will be used to predict the identity of isolated antimicrobial agents as well as guide experiments aimed towards determining the mechanism of action, minimum inhibitory concentration (MIC) and cellular toxicity.

In addition, molecular and culture-independent methods will be used to present the first ever characterisation of the overall bacterial microbiota of the sponges examined, as well as that of sediment samples obtained from two separate sampling sites. Taxonomic classification of 16S rDNA sequences obtained will also aim to explore the differences between both sponge and sediment samples, identify intra-sample and site-specific differences as well as provide information on the structure of the core and species-specific microbiota. Lastly, the taxonomic classification of sponge reads will also be used to assess the presence of isolates obtained using culture-dependent methods, and provide an indication as to the overall proportion of cultivable microbiota.

Chapter 2

Impact of growth media and pressure on the diversity and antimicrobial activity of isolates from two species of Hexactinellid Sponge

Part of the data in this Chapter is also published in Koch et al., 2021, *Microbiology* (Reading). 2021; 167(12): 001123

2.1 Introduction

Antimicrobial resistance has been classified as one of the greatest threats to human health by the World Health Organisation (15) and was the subject of a UK governmental report in 2016 (7). Historically, many of the clinically available antimicrobials have been derived from bacteria associated with the soil microbiota and have been the result of screening efforts aimed at discovering compounds (14). The spread of antimicrobial resistance mechanisms as well as Issues in the supply chain of novel classes of antimicrobials have led to an urgent need to innovate by investigating underexplored areas and improving culture methodology.

Sponges (Porifera) are the oldest known marine invertebrates (39,40). It has become apparent in recent years the microbes associated with sponges are responsible for many of the novel antimicrobial agents associated with them (22), a finding which has provided the rationale for the culture-dependent approach of many studies seeking to optimise bacterial recovery and identify novel natural products (75,77,81,101).

The cultivation of sponge-associated microbes has traditionally been limited by poor access to samples (56) or difficulty in providing suitable culture parameters (102,103). Efforts to improve the cultivation have included an analysis of different methodologies, such as agar-based recovery (104), the use of diffusion chambers (105), liquid culture and floating-filter cultivation (81). Agar-based methods have shown greater success in cultivating an increased bacterial diversity from *Haliclona* spp., compared to liquid and floating-filter methods (81). *In-situ* implantation of diffusion growth chambers (DGC) within the living tissue of *Rhabdastrella globostellata* sponge have also resulted in the improved recovery of bacteria belonging to the Actinobacteria, Alphaproteobacteria and Gammaproteobacteria (105), many of which were deemed

to be novel. This represents a promising method for the cultivation of bacteria from larger, shallow water sponges, but the *in-situ* nature of the methodology would make implementation on deep-sea sponges more problematic.

For every depth increase of 10.06m, pressure increases one atmosphere. Therefore, the retrieval of sponge samples from deeper waters brings with it the potential to isolate bacteria adapted to life at both cooler temperatures and higher pressures. Bacteria adapted to survive in such conditions can be separated into several categories. Piezotolerant bacteria are those capable of surviving at increased atmospheric pressures, but at which their optimal growth does not occur. In contrast, piezophilic bacteria grow more favourably at higher pressure, while hyperpiezophilic are those that only grow at increased atmospheric pressure (106). Whilst research has revealed the extent to which piezotolerant/piezophilic bacteria participate in ecological cycles such as nutrient cycling and degradation (107), it has been remarked upon that the effect of host-microbe interactions on the ability of bacteria to thrive in increased atmospheric pressures is poorly understood (108). To the best of our knowledge, the use of increased atmospheric pressure to improve the cultivability of sponge bacteria has not yet been explored.

The majority of culture-dependent sponge research has explored the microbes assoied with members of the Demosponge class, with the Hexactinellid, or ‘Glass’ sponges representing an untapped ecological niche, in relation to their microbiota and the bioactive potential of associated microbes (3,4). Mangano et al., (3), however reported the first ever recovery of bacterial isolates from a deep-sea Hexactinellid sponge (*Anoxycalyx joubini*), in a study that included both Demosponges and the

Hexactinellids. Similarly, Xin et al. (4) explored the cultivable diversity of two species of Hexactinellid sponges, *Rossella nuda* and *Rossella racovitzae*, resulting in the culture of bacteria including the cultivation of a potentially novel group of previously uncultured isolates. This suggests a potentially distinct Hexactinellid-specific microbiota and is further supported by recent 16S rRNA amplicon sequencing and metagenomic surveys (86–88). The evidence that bacterial genomes associated with *Vazella pourtalesii* display genome reduction is potentially indicative of specialised, Hexactinellid-specific host-microbe interactions (86). These reports highlight a potentially diverse but uncharacterised microbiome specific to individual sponge-species, which opens up an opportunity to investigate this unique flora for novel antimicrobial compounds.

The current lack of information regarding the cultivable sponge-associated inhabitants of Hexactinellid sponges and their antimicrobial potential represents a knowledge gap in the current literature. Therefore, the aim of this study is to utilise novel media and pressure culture methods to improve recovery of Hexactinellid-associated bacteria in the search for novel antimicrobial producers.

2.2 Materials & Methods

2.2.1 Sample Collection

Sponge samples were collected from the North East Atlantic deep-sea, as part of two different research programmes: the NERC funded DeepLinks Project in 2016 (RRS James Cook - JC136), the Sensitive Ecosystem Assessment and ROV Exploration of Reef (SEAROVER) project in 2017 (Irish Light Vessel Granuaile - GRNL2017, RH17001), and again in 2019 (RV Celtic Explorer CE19015). Sample collection sites are displayed in **Figure 2.1.**

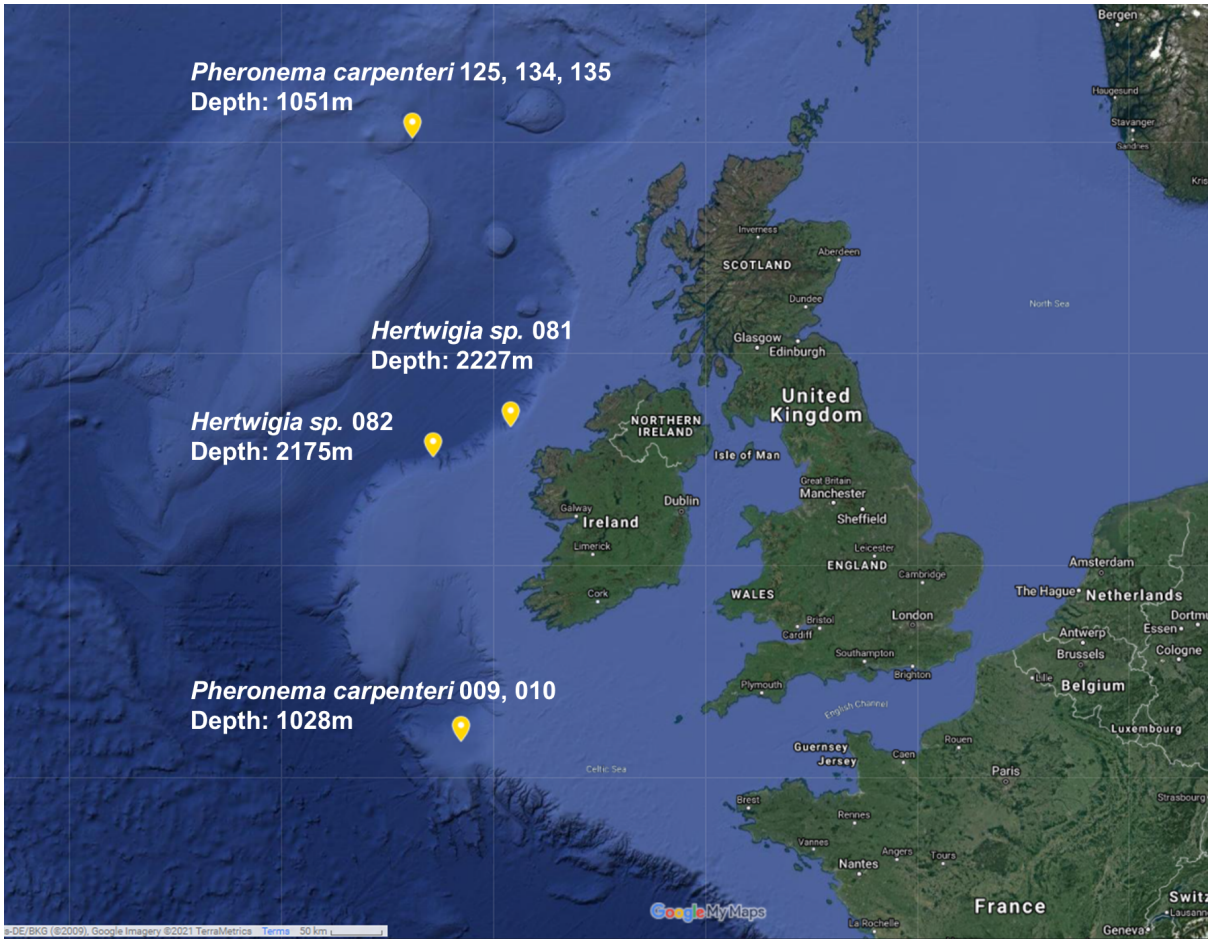

Figure 2.1 – GPS co-ordinates of collection sites for sponges used in this study. Picture obtained by inserting sample co-ordinates into Google Maps.

Sample co-ordinates and metadata displayed in **Table 2.1**

Table 2.1 – Samples collection metadata for sponges used in this study

Cruise	ROV	Sample ID	Date	Latitude	Longitude	Depth (m)	Pressure (bar)	Temp (°C)
JC136	Isis	JC136_134	6/16/2016	58.8546885	-13.3994155	1051	107	6.39
JC136	Isis	JC136_125	6/16/2016	58.8547103	-13.3994087	1051	107	6.39
GRNL 2017	Holland I	GRNL_081	7/20/2017	54.1867235	-12.8472535	2228	225	3.49
GRNL 2017	Holland I	GRNL_082	7/20/2017	54.18651317	-12.847798	2175	220	3.5
CE19015	Holland I	Sponge_009	8/13/2019	49.534534	-12.10624333	1208	122	6
CE19015	Holland I	Sponge_010	8/13/2019	49.53452567	-12.10614217	1208	122	6

Both cruises conducted sampling of a wide range of deep-sea organisms. Sponges were collected by Remotely Operated Vehicles (ROVs) and photographed *in situ* before removal (**Figure 2.2**).

Figure 2.2 – Photos of sponges taken *in situ* before sample collection. Top left/right: *Pheronema carpenteri* sponges (JC136 cruise). Bottom left/right: *Hertwigia* sp. sponges (GRNL17).

On surfacing, sponges were transferred from the ROV into buckets containing *in situ* seawater and taken into the laboratory for processing. Sponge samples were photographed and a small tissue sample taken for genetic analysis. The remaining sponge sample was then placed in a plastic zip-lock bag and frozen at -20°C for the

remainder of the cruise. Upon return to land, frozen samples were transported in dry ice and maintained at -80°C.

2.2.2 Sponge Identification

Sponges were identified by scientists in the School of Biological Sciences at the University of Plymouth, from the analysis of internal and external morphological features (i.e. body shape, type, size, and arrangement of spicules) following the Systema Porifera classification system (84). For spicule analysis, under sterile conditions using ethanol washed and flame sterilised scalpels, cuttings of approximately 1 cm^3 were taken from the three regions on the sponge body, mesohyl, atria, and the prostalia. Tissues were placed inside Eppendorf tubes (2 mL), covered with 65% Nitric Acid and left for 2 h for spongin tissue to dissolve. The tubes were gently centrifuged at 600 x *g* for 2 min. The supernatant was carefully discarded and the pellet containing spicules re-suspended in water three times to wash all remaining acid. Spicules were then washed in >95% ethanol twice before being left at room temperature for the ethanol to evaporate. Dry spicules were inspected under a compound light microscope and identified (84).

2.2.3 Sample Processing

For isolation of bacteria, sponge samples were allowed to come to room temperature naturally. Sections of the sponge mesohyl were cut from the sponge using a sterile scalpel. Individual tissue segments (~10g) were then homogenised using a sterile mortar and pestle and transferred to a sterile 50 mL falcon tube (Fisher Scientific, UK). Large and un-degradable (spicular) debris was left to settle for 5min and the remaining suspended homogenate was transferred to a new sterile 50 mL falcon tube. The homogenate was then centrifuged (4696 x *g,* 20 min) to obtain a pellet. The pellet was

then re-suspended in 2 mL sterile phosphate-buffered saline (PBS) and 100 µL was spread onto individual agar plates. To minimise the effects of repetitive freezing on the original sponge sample, as well as to aid replicability, all sponge segments were processed at the same time. Unused bacterial cell suspensions and sponge tissue segments were stored at -20°C in Natural Seawater (NSW) + 50% Glycerol for later use.

2.2.4 Agar-Based Comparison of Bacterial Richness and Abundance

A range of solid-growth media was used for bacterial recovery. Abbreviations in the text and figures are as follows. MA: Marine Agar; MC: Marine Agar + Carnitine Hydrochloride (0.2g/l); LB: LB Agar; LC: LB Agar + Carnitine Hydrochloride (0.2g/l); RC: R2A Agar + Carnitine Hydrochloride (0.2g/l); OM: Oatmeal Agar; SYP-SW: Starch-Yeast-Peptone-Seawater Agar (109); ABC: PS Medium (110). A full list of media used is contained within the **Appendix, Table S1**. Bacterial cell suspension was spread evenly across agar plates. Where agar contained Carnitine Hydrochloride, 0.2g/L Carnitine hydrochloride (Sigma-Aldrich) was added before autoclaving. For each condition tested, 3 technical replicates were performed for each biological sponge replicate. For assessing the impact of different media on cultivation, all plates were incubated in the dark at 20°C for a total of 40 days, when all growth measurements were taken.

For pressurised culture, agar plates spread with bacterial cell suspensions were placed into stainless steel containers (650x300mm) (Southwestern Engineering, UK). Gas mixtures were prepared at either 4% or 21% O_2 prior to being pumped into the chambers. Chambers were filled with gas mixtures until the desired pressure had been

reached. This work was carried out in collaboration with Dr Gary Smerdon at the Diving Diseases Research Centre, Plymouth Science Park.

2.2.5 Dilution to Extinction – Cell Counting and Dilution

Bacterial cell suspensions from *P. carpenteri* (Cruise JC126, samples 125/134) and *Hertwigia* sp. (GRNL_081/082) were prepared according to the steps outlined above. Approximate bacterial concentration was determined with the use of a haemocytometer. Cell suspensions were then diluted to approximately 3-4 cells per mL, and 333µl was added to each well of a 96-well plate, to give an approximate total of ~1 cell per well. A total of 288 wells were inoculated in total. Plates were incubated at 20°C for a period of 40 days. The calculations for the actual counts and dilutions used are as follows:

***Hertwigia* sp.**

Original bacterial cell suspension was diluted 1:10 ($1x10^{-1}$) and counted on a haemocytometer. The suspension was thereby deemed to contain ~12,000,000 cells/mL. The cell suspension was split into 3x333µl (4,000,000 cells/mL each) and each was diluted 1:10,000 using either ½ Marine Broth, ABC media or LNHM (see media list). An aliquot (500µl) was then added to 49.5 mL of the appropriate media (1:100) giving an approximate concentration of 4 cells/mL and 330µl was then added to each well of a 96-well plate to give an approximate concentration of 1.33333 cells/well.

Pheronema carpenteri

Original cell suspension was diluted 1:10 ($1x10^{-1}$) and counted on a haemocytometer. The suspension was thereby deemed to contain ~22,500,000 cells/mL. This cell suspension was split into 3x333µl (7,500,000 cells/mL each) and each was diluted 1:10,000 using either ½ Marine Broth, ABC media or LNHM (see media list). Each dilution was then diluted 1:2 (500µl cells in 500µl media) (~375 cell/mL). An aliquot (500µl) was then added to 49.5mL of the appropriate media (1:100) giving an approximate concentration of 3.75 cells/mL and 330µl was then added to each well of a 96-well plate to give an approximate concentration of ~1.25 cells/well.

2.2.6 Antimicrobial Screening using Simultaneous Antagonism

Cell suspensions of the organism being screened against (the indicator) were prepared to specific OD_{600} readings for each species. Indicators used for preliminary screening were *Micrococcus luteus* (OD_{600} 0.5), *Staphylococcus aureus* NCTC12493 (OD_{600} 0.5), and *Escherichia coli* NCTC10418 (OD_{600} 0.4). Isolates obtained from bacterial culture were screened for antimicrobial activity using the simultaneous antagonism method (111).

Each well-plate was wrapped in foil to ensure darkness and was incubated at 20ºC whilst shaking at 100rpm. Growth was assessed by the presence of visible growth after 40 days. Aliquots (100µl) from each growth-positive well was streaked onto 1/10 R2A and incubated in the dark (112). Upon the growth of colonies, each individual colony type (assessed by visual morphology) was sub-cultured onto a separate agar plate.

2.2.7 DNA Extraction and Amplification

Genomic DNA was extracted from isolates using the DNeasy Powersoil Kit (Qiagen, UK) according to manufacturer's conditions. DNA was quantified using a Qubit Fluorometer (Thermofisher Scientific). PCR reactions (50µL) were set up, consisting of 25µL 2x DreamTaq Green PCR Master Mix (Fisher Scientific, UK), 2.5µL 27F 16S Primer (5'-3' AGAGTTTGATCATGGCTCA), 2.5µL 1492R 16S Primer (5'-3' TACGGTTACCTTGTTACGACTT) (Eurofins Genomics Standard Primers) (113–116), 5µL DNA Template (50-100ng), 15µL nuclease-free water (Merck). PCR conditions for the amplification of the 16S rRNA gene consisted of an initial denaturation step of 5 minutes at 94°C, followed by 30 cycles of 30 seconds at 94°C, 60 seconds at 52°C, 90 seconds at 72°C and a final extension step of 10 minutes at 72.

2.2.8 Bacterial Sequence Classification and Tree Building

Amplicons of the 16S rRNA gene were sequenced using Sanger Sequencing (LGC Genomics Ltd, Germany). The forward and reverse strands of the 16S rDNA gene were sequenced separately and trimmed to remove regions that had more than a 5% chance of per-base error. Forward and reverse sequences were then aligned to each other in order to provide a consensus sequence. Sequences were compared against the NCBI Nucleotide collection (nr/nt) database using the BLAST function in Geneious Prime v2020.2.2 with standard parameters. A phylogenetic, neighbour-joining tree was constructed using a Tamura-Nei distance model (117). Tree-building was performed in Geneious Prime using the Geneious Tree Builder tool with standard parameters. The tree was exported as Newick-format and uploaded to iToL (https://itol.embl.de/) for visualisation.

2.3 Results

2.3.1 Low-nutrient media recovers highest bacterial abundance and diversity for *Pheronema carpenteri* and *Hertwigia* sp.

Preliminary optimisation of bacterial culture was carried out for two species of deep-sea hexactinellid sponges using a range of solid growth media. Abundance counts were recorded as counts of individual colonies, irrespective of morphotype, while diversity counts record different morphotypes. The word morphotype here refers to bacterial colonies that were distinguishable using the naked eye. Each colony present on a particular agar was cross-referenced by searching for a colony of the same visible morphology on all other plates of that media type. Parameters including colour, size, border, opacity, and profile were taken into account. It should also be noted that these reports of abundance and diversity refer explicitly to cultivability, and not to the overall microbial communities of the sponges. For all media trialled, Marine Agar (MA), Marine Agar + Carnitine (MC) and half-strength Marine Agar (½ MA) consistently yielded higher colony forming units per gram of wet weight of sponge (CFU/gww) across both sponge samples tested (**Figure 2.3A, B, D, E**), while Oatmeal Agar (OM) produced the lowest (**Figure 2.3A, D**). Of the three, ½ MA was the most successful in recovering bacteria from *Hertwigia* sp., with an average of 99.7 CFU/gww (**Figure 2.3A**), while MC was the most successful for *P. carpenteri* samples (**Figure 2.3D**), averaging 9.3 CFU/gww. Furthermore, the trend across all media types indicated an approximate 10-fold greater recovery of bacteria from *Hertwigia* sp. samples compared to those from *P. carpenteri*. A significantly higher bacterial abundance was obtained from *Hertwigia sp*. across 6 of the 10 media used. Media that produced a significantly higher bacterial abundance were LB (p-value:0.0077), RC (p-value:0.0303), R2a (p-

value:0.0024), ½ MA (p-value:<0.0001), MA (p-value:<0.0001) and MC (p-value:<0.0001).

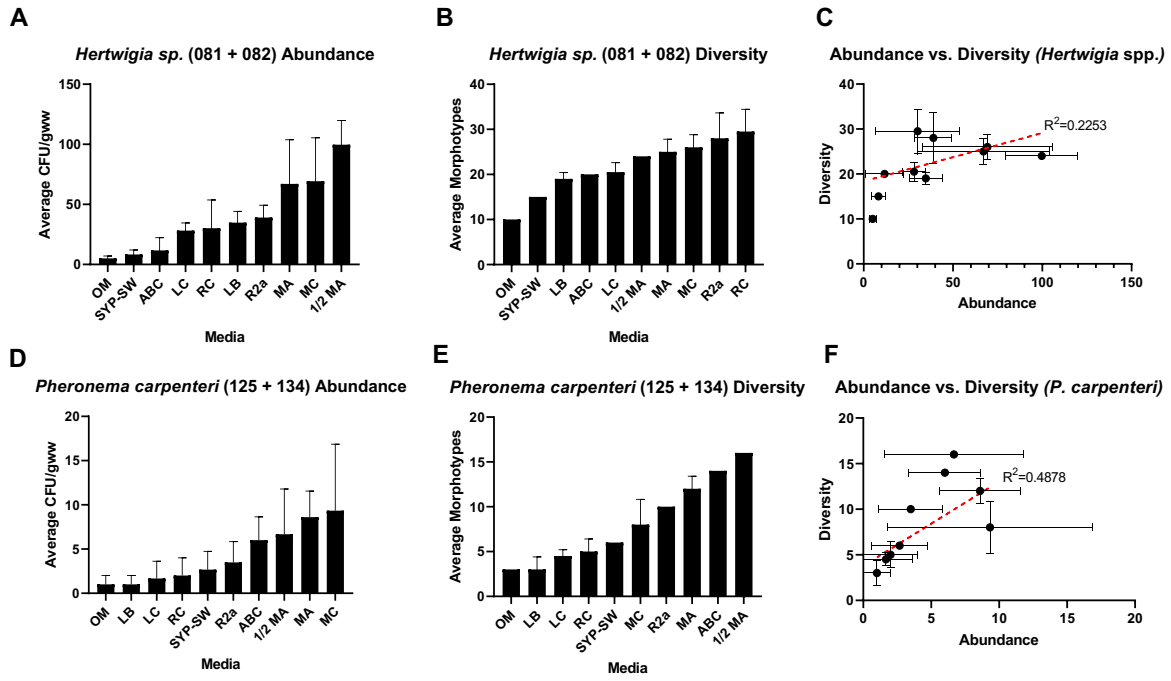

Figure 2.3 – Recovered CFU/gww counts for isolates obtained from two different samples of two species of Hexactinellid sponge. **A, D)** Abundance counts for bacteria grown across different media for *Hertwigia* sp. and *P. carpenteri*, respectively. Bars: Mean + Standard Deviation (SD). **B, E)** Number of bacterial morphotypes grown across different media for *Hertwigia* sp. and *P. carpenteri*, respectively. Media without bars represent counts taken only for GRNL_081. **C, F**)**.** Linear regression analysis between CFU/Morphotypes obtained across different media for *Hertwigia* sp. and *P. carpenteri*, respectively (dots represent individual growth media). Bars represent Standard Deviation. All media were inoculated in triplicate. Number in parentheses in individual graph title represents sponge replicate ID. Abbreviations: OM, Oatmeal Agar; SYP-SW, Starch-Yeast-Peptone Seawater Agar; ABC, 'ABC' Agar; LC, LB +

Carnitine Hydrochloride; RC, R2a + Carnitine Hydrochloride; LB, LB Agar; MA, Marine Agar; MC, Marine Agar + Carnitine.

Of the media examined, R2a + Carnitine Hydrochloride (RC) agar yielded the highest number of bacterial morphotypes for *Hertwigia* sp. (29.5 morphotypes/gww) while ½ MA produced the highest number of bacterial morphotypes for *P. carpenteri* (16 morphotypes/gww) (**Figure 2.3B, E**). The correlation between the number of bacterial isolates and the number of bacterial morphotypes present on each growth medium after 40 days of incubation was quantified. For both sponges, there was a positive correlation between the abundance of bacteria and the diversity as measured by Pearson's correlation co-efficient (r = 0.4878, *P. carpenteri*; r = 0.2253, *Hertwigia* sp. (**Figure 2.3C, F**).

2.3.2 P. carpenteri and *Hertwigia* sp. display low overlap in cultivable morphotypes

Analysis of the percentage of bacterial morphotypes shared between the two *Hertwigia* sp. biological replicates (GRNL_081 and GRNL_082) (18.37%) was higher than for *P. carpenteri* replicates (JC136_125 and_134) (5.48%). The number of morphotypes that were shared between sponge species was (2.28%) (**Figure 2.4**).

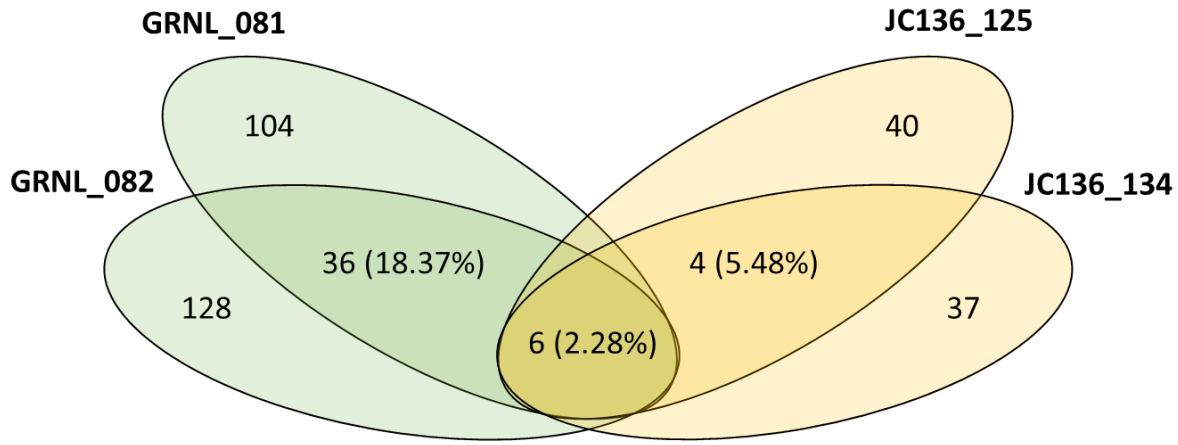

Figure 2.4 –Venn diagram of shared diversity between *Hertwigia* sp. replicates (in green) and *Pheronema carpenteri* replicates (in yellow). The number on the outer edges of the ellipses denote the number of morphotypes for each individual replicate. The percentage number in the corresponding colour denotes the shared morphotypes between replicates of the same type. The central figure denotes the number of shared morphotypes between all *Hertwigia* sp. and *Pheronema carpenteri* replicates as a whole.

2.3.3 Dilution to extinction (DTE) culture produces more bacterial isolates from *P. carpenteri* than from *Hertwigia* sp.

Bacteria were grown from *Hertwigia* sp. (GRNL_081) and *P. carpenteri* (JC136_125) samples using a dilution to extinction (DTE) method (112,118).

For *P. carpenteri*, 21 isolates were recovered on ½ MA, equal to the number of growth positive wells (**Figure 2.5A**). For *Hertwigia* sp., 16 isolates were recovered, higher than the number of growth-positive wells observed (**Figure 2.5A**). For both sponges, several morphotypes were recovered from some individual wells, indicating mixed cultures (**Figure 2.5B**). No bacteria were recovered on solid media from well-cultures of ABC media or LNHM. A higher number of growth-positive wells, as well as a higher

number of bacterial isolates were obtained from *P. carpenteri* (**Figure 2.5A**). A total of 37 bacterial isolates were cultured.

A

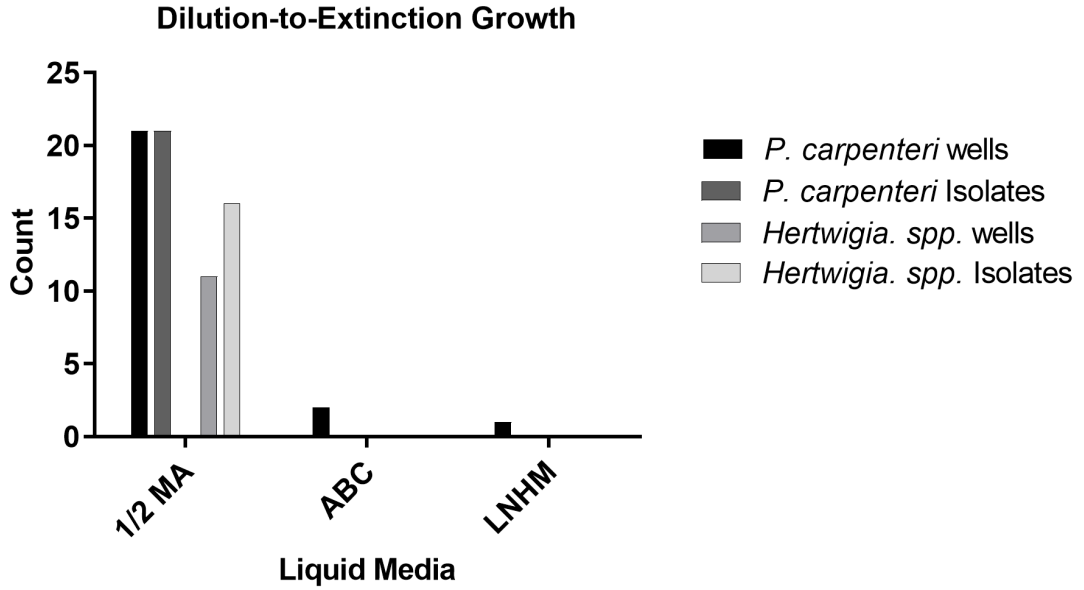

B

Dilution to Extinction Culture Statistics							
Sponge	Growth-Positive Wells	Recoverable Wells	Isolates	Singles	Doubles	Triples	Multiples
P. carpenteri	24 (8.33%)	18 (75%)	21	16 (88.89%)	1 (5.56%)	1 (5.56%)	2 (11.11%)
Hertwigia spp.	11 (3.82%)	9 (81.82%)	16	4 (44.44%)	3 (33.33%)	2 (22.22%)	5 (55.56%)

Figure 2.5 – A) Growth statistics for bacteria grown in different media using the dilution to extinction method. **B)** Table displays statistics for number of bacteria recovered from each treatment. Single, Double and Triple refers to the number of wells from which 1, 2 or 3 different morphotypes, respectively, were recovered when liquid from wells was plated onto solid media.

The percentage cultivability of each sponge [based on the Button et al. (118) and Connon & Giovannoni (112) methodology], was predicated to be 1% for *P. carpenteri* and 0.1% for *Hertwigia* sp. The number of wells containing pure cultures was predicted to be 34.7% for *P. carpenteri*. Actual percentage of wells containing pure cultures, as

measured by counting morphotypes cultured on solid media was 16.7%. The number of wells containing pure cultures was predicted to be 10.8% for *Hertwigia* sp., though actual recoverable morphotypes was 4.2%. Cell counting of a bacterial suspension from each sponge using a haemocytometer suggested there to be around twice as many cells present in the *P. carpenteri* suspension; ~2.25x10^7 cells/mL compared to ~1.2x10^7 cells/mL for *Hertwigia* sp.

2.3.4 Culturing under altered atmospheric pressure/O_2 reveals additional bacterial genera from *P. carpenteri.*

Further bacterial cultivation was carried out for two separate sponges of *P. carpenteri* (hereafter named Sponge_009 and Sponge_010) collected from a later cruise (**Table 2.1**). Further work was carried out on *P. carpenteri* given that a higher number of isolates recovered under normal atmosphere from this sponge displayed antimicrobial activity than was observed for *Hertwigia* sp. (**Table 2.2**, below). Increased pressures were generated with the use of stainless steel chambers (**Appendix, Figure S1**), with the pressure limits determined by the capacity of the chambers used. Gas mixtures were prepared at either 4% or 21% O_2 prior to being pumped into the chambers. Sealed chambers were filled with gas mixtures until the desired pressure had been reached. The pressure simulated in this study (5 bar) was equivalent to 4.93 atmospheres, which is representative of an ocean depth of almost 50m.

Culturing *P. carpenteri* samples at increased pressure (21% O_2/5 bar) resulted in a reduced bacterial abundance when compared to those grown under the control conditions (21% O_2/1 bar) (**Figure 2.6A**). A similar result was also seen for those samples cultured at 5 bar pressure combined with a lower oxygen concentration (4%). A significant reduction in bacterial diversity was also seen for Sponge_009 samples

incubated on R2a at 21% O_2/5 bar, when compared to the control group using a 2-way ANOVA (p-value: 0.0482) (**Figure 2.6B**). A reduction was also observed for those incubated in the lower oxygen concentration, however the difference was not significant (p-value: 0.7793). This indicates that, in these experiments, increased pressure did not improve the abundance or diversity yields from *P. carpenteri* cultured on R2a medium over that of the control conditions.

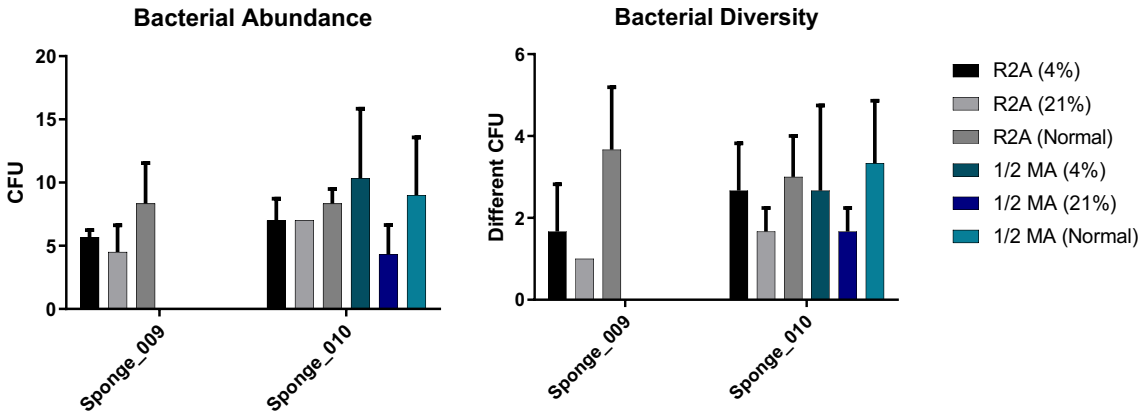

Figure 2.6 – Abundance and diversity measurements for bacteria recovered from *P. carpenteri* and cultured under altered atmospheric conditions. **A)** abundance counts. **B)** Diversity counts. Bars: Standard Deviation across 3 technical replicates.

Bacteria from each environmental condition were sub-cultured onto solid media in non-pressured conditions and genomic DNA extracted from each individual morphotype that was cultured. Sequencing, quality-trimming and aligning of the forward and reverse 16S rRNA gene sequence resulted in data for 31 isolates, as shown in the histograms for sequence length, query cover (%) and identical sites (%) of all BLASTn queries (**Appendix, Figures S2, S3, S4**).

The top BLASTn hit for all 16S rDNA sequences were filtered to those that matched with 100% query cover and a <97% site identity. Filtering sequences in this way

revealed the presence of a single 16S rDNA sequence that may represent a potentially novel *Bacillus* species. The sequence was from an isolate recovered at 21% O_2/Atmospheric bar and matched most closely to *Bacillus sp.* ITP29 with an identical site percentage of 96.6% The filtering cutoffs were relaxed to also include those that had an identical site percentage of <99%, in accordance with updated Operational Taxonomic Unit (OTU) clustering recommendations (119). By including all 16S rDNA sequences that were divergent from those in the NCBI database by >1%, rather than by >3%, the number in the filtered list increased from 1 to 8, as only one sequence had an identical site match of <97%. The 8 16S rDNA sequences that had an identical site match of <99% matched to sequences related to *Psychrobacter* sp., *Pseudomonas* sp., *Erythrobacter* sp., *Dermacoccus nishinomiyaensis*, *Bacillus* sp. and 'Uncultured bacterium clone Md-9.

Of the 31 isolates, 10 were obtained from Sponge_009, whereas 21 were obtained from Sponge_010. All 10 sequences from Sponge_009 had unique BLASTn identities, 8 of which (80%) were unique to Sponge_009. A total of 16 of the 21 sequences from Sponge_010 had unique BLASTn identities, 14 of which (87.5%) were unique to Sponge_010. A total of 2 sequences from each sponge had a shared BLASTn identity. Of the 24 unique BLASTn identities, 22 (91.7%) of these were unique to a particular sponge.

A Neighbour-joining tree of all 31 16S rDNA sequences (alignment length 1621nt) from each sample treatment revealed that they did not cluster together at species level - indicating that isolates from each sample treatment were not more closely related to each other than those from different samples (**Figure 2.7**).

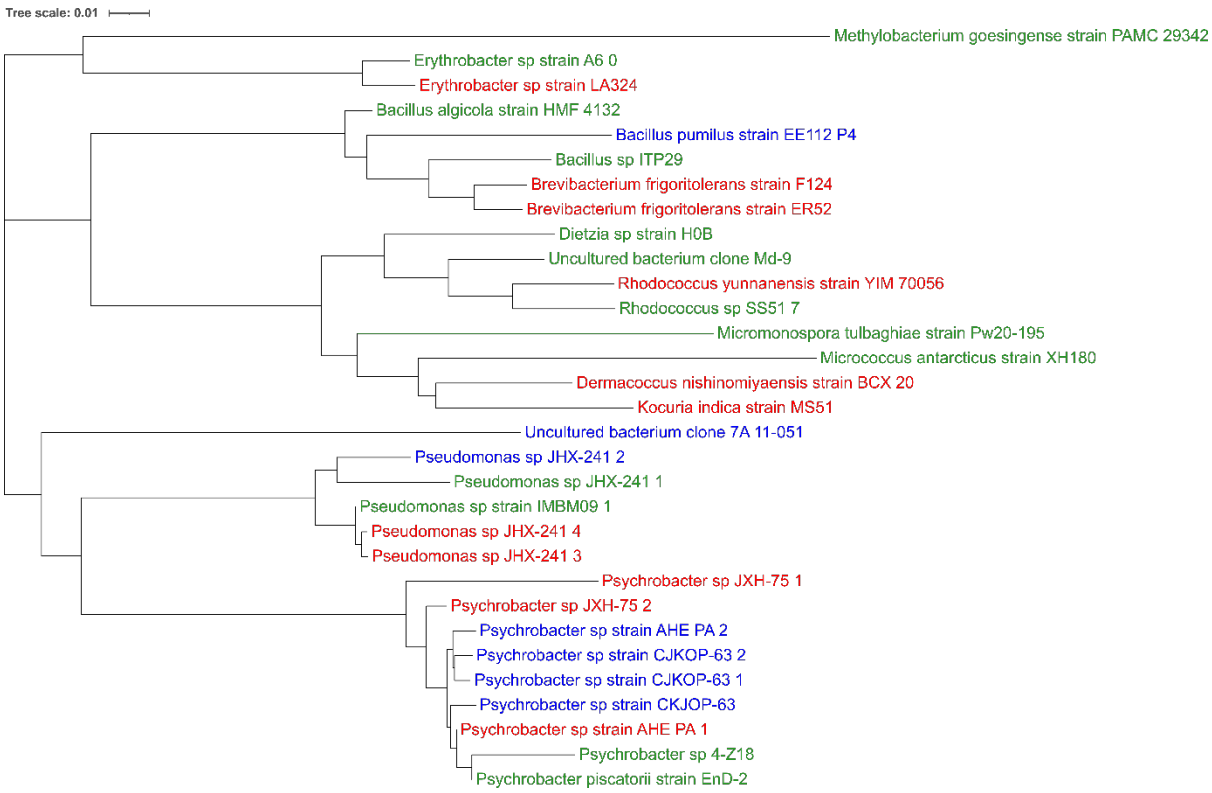

Figure 2.7 – Neighbour-joining tree of 16S rDNA sequences obtained from bacterial isolates cultured from *P. carpenteri*. Taxonomic ID's represent the top BLASTn hit for each sequence. Colours represent treatment at which isolate was recovered. Green: 21% O_2/1.01 bar, Blue: 21% O_2/5 bar, Red: 4% O_2/5 bar.

A total of 31 different morphotypes were recovered from the *P. carpenteri* samples, belonging to 14 genera (**Figure 2.8A**) within the Proteobacteria, Actinobacteria and Firmicutes phyla (**Figure 2.8B**). Of these, thirteen (41.9%) were from 21% O_2/1.01 bar, seven (22.6%) from 21% O_2/5 bar, and eleven (35.5%) from 4% O_2/5 bar. The most common genus recovered was *Psychrobacter* (29%), a proteobacterium present in all three sample types (**Figure 2.8C**). Bacteria from all three phyla were recovered

from 21% O_2/1.01 bar, however, no Actinobacteria were recovered from 21% O_2/5 bar and no Firmicutes were identified in the 4% O_2/5 bar (**Figure 2.8D**).

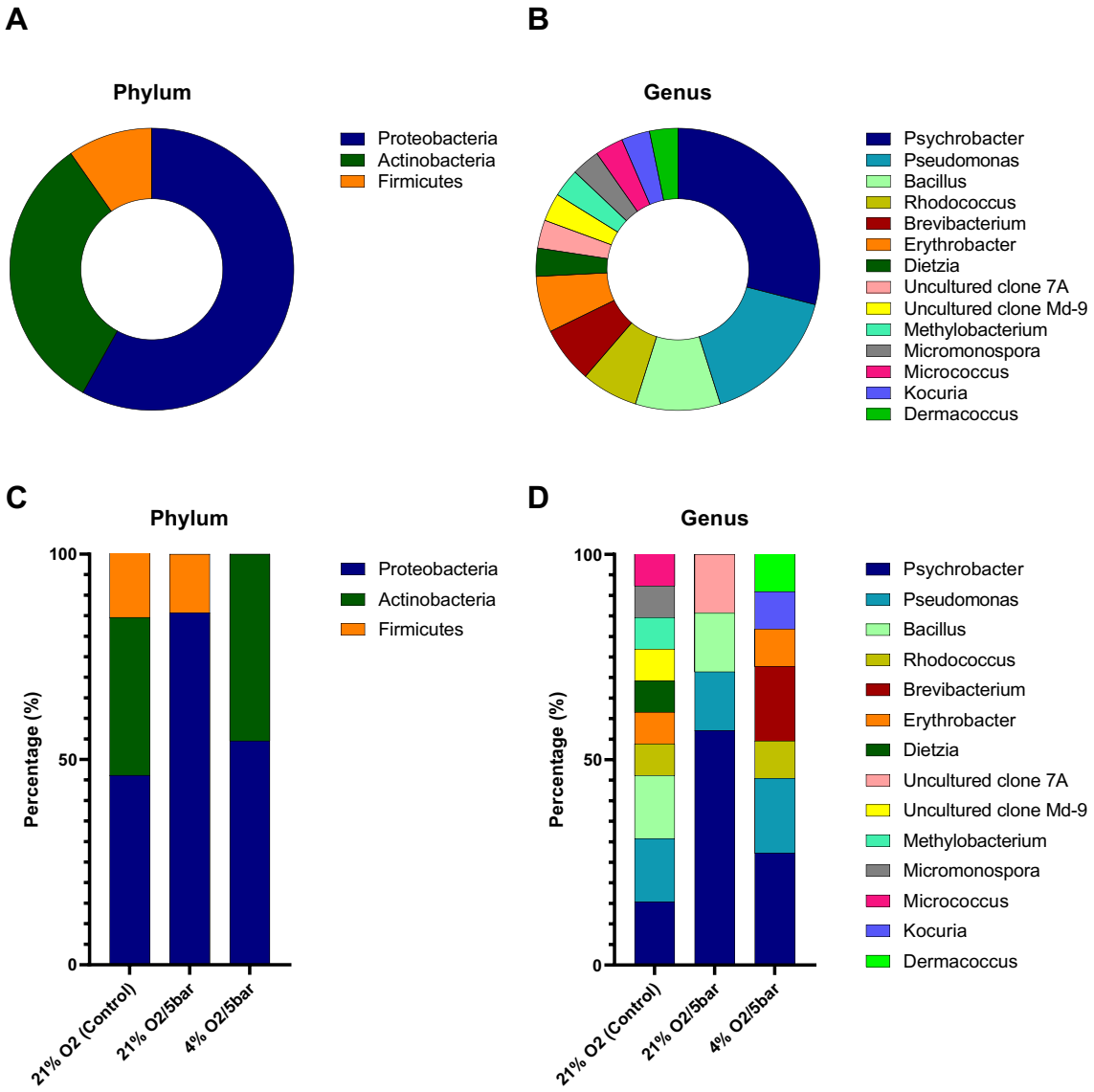

Figure 2.8 – A) Phylum- and **B)** Genus-level distribution of all *P. carpenteri* isolates sequenced. **C)** Phylum- and **D)** Genus-level distribution of isolates recovered, split by sample treatment.

While increased pressure reduced overall bacterial abundance, it appeared to promote the recovery of certain genera that were not cultured under the control conditions. The isolate 'Uncultured clone 7A' was found in the samples incubated at 21% O_2/5 bar but

not at 21% O_2/1.01 bar or at 4% O_2/5 bar, indicating that a combination of higher oxygen and pressure may favour the recovery of this specific strain. *Dermacoccus*, *Kocuria* and *Brevibacterium* were only cultured on R2a at 4% O_2/5 bar, while *Micrococcus, Micromonospora, Methylobacterium* and *Dietzia* were only cultured at 21% O_2/1.01 bar (**Figure 2.8D**), further evidencing the need to implement different environmental factors when attempting to improve recovery of sponge bacterial diversity.

2.3.5 Bacteria from Hexactinellid sponges display antimicrobial activity against clinically-relevant bacterial strains

A total of 331 bacterial isolates were screened for antimicrobial activity using a simultaneous antagonism assay. Briefly a confluent lawn of an indicator organism was spread across an agar plate and 'spotted' with sponge isolates. The plates were incubated and assessed visually for a 'zone of inhibition' around each sponge isolate, with a total of 212 (64%) isolates from *Hertwigia* sp. and 119 (36%) from *P. carpenteri*. The potential screening of duplicate strains was a possibility given isolates were obtained at different stages and via different methods. Each isolate was initially screened for antimicrobial activity against the three test bacteria; *M. luteus*, *S. aureus* and *E. coli* (**Table 2.2**). *S. aureus* and *E. coli* were chosen for their clinical relevance as well as to represent both Gram-positive and Gram-negative bacteria. *M. luteus* in particular was chosen due to its relative susceptibility to antimicrobials, thought to be a reflection of its small genome and resulting lack of certain resistance proteins found in other Actinobacteria (120). *M. luteus* was therefore considered a good target, or 'wide net' for first-pass antimicrobial detection. Of the 11 isolates that displayed antimicrobial activity, 9 (81.8%) were active against both Gram-positive organisms,

while 1 isolate, *Micrococcus antarcticus* showed activity against *M. luteus* only. Two isolates (18.2%) were active against both Gram-positive and Gram-negative organisms, with those that were identified coming from Actinobacteria and Firmicutes, while only one isolate (9.1%) was solely active against *E. coli*. Eight (72.7%) of active isolates were obtained from *P. carpenteri*, while three (27.3%) were obtained from *Hertwigia* sp.

Table 2.2 – Isolates obtained from Hexactinellid sponges that displayed antimicrobial activity in a simultaneous antagonism assay.

			Activity vs.		
Parent sponge-Isolate ID	**16S rDNA Identity based on closest database match**	**Isolation Medium**	***M. luteus***	**MRSA**	***E. coli***
***P. carpenteri* -Ph28**	*Bacillus altitudinis*	LB	+	+	+
***P. carpenteri*-RC14**	*	RC	+	+	-
***P. carpenteri*-RC15**	*	RC	+	+	-
***P. carpenteri*-RC17**	*	RC	+	+	-
***P. carpenteri*-A11**	*Streptomyces* sp.	RC	+	+	+
***P. carpenteri*-Ph7**	*Streptomyces* sp.	½ MA (DTE)	+	+	-
***P. carpenteri*-NS98**	*Micrococcus antarcticus*	R2A	+	-	-
***P. carpenteri*-NS10M4**	*Bacillus sp.*	½ MA	-	-	+
***Hertwigia* sp-RC57**	*	RC	+	+	-
***Hertwigia* sp-SYP-1**	*	SYP	+	+	-
***Hertwigia* sp-SYP-2**	*	SYP	+	+	-

M. luteus: *Micrococcus luteus* (lab strain); MRSA: *Staphylococcus aureus* NCTC 12493; *E. coli*: *Escherichia coli* NCTC 10418. Isolation media abbreviations as previously described. *Isolates with low level activity were not identified using 16S rRNA gene sequencing.

2.4 Discussion & Conclusions

2.4.1 Culture Using Solid Media and Community Dissimilarity

Most studies investigating bacteria with antimicrobial activity from sponge microenvironments have focused on those sponges collected from shallow waters

(<200 metres deep) and those from the class, Demospongiae. To optimise the culture of bacteria from two previously uncharacterised species of Hexactinellid sponge, bacteria were cultured on a range of solid-growth media, representing the first culture-based microbial analysis of these two sponges. The number of CFU and the number of distinct morphotypes (i.e. abundance and diversity) were also compared between isolates obtained from *P. carpenteri* and *Hertwigia* sp. In general, this revealed a higher abundance of isolates from *Hertwigia* sp. and the positive impact of lower-nutrient media designed to mimic the marine environment, across both sponge species. The inclusion of seawater in culture media (SYP-SW), whilst resulting in low bacterial abundance, did produce a relatively high number of bacterial morphotypes, particularly in the case of *Hertwigia*. The use of carnitine, a substrate for which sponge bacteria have previously been shown to display metabolic specialisation (121) did not appear to significantly increase the number of bacterial CFU or morphotypes.

Maximising the chance that recovered bacterial isolates are derived from the marine/sponge environment attempts to reduce the chance for re-discovery of previously characterised antimicrobials by taking advantage of the increased species and functional richness associated with deeper waters (82,95) and the number of marine NPs that have been discovered from the marine environment in recent years (21,41). It is also important for studies seeking to screen recovered isolates for antimicrobial activity to consider which media produce the highest number of distinct bacterial morphotypes (i.e. diversity), rather than just abundance - a higher number of individual morphotypes provides a higher number that can be screened. It should be noted that whilst two isolates display similar morphologies, this does not mean that they will produce the same profile of secondary metabolites. Distinguishing colonies based on visual morphology attempts to provide an early, simple de-replication step

in the process of identifying potentially novel antimicrobial candidates. This however is limited by the fact that strains may display different morphologies when using different culture media, and that different bacteria may display highly similar morphologies that may be indistinguishable with the naked eye.

The positive impact on bacterial culture of low-nutrient media, as well as the inclusion of seawater provide an initial reassurance that the bacteria cultured are more likely to be those present in the marine environment, rather than the result of terrestrial contamination. Whether or not the bacteria cultured are truly ‘sponge-associated’ as opposed to being just from the marine environment in general was not investigated, and is unknowable without further investigation of metabolic and/or genetic specialisation. This indication was further explored by the molecular characterisation of isolates obtained from culture at altered atmospheric pressure, as will be discussed later.

The use of solid growth media resulted in a ten-fold increase in the number of colonies recovered from *Hertwigia* sp., although a similar increase was not observed for diversity, suggesting the *Hertwigia* sp. microbiota is dominated by either one or a small number of bacterial species that cannot be cultured. Cell counting techniques used in dilution-to-extinction experiments indicated there to be around twice as many cells present in the *P. carpenteri* suspension. Whilst cell counting techniques using only a haemocytometer are rudimentary, it does perhaps suggest the *P. carpenteri* sponge does not only have a higher bacterial density but also a higher number of constituents that were either ‘uncultivable’ under the conditions applied, or perhaps unviable. Use of dilution-to-extinction experiments indicated that *Hertwigia* sp. have a much lower microbiome cultivability (0.097%) than *P. carpenteri* (1.039%). The formula for

calculating percentage cultivability of bacteria devised by Button et al. (118) has since been updated to include information concerning the relative abundance of particular species within bacterial suspensions (103). Culture of bacteria here by DTE would benefit from a 16S rRNA taxonomic survey of the host microbiota, in order to provide this information.

Another initial indication of the community dissimilarity of each sponge species is the markedly low overlap between shared morphotypes [6 (2.26%) of 269 isolates]. Whilst this observation is limited by the small number of isolates obtained from *P. carpenteri*, it is supported by the fact that 91.7% of the 16S rDNA sequences obtained from *P. carpenteri* had BLASTn identities that were found in only a particular sponge replicate. It also appears that the different media used herein revealed distinct groups of bacterial morphotypes. This was noted in visual observations and is also highlighted by the lack in correlation between an increase in abundance and diversity. The increase in number of bacterial colonies recovered did not lead to a significant increase in a specific morphotype, with the increase being made up of representatives of numerous morphotypes.

2.4.2 Comparison Between Biological Replicates

Due to the lack of information available on the Hexactinellid microbiota, it is unknown how much variation exists between biological replicates of the same species. Perhaps the most extensive overview of the sponge microbiota to date included <5 biological replicates for the majority of species analysed (43). It is interesting to note than even for species for which a high number of biological replicates was provided, there was still a high degree of variation in community dissimilarity as determined by 16S rDNA sequence profiling (43). In our efforts to observe the effects of isolation media,

temperature, and supplementation on culturing effects, we observed significant differences between biological samples belonging to the same species. In this study, sponge samples were classified as biological replicates if belonging to the same species and if they were retrieved from the same sampling event and depth. This attempts to control the effect that depth, a proxy for temperature and pressure, may have on the recoverability of sponge-associated bacteria. The *P. carpenteri* sponges JC136_125 and 136 were both sampled from the same location at 1,051 m depth, whereas the two *Hertwigia* sp. sponges were sampled at 2,175 m (GRNL_82) and 2,227 m (GRNL_81) depth (**Table 2.1**).

The most comprehensive analysis of the Hexactinellid microbiota to date included 3-4 replicates of each species from 770-4160m depth (87), reporting that the relative abundance of each taxon varied more widely between biological replicates of Hexactinellid sponges than for Demosponges. Members of the *Hertwigia* and *Pheronema* genera were absent from the Steinert study. Using the amplicon sequence variant (ASV) technique of classification (122), a greater dissimilarity in alpha-diversity was also observed between 33 replicates of the Hexactinellid *Vazella pourtalesii*, compared to the microbiome of surrounding seawater and sediment, at ASV and Phylum level (88). It is therefore relevant to consider the differences in community composition between biological replicates of the same host species, particularly for those that have not been previously investigated. It appears from the preliminary investigation conducted here that cultivable differences are more pronounced between sponge species than for replicates of the same sponge species. Further in-depth 16S rRNA gene or

metagenomic community profiling would be recommended to fully explore these inter- and intra-sponge differences and is covered in **Chapter 4**.

2.4.3 Dilution-to-Extinction Culture

Bacteria from *Hertwigia* sp. and *P. carpenteri* were cultivated using the DTE method. Whilst the use of ½ MA produced colonies in 11/96 and 24/96 wells for *Hertwigia* sp. and *P. carpenteri*, respectively, the use of ABC and LNHM produced only a small number of colonies for *P. carpenteri* and none for *Hertwigia* sp. Inoculation of LNHM (123) and sterilised seawater (112) has previously been used for the cultivation of isolates from marine water. Given the reported success of ABC media in improving the diversity of bacteria recovered on solid media in this study and its original report (110), it is surprising that such a low number were produced using DTE in the current study. A theoretical outcome of using DTE is that wells are more likely to contain members of the most highly abundant species present in the original sample. The observation that a lower number of isolates were obtained from *Hertwigia* sp. may support the concept that the microbiota is dominated by one or several 'uncultivable' species. This however does not provide an explanation for why such a low number of isolates were produced from *P. carpenteri* when using ABC and LNHM. The calculated cultivability value was much lower for *Hertwigia* sp.

2.4.4 Culture at Increased Atmospheric Pressure

Bacteria from the phyla Proteobacteria, Actinobacteria and Firmicutes were recovered from *P. carpenteri* samples cultivated at 21% O_2/1 bar. Interestingly, the use of 4% O_2/5 bar prevented the growth of Firmicutes, and the use of pressure (21% O_2/1 bar) prevented the growth of Actinobacteria. The addition of pressure to culture conditions appeared to increase the overall percentage of Proteobacteria isolates. The control

group (21% O_2) resulted in the highest abundance and diversity recovered, while lowering the O_2 to 4% resulted in no Firmicutes being recovered but increased the percentage of Actinobacteria isolates. Bacteria cultured under the same atmospheric pressure/O_2 did not appear to be more closely related, or cluster together in terms of 16S rRNA gene similarity. There were, however, species that were unique to each atmospheric condition.

The addition of pressure (21% O/5 bar) reduced the overall number of bacteria cultured, however produced an 'uncultured bacterial clone'. Isolates grown under a low-O_2, pressurised environment (4% O_2/5 bar) included members of *Dermacoccus*, *Kocuria* and *Brevibacterium*. Isolates belonging to the *Micrococcus*, *Micromonospora*, *Mehylobacterium*, 'Uncultured clone Md-9' and *Dietzia* genera were only present in the control group.

The lack of data from 4% O_2 at atmospheric bar in this study prevents a more comprehensive analysis into whether certain isolates were selectively cultured by the combination of low O_2 and pressure. The ability of all isolates to grow in non-pressurised environments once sub-cultured however, demonstrates that none of them require pressure for their growth. It may also be the case that the combination of pressure and low O_2 concentration prevented the growth of competing bacteria in the first instance. Isolates that did not require pressure for their growth may also have grown more favourably under pressurised conditions. Isolates belonging to the psychrotolerant *Psychrobacter* (124) were the most common across all sample treatments; a psychrotolerant microbe that has previously been isolated from a fish processing plant (125) and a deep-sea hydrothermal vent (124).

The sponges used in this study were obtained from depths ranging between 1051-2228m, which is equivalent to ~105-223 atmospheres of pressure. The pressure simulated in this study (5 bar) was equivalent to 4.93 atmospheres, which is representative of a depth of almost 50m. Previous work detailing the range of cellular processes affected by pressure suggest that essential biological processes (in *E. coli*) are not prevented until pressures much higher than this (126). Therefore, it is assumed that many bacterial species associated with *P. carpenteri* and *Hertwigia* sp. may be cultivable at much higher pressures than those used in this study. Further work in assessing the impact of higher pressure on the cultivation of sponge-associated bacteria, and their ability to thrive and survive at such pressures would be of benefit in exploring this, though the practicalities of doing such work may represent a significant hurdle. The pressures at which bacteria were grown here were determined by the pressure capacity of the containers used.

2.4.5 Antimicrobial Screening

A total of 11 (3.32%) of the 331 isolates screened displayed antimicrobial activity. Previous reports of antimicrobial screening vary with respect to sample and methodology. Previous studies from sponges have reported hit rates between 8.4-41% without dereplication strategies (127–129). Previous studies in soil and wastewater have reported hit rates between 1.3-42.4% (130,131). High-throughput studies screening small molecule libraries report a hit rate of ~0.5% (132). Of the 11 isolates that displayed antimicrobial activity, 8 were recovered from *P. carpenteri*. This is perhaps surprising considering the much lower number of isolates obtained from this sponge, compared to the *Hertwigia* sp. samples. The prevalence of active isolates was used to select a sponge for bacterial culture at increased pressure, but it remains

to be seen whether the *P. carpenteri* microbiota contains more bacteria that produce antimicrobial compounds *in vitro*. Observations about the potential composition of the *P. carpenteri* microbiota provided by DTE culture may become relevant if bioactive bacteria cultivated from *P. carpenteri* are found to include members of the rare biosphere. The majority of isolates that displayed antimicrobial activity did so against Gram-positive organisms, while several were also active against *E. coli* NCTC10418. The need for the discovery of novel antimicrobial agents active against Gram-negative organisms is of particular importance, given the lack of available agents effective against drug-resistant members of this group (133). Isolates that appeared to display inhibitory activity towards *E. coli* NCTC10418 were recovered from both sponge species studied here, indicating the value in continued investigation of the bioactive potential of their associated microbiota.

An evaluation of bacterial culture-based methods was carried out for two previously uncharacterised species of the Hexactinellid sponge, revealing a higher number of cultivable isolates from *Hertwigia* sp. and a higher proportion of bioactive isolates from *P. carpenteri*. The use of elevated atmospheric pressure was demonstrated to have an impact on the bacterial genera that were capable of being recovered. Isolates were screened for antimicrobial activity, producing several isolates of interest, active against Gram-positive and Gram-negative bacteria. These have been prioritised for downstream analysis. This study constitutes the first exploration of the diversity and antimicrobial potential of the microbiota from *P. carpenteri* and *Hertwigia* sp. sponges, as well as the use of pressure in culturing bacteria from such samples. It appears that the cultivation of isolates with antimicrobial potential from *P. carpenteri* is more likely than from *Hertwigia* sp. However, there also exist intra-species dissimilarity between

cultivable bacteria from both sponges. Further molecular, microbiome-level investigation would be recommended in order to examine trends in detail. Overall, the isolates obtained herein provide a promising avenue for further investigation and indicate that *Pheronema* sponges are promising targets for the isolation of novel antimicrobial candidates. The 16S rRNA gene sequences generated by this study were submitted to genbank under the accession numbers MZ723441 to MZ723479. A full list of accession numbers can be found in the (**Appendix, Table S2**).

Chapter 3

Purification and characterisation of an antimicrobial agent from a sponge-derived *Streptomyces* sp. strain

3.1 Introduction

3.1.1 Sponge Actinobacteria-derived Antibacterials

The culture of Actinobacteria from sponge samples has been a focal point for many culture-dependent studies (23,29–35). Historically, soil-derived Actinobacteria have been a prolific source of antimicrobial compounds (14). With regards to sponge-associated antimicrobials, the Actinobacteria have also been shown to be a major source of antimicrobials. A survey of antibacterial compounds isolated from sponge-derived bacteria revealed that they have thus far been the most prominent source (~21%) (1). This is likely to be due to a combination of their natural propensity for production of antimicrobials and/or secondary metabolites and the number of culture-dependent studies that have focused specifically on their isolation.

Sponge-associated Actinobacteria that have previously been cultivated from sponges belong largely (38.5%) to the genus *Streptomyces* spp. **(Figure 3.1)**. A similar trend has been reported for the *Actinobacteria* genera responsible for production of antibacterial agents (**Figure 3.1 Inset**).

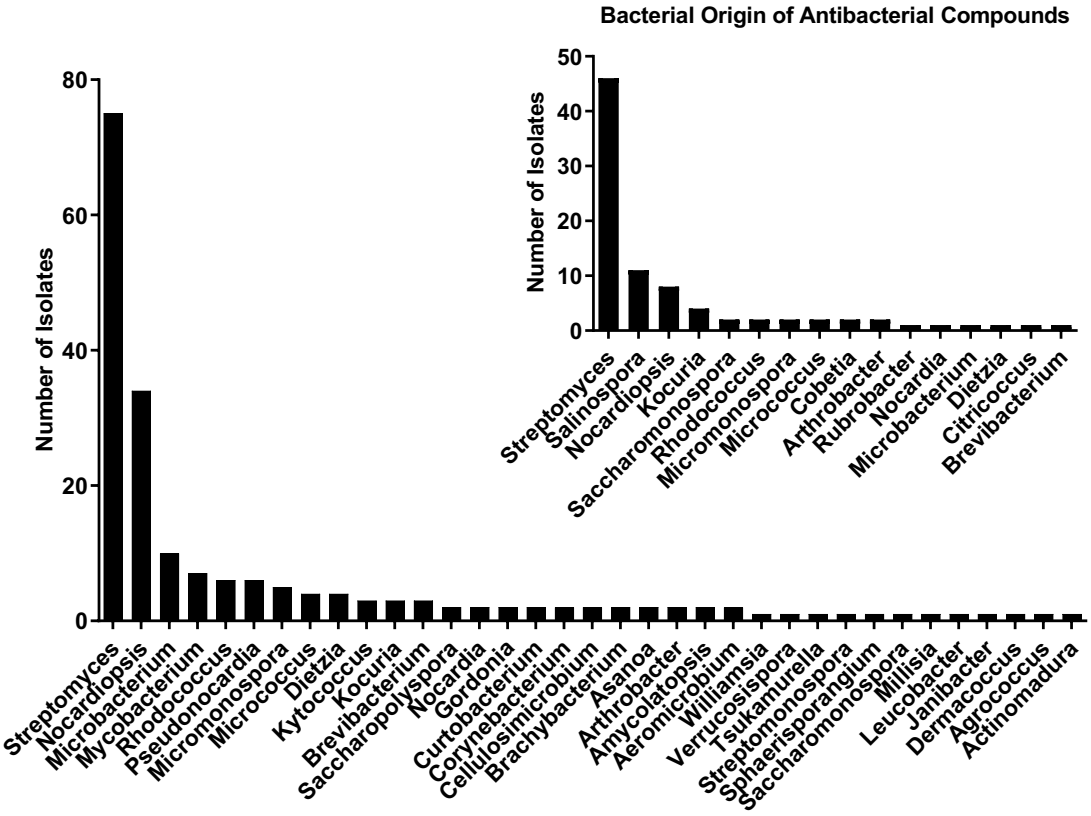

Figure 3.1 – Number of bacterial sequences deposited to NCBI for cultivated Actinobacteria from sponge samples. Search criteria: (((sponge* or porifera*) and (cultured* or cultivated*) NOT (uncultured* or uncultivated*))) AND "actinobacteria". **Inset:** Number of Sponge Actinobacteria-derived antibacterial compounds reported by Indraningrat, Schmidt & Sipkema (1).

3.1.2 Antibacterials from Sponge-derived *Streptomyces* spp. isolates

Previous antimicrobials isolated from sponge-derived *Streptomyces* sp. include Mayamycin (28), a cytotoxic polyketide with demonstrated activity against both microbes and human cancer cell lines. The siderophore 2-pyrrolidine isolated from a sponge *Streptomyces* sp. displayed weak antimicrobial activity against both Gram-negative and Gram-positive organisms (MIC 400-700 μg/mL) (134). Streptophenazines A-H were purified from fermentation cultures of a sponge-derived

Streptomyces sp. (135). Reiner et al. in 2015 reported the elucidation of a napthacene glycoside given the title of SF2446A2 that displayed the ability to inhibit chlamydia proliferation in HeLA cells (136). Several antibacterial agents of the Antimycin family were isolated from a marine sponge-derived *Streptomyces* sp. Purified fractions were found to inhibit *Bacillus subtilis* with MICs ranging from 7.47-400 µg/mL (137).

The list of examples provided here may not be exhaustive, however represents those reported in the literature at time of review, to the best of the author's knowledge.

3.1.3 Culture-dependent vs. Culture-independent Antimicrobial Detection

With regard to the culture of microorganisms, the widely accepted 'Great Plate Anomaly' phenomenon suggests that 99% of bacterial species present in environmental samples are recalcitrant to cultivation (102). Whilst considerable efforts have been made to widen the diversity of cultivable bacterial isolates (103,138), the fact remains that the vast majority of bacterial species remain uncultivable under normal laboratory conditions (139) - thereby limiting the number of available strains that may be screened for antimicrobial agents. The use of Next-Generation Sequencing (NGS) for the purpose of genome-mining has also been used to identify potentially novel secondary metabolites (140,141). The use of genome mining in order to identify potential candidates, whilst providing an insight into the antimicrobial potential of a particular sample does not lead directly to the isolation of the antimicrobial agent in question. Similarly, it is unknown upon the detection of an antimicrobial candidate within a genome whether it will exhibit the predicted action (based on homology to known agents) *in vitro*, once isolation, recombinant expression or synthesis has been achieved (142). By sequencing the isolate of interest derived from culture-dependent studies, clues can be obtained as to the identity, mechanism

of action and methods that could be used for the improved antimicrobial production from bacterial strains.

The use of online tools for the prediction of BGCs can be combined with laboratory-based investigations for a more complete and multi-faceted approach to determine the identity of potential drug candidates. Pursuing each avenue of enquiry in tandem helps to provide an earlier indication as to whether the candidate is worth further investigation.

3.1.4. Protease Inhibitors in *Streptomyces*

Protease inhibitors are molecules that inhibit the enzymatic breakdown of proteins. They are divided into 48 families that are each in turn grouped according to the mechanism of protease they inhibit (e.g. serine, cysteine or metalloprotease inhibitors) (143). Protease inhibitors have been previously investigated for their capacity as anti-cancer, antimicrobial and broadly applicable industrial agents (144–146). More recent work has examined the possibility for the repurposing of currently available anti-viral protease inhibitors for treatment of SARS-CoV-2 infection (147). Efforts have thus been made at screening libraries of *Streptomyces* for the isolation of novel protease inhibitors (148).

Cellular differentiation in the growth cycle of *Streptomyces* sp. is a complex and highly regulated process (5,149). Proteases and protease inhibitors are key players in the transition from substrate mycelium to the growth of aerial hyphae (150,151) – a process regulated by the *bld* and *whi* regulatory systems in response to nutrient limitation (152,153) (**Figure 3.2**).

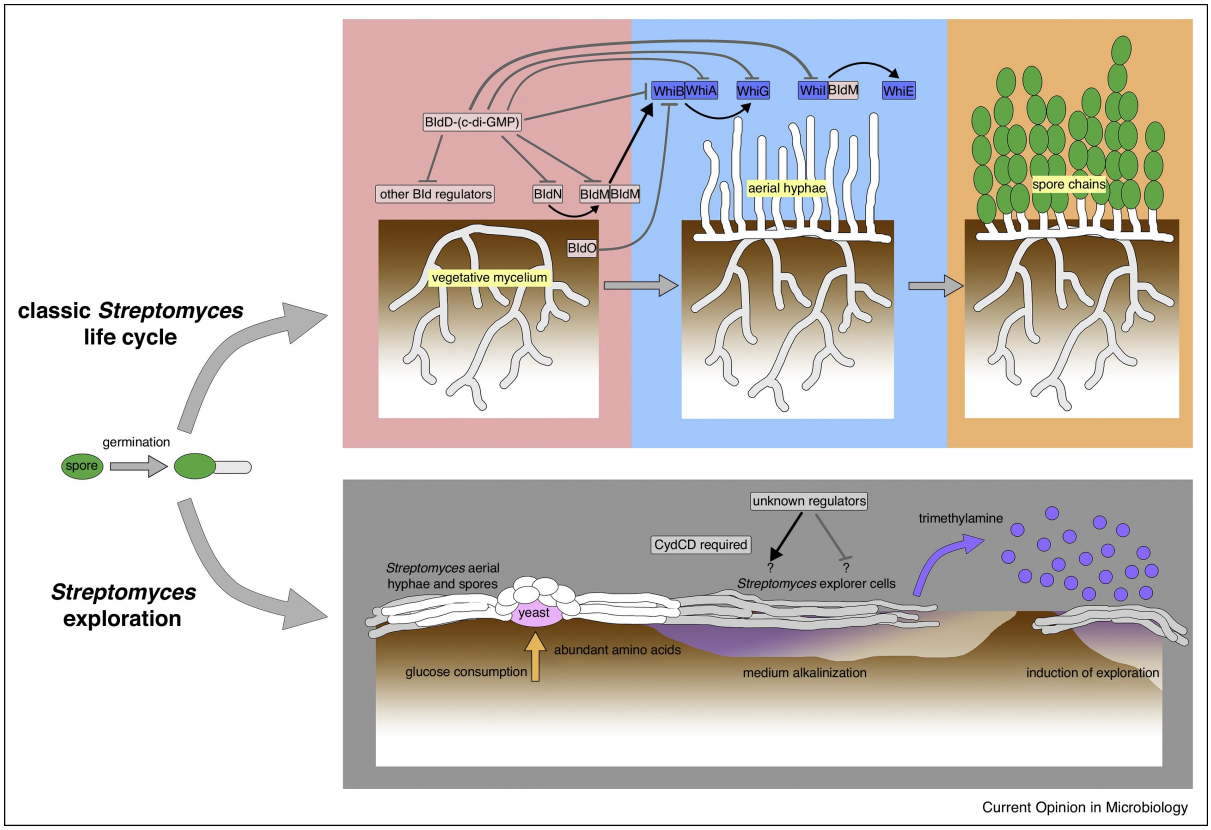

Figure 3.2 – Factors regulating the formation of aerial hyphae development in *Streptomyces* sp. (5). Text in rectangular boxes represent genes involved in the signalling pathways indicated in the regulation of the formation of aerial hyphae, and signalling factors involved in the same process

The production of extracellular proteases, and in turn the inhibitors that inactivate them is thought to be involved in several processes governing aerial hyphae production (151). These processes include the degradation of substrate mycelium (154,155), the regulation of transglutaminases (156) and SapB activation – a biosurfactant lanthipeptide that is essential for hyphae formation in certain *Streptomyces* sp. (157).

The work in this chapter aimed to purify and characterise the agent responsible for the antimicrobial activity demonstrated by a bacterial isolate obtained from the culture-dependent work outlined in **Chapter 2**. In addition, the work outlined here aimed to

identify the isolate in question and reveal information about its potential for the production of secondary metabolites. The investigation of this isolate consisted of fermentation, secondary metabolite purification using reverse-phase chromatography, minimum inhibitory concentration (MIC) assessment. The use of whole-genome sequencing was also carried out in order to identify the isolate and predict secondary metabolite production using *in silico* mining tools. Information obtained from *in silico* mining was also used to predict the identity of the purified agent as well as it's mechanism of action and supported work to determine its biological activity as a protease inhibitor.

3.2 Materials & Methods

3.2.1 Sample Collection and Processing

Sponge tissue processing, plating for culture-dependent work and antimicrobial screening were carried out according to **Chapter 2.** The isolate described herein, strain A11, was obtained from Sponge_125 via culture on R2A + 0.2g/L carnitine hydrochloride.

3.2.2 DNA Extraction & Genome Sequencing

Two replicate streak-plates plates of strain A11 were gown using R2A media. DNA was extracted from colonies from the first streak-plate using the DNeasy Powersoil kit (Qiagen, UK) as per manufacturer's instructions. DNA was eluted in 50 µL nuclease-free water. Library preparation for MinION sequencing was carried out using the Oxford Nanopore Ligation Sequencing Kit (SQK-LSK109) and quality assessed using a Qubit fluorometer according to the barcoding kit instructions. DNA was sequenced in-house using the MinION sequencing platform. Satisfactory flow cell performance

was confirmed prior to sequencing as part of the built-in pre-run check using the MinKnow software. All of the bacterial biomass was taken from the second streak-plate and sent to MicrobesNG (UK) for Illumina whole-genome sequencing using the 'Standard Whole Genome Service' and preservative beads that they supplied: https://microbesng.com/our-services/. Genomic reads were provided by MicrobesNG in the form of 2x250bp paired-end reads with associated quality score data.

3.2.3 Antimicrobial Screening & Growth Curve Determination

Antimicrobial activity was detected for isolate A11 using the agar-plug diffusion method as a primary screen (158). Cotton swabs were dipped into 1 mL cell suspensions of the indicator organism (Indicators used: *Micrococcus luteus:* OD_{600}: 0.14-0.16; *Escherichia coli* NCTC10418*:* OD_{600}: 0.08-0.1) and swabbed over the surface of individual agar plates (TSB Agar) in order to create a 'lawn' of the indicator organism. An agar plug was taken from around the base of a 3-day colony of A11 using a sterile scalpel. The agar plug was placed onto the plate containing the indicator lawn and incubated for 18hr at 37°C to allow growth of the indicator organism. The presence of antimicrobial activity was assessed by the presence of a zone of inhibition around the agar plug.

For production in liquid culture, bacterial suspensions were placed in 10 mL Marine Broth, ½ Marine Broth, TSB and LB at an optical density of 0.100 (OD_{600}) in order to assess the impact of culture conditions and nutrient availability on the rate of antimicrobial production. Cultures were incubated at 20°C, 120rpm for a total 4 days and 50µL was taken every 24hrs for antimicrobial testing. The production of an antimicrobial agent was assessed by well diffusion assay: 13.5 mL cooled molten LB Agar was added to 1.5 mL suspension of the indicator organism (*M. luteus*: $0D_{600}$ 0.5;

E. coli: OD_{600} 0.4) and the agar poured into a petri dish. Once dried, uniform wells (5mm diameter) were made in the agar plate using a vacuum-pump (**Figure 3.3**) and 50 µL supernatant was added to each well. Plates were incubated at 37°C.

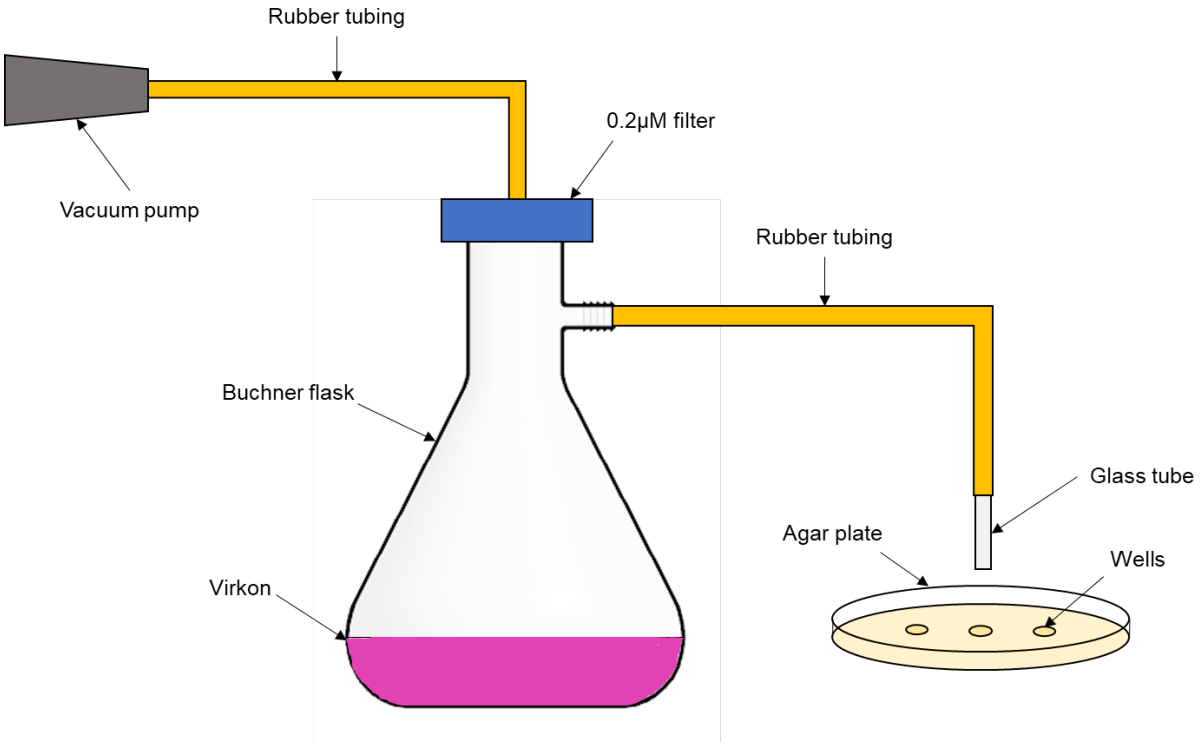

Figure 3.3 – Graphical representation of the apparatus used to create wells in agar diffusion plates

Aliquots (3 x 100µL) of the 10 mL cultures were also taken every 24hrs for dilution and CFU/mL counting (159). Broth cultures for CFU counts were centrifuged (4696*g*, 20min) and the supernatant was transferred to sterile Eppendorfs. CFU/mL counting was performed using 10-fold dilutions on R2A agar plates that were incubated at 20°C.

3.2.4 Fermentation and Purification of antimicrobial compounds

Scale-up of bacterial growth and antimicrobial production was carried out using the culture media demonstrated to result in the highest rate of antimicrobial production

(LB, Miller). A 50 mL starter culture was grown for 3 days before being added to 450 mL broth of the same culture media (final volume: 500 mL). The 500 mL cultures were then re-incubated for a further 3 days. Broth was then centrifuged (8500 *g*, 40 min). The supernatant was filtered through a 0.2μm filter to remove bacterial cells/spores and kept for downstream purification.

A 50 μL aliquot of supernatant was tested by well diffusion to assess the presence of antimicrobial activity. The supernatant was then pH adjusted to pH 6.0 with the use of HCl and 50 μL was assayed by well diffusion to confirm that the antimicrobial activity was not altered as a consequence of the pH adjustment. The remaining supernatant was passed through a Strata–C18E column (Pheromenex. UK) and eluted in 4x15 mL aliquots of 50%, 70% and 90% MeOH with 0.01% (v/v) Trifluoroacetic Acid (TFA). Each 15 mL elution was assayed for the presence of antimicrobial activity using the well assay method described above. In the case that multiple fractions displayed antimicrobial activity, all active fractions were combined and concentrated to a volume of 5 mL using the Biotage V-10 Touch evaporator (Biotage, Sweden).

The MeOH/TFA eluent demonstrated to possess antimicrobial activity was injected into a second C18 column (Biotage® SNAP Ultra C18, 12g) and eluted with a linear gradient of 5-50% Acetonitrile with 0.01% (v/v) TFA (t=26m) in water using the Biotage® Isolera. Fractions were collected based on UV detection (λ: 200-400nm) with a minimum detection threshold of 10mAU. Aliquots (50 μL) of each fraction were assayed for antimicrobial activity via well diffusion assay.

The antimicrobial fraction demonstrated to possess antimicrobial activity from the second round of C18 chromatography was injected into a size exclusion column (Superdex 200 10/300 GL) and fractionated using the Äkta Pure (GE Healthcare Life Sciences). Sample fractionation was based on UV detection at wavelengths of 220, 254 and 280mn with a minimum detection threshold of 10mAU. Fractions were eluted in 150mM NaCl saline solution. Fractions were assayed for antimicrobial activity via well diffusion assay. Solvent/eluent controls were included for each chromatography fractionation in order to eliminate the occurrence of false positives.

LC/MS analysis was performed by researchers at the University of Bristol on an LC/MS Waters 2767 Autosampler, Waters 515 HPLC Pump, Waters 2998 Photodiode Array Detector, Waters 2424 ELS Detector and a Waters Quattro Micro Mass Spectrometer. A 20µL sample was injected into a Phenomenex Kinetex C18 column (250mmx4.6mm) and eluted across a linear gradient of 5-95% ACN + 0.05% formic acid (t=30min). Spectra were visualised in MassLynx (Waters, US).

3.2.5 Pierce BCA Protein Quantification Assay

Quantification of the concentration of purified antimicrobial agent was carried out using a Pierce BCA Protein Quantification Assay according to the manufacturer's instructions, using the standard working range of 20-2000 µg..

3.2.6 Minimum Inhibitory Concentration (MIC) Testing

MIC testing was performed in 96-well microtitre plates according to the broth microdilution method outlined by Weigand, Hilpert & Hancock (160). Antimicrobial agent was tested between the concentrations of 32-1 µg/mL. Müller-Hinton II Broth (Sigma) was used for all antimicrobial screening.

3.2.7 *Galleria mellonella* Toxicity Screening

Larvae were purchased from Livefoods UK Ltd (Somerset, UK) and stored in the dark at 4°C for up to 7 days with no food. Larval injection was carried out as per Hesketh-Best et al. (161). Larvae were injected with 10µL antimicrobial test compound suspension (in PBS) in the left penultimate foreleg using a 50µL Hamilton 750 syringe (Hamilton Company, UK). Syringes were cleaned between each injection using 3 x 50µL washes with sterile dH_2O, 3x 50µL washes of 70% ethanol, and a final 3 x 50µL washes of dH_2O. The control group was injected with 10µL sterile PBS in order to account for physical stress incurred by injection. After injection, larvae were kept in the dark at 37°C for a total of 5 days and visually inspected at 24hr intervals for signs of melanisation and death.

3.2.8 Hybrid Genome Assembly & Genome Analysis

Short A11 reads obtained by sequencing using the Illumina platform (MicrobesNG, UK) were aligned with long reads obtained from in-house MinION sequencing (Oxford Nanopore, UK) using Unicycler (162) in order to obtain a hybrid assembly. Oxford Nanopore fast5 files were base-called using Guppy basecaller using standard parameters. Concatenated fastq files for A11 were quality-filtered with NanoFilt using a quality cutoff of Q11. A histogram for the length and quality of sequencing reads is displayed within **Appendix, Figures S5; S6**. Samples were de-multiplexed using porechop with standard parameters.

A full protocol for the hybrid assembly procedure can be found at https://galaxyproject.github.io/training-material/topics/assembly/tutorials/unicycler-assembly/tutorial.html#assembly-with-unicycler. The hybrid whole-genome assembly was submitted for identification using BLASTn using the nr/nt database. The assembly was then aligned to the top BLAST hit using the ‘progressiveMauve’ algorithm (163)

using standard parameters. The aligned A11 sequence was mined for the presence of BGCs using AntiSMASH (164). Open Reading Frames (ORFs) were assigned 'identities' (**Table 3.4**) from the nr/nt NCBI database using BLASTn.

3.2.9 Protease Inhibition Assays – Skim Milk Plates

Skim Milk Agar plates were made (skim milk powder,10g/L, Agar, 15g/L) (165). Uniform wells were created using the vacuum pump previously described and 50µL trypsin (100 µg/mL) was combined with 50µL test compound (90 µg/mL, final concentration: 45 µg/mL) in each well. Antipain+Trypsin was used as a positive control for protease inhibition. Epidermicin+Trypsin was used as an internal negative control. Trypsin (50µL; 100 µg/mL) was used as a protease control. Plates were incubated at 37°C and assessed for protease inhibition after 1 hour. The trypsination of milk proteins was assessed by measuring the presence of a zone of clearance, or degradation around the well. Protease inhibition was measured by a reduction or lack of a zone of degradation.

3.2.10 Protease Inhibition Assays – BAPNA Microplate Assay

Inhibition of the trypsination of Na-Benzoyl-DL-Arginine-p-Nitroanilide (BAPNA) by **C-A11** was measured. Trypsin cleaves BAPNA to produce Na-Benzoyl-DL-Arginine and p-Nitroaniline. The amount of p-Nitroaniline in solution can be detected by measuring the absorbance of light at a wavelength of 410 nm (166).

Aliquots (50µl) of test compounds – either: Antipain dihydrochloride (0.1M Tris-HCl Buffer, pH 8.2); Epidermicin (0.1M Tris-HCl Buffer, pH 8.2); or C-A11 (0.1M Tris-HCl Buffer, pH 8.2) were placed into wells (in triplicate) of a 96-well microplate, at

concentrations of 90, 45, 22.5 and 11.25 µg/mL (**Figure 3.4**). Then, 50µL 1 mg/mL trypsin (0.1M Tris-HCl Buffer, pH 8.2) was added into each well, to give a final concentration of 500 µg/mL. Final concentrations of test compound were 45, 22.5, 11.25 and 5.5125 µg/mL. These concentrations were determined by the amount of **C-A11** that was able to be generated from purification. Each concentration of test compound was also added to 3 separate wells, into which 50µL of buffer (0.1M Tris-HCl Buffer, pH 8.2) was added as a 'no trypsin' control and 100µL of buffer was placed into 3 separate wells as a buffer/negative control or 'blank'. The positive control was 50µl of buffer and 50 µl of trypsin (1 mg/mL), which was also placed into 3 separate wells. Plates were subjected to a 15m pre-incubation step at 37ºC, 130rpm after which 50µl of 0.1mM BAPNA (0.1M Tris-HCl Buffer, pH 8.2) was pipetted into each well of the 96-well plate. The absorbance of each well at 410 nm was read at 1min intervals over a 30min time period, with continuous incubation at 37ºC using a SPECTROstar® Omega microplate reader (BMG Labtech, Germany).

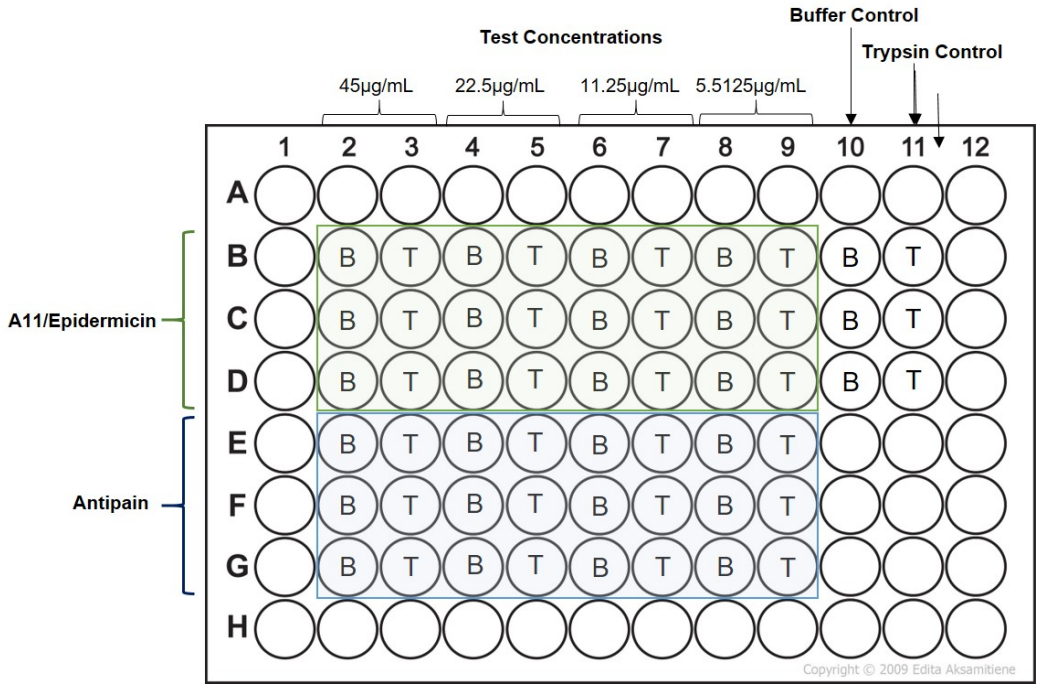

Figure 3.4 – Diagram (produced by the author) to represent the set-up of microtitre-plate protease inhibition testing. B refers to Buffer. T refers to Trypsin.

The percentage inhibition caused by **C-A11 (**45 µg/mL) was calculated using:

$$PI = 100 - ((T \times 100) \div C),$$

where PI = percentage of inhibition, T = mean absorbance of the treated sample and C = mean absorbance of the control sample (167).

3.3 Results

3.3.1 Isolate Growth and Identification

Isolate A11 was obtained during the culturing of bacteria from *Pheronema carpenteri*, using R2A media (Oxoid) incubated at 20°C. Isolate A11 appeared as a dull grey/purple colony. Formulation of aerial mycelium and sporulation was observed when the isolate was cultured on low-nutrient media such as R2A or Oatmeal Agar (**Figure 3.5**). A11 was capable of growth on solid media prepared with seawater, however it did not require it for growth. DNA extracted from Isolate A11 was sequenced using both the Oxford Nanopore (in-house) and Illumina platforms (MicrobesNG, Birmingham) (Methods). A hybrid assembly was constructed from both sequences using Unicycler (162) (**Table 3.1, next page)**.

Table 3.6 – Genome statistics for reads obtained from each sequencing platform. N50 refers to average read length as opposed to median. All lengths given in base pairs.

	Oxford Nanopore	Illumina (2x paired-end)	Hybrid Assembly
Contigs	101	819765	434
Read length (N50)	63650.2	199.3/186.4	19910.62
Summative Length	6428674	163398705/152787854	8641208
GC Content	70.69	70.26/70.2	71.61%

Despite the increase in number of contigs from 101 to 434 as a result of hybrid assembly, the assembly was judged to represent a more complete genome owing to its size as well as 'max score' and similarity to hits obtained using BLASTn. Information on the top BLASTn results for both Oxford Nanopore and Illumina genomes are displayed in **Appendix, Table S3**). The hybrid assembly of A11 was submitted to BLASTn (**Figure 3.5**), revealing the highest overall sequence similarity to *Streptomyces* sp. 3211.

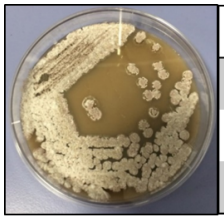

Identity (#1; #2; #3)	QC (%)	Identity (%)	Max Score	Total Score	E-Score
Streptomyces sp. 3211	75	92.38%	69549	9.66E+06	0
Streptomyces sp. Sge12	75	91.91%	50122	9.62E+06	0
Streptomyces venezuelae strain ATCC 21018	71	93.85%	46928	8.93E+06	0

Figure 3.5 – Picture (left): Isolate A11 grown on Oatmeal Agar. Table: Top 3 BLASTn hits obtained using the draft genome sequence. 'QC' refers to Query Cover of top BLASTn hit. 'Identity' refers to identical nucleotide site match with highest BLASTn hit. 'Max Score' refers to highest alignment score of a particular genome segment. Total

score refers to the sum of the alignment scores of all segments. E-Score refers to number of hits expected at that level of identity (score) by chance.

The assembly was aligned to the top BLASTn hit (*Streptomyces* sp. 3211) using the progressive mauve algorithm (**Figure 3.6, next page**), displaying conservation of large genomic regions despite the high number of contigs obtained for A11.

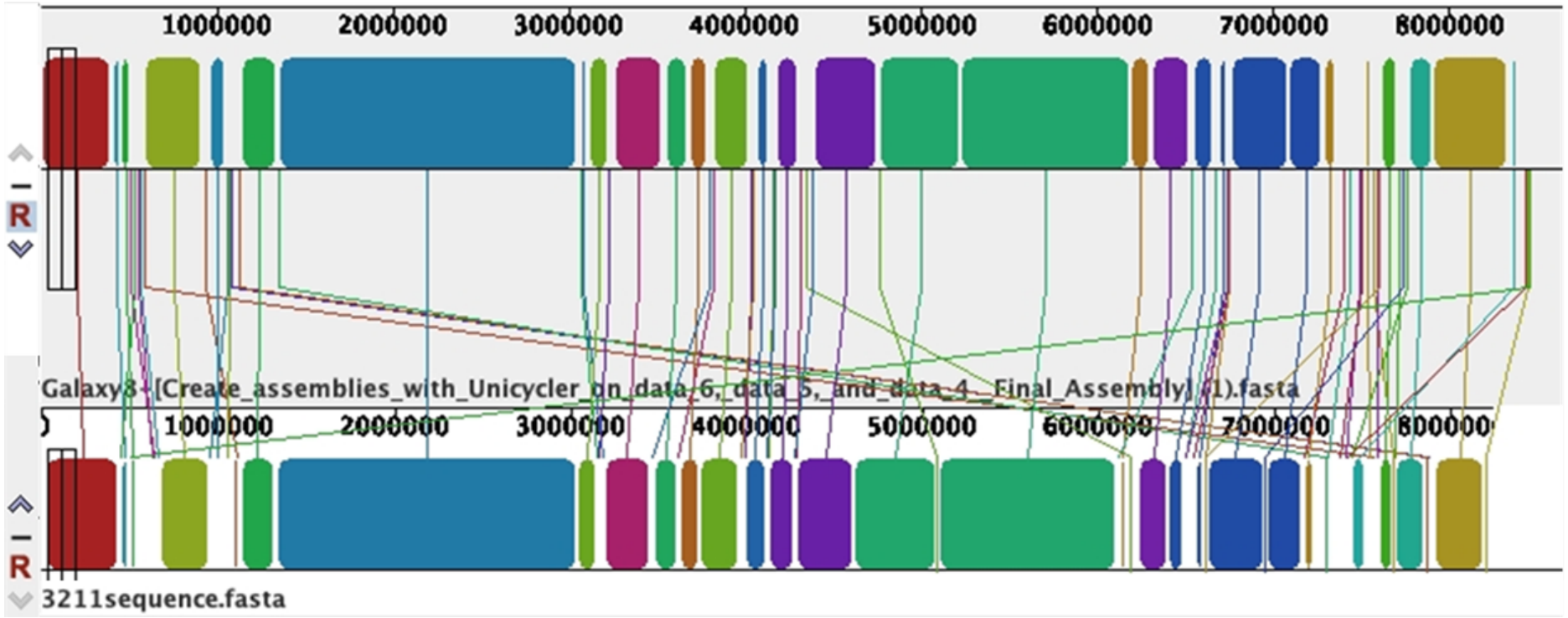

Figure 3.6 – Mauve alignment of A11 with *Streptomyces* sp. 3211. Upper alignment displays contigs for A11. Lower alignment displays contigs for *Streptomyces* sp. 3211. Lines show position of each region in each genome.

The alignment was submitted for BGC detection using antiSMASH v5.0 (164). Use of antiSMASH software facilitated identification of 31 biosynthetic gene clusters (**Figure 3.7, next page**).

Region	Type	From	To	Most similar known cluster		Similarity
Region 1	ectoine	161,327	171,695	kosinostatin	NRP + Polyketide	8%
Region 2	butyrolactone , NRPS-like	200,360	246,189	lactonamycin	Polyketide	10%
Region 3	NAPAA	318,479	352,231	chalcomycin A	Polyketide	4%
Region 4	CDPS	354,991	375,731			
Region 5	T3PKS	424,930	465,859	alkylresorcinol	Polyketide	100%
Region 6	siderophore	508,250	519,962			
Region 7	melanin	597,439	624,391	istamycin	Saccharide	4%
Region 8	terpene	630,739	650,618	monensin	Polyketide	5%
Region 9	terpene	778,636	798,611	ebelactone	Polyketide	5%
Region 10	PKS-like	916,344	957,399	colabomycin E	Polyketide:Type II	4%
Region 11	NRPS-like	1,020,013	1,062,367	deimino-antipain	NRP	33%
Region 12	lanthipeptide-class-ii	1,066,999	1,089,209			
Region 13	lanthipeptide-class-iii	1,091,574	1,114,219			
Region 14	hglE-KS	1,485,114	1,531,692			
Region 15	terpene	1,603,901	1,630,416	hopene	Terpene	61%
Region 16	terpene	1,994,783	2,016,999	toxoflavin / fervenulin	Other	10%
Region 17	RiPP-like	2,122,632	2,131,562			
Region 18	NRPS	2,195,051	2,255,362	paenibactin	NRP	66%
Region 19	siderophore	2,496,779	2,504,891			
Region 20	RRE-containing , NRPS , NRPS-like	4,242,766	4,324,890	friulimicin A / friulimicin B / friulimicin C / friulimicin D	NRP	21%
Region 21	butyrolactone	4,967,036	4,977,212	methylenomycin A	Other	9%
Region 22	furan	4,980,952	5,002,160	colabomycin E	Polyketide:Type II	15%
Region 23	siderophore	5,445,655	5,456,534	desferrioxamin B	Other	100%
Region 24	NRPS	5,555,744	5,599,529	BE-43547A1 / BE-43547A2 / BE-43547B1 / BE-43547B2 / BE-43547B3 / BE-43547C1 / BE-43547C2	NRP:Cyclic depsipeptide + Polyketide:Modular type I	13%
Region 25	RiPP-like	5,939,316	5,949,771			
Region 26	butyrolactone	7,187,366	7,196,115	sanglifehrin A	NRP + Polyketide	4%
Region 27	T1PKS , NRPS	7,327,065	7,389,899	coelichelin	NRP	72%
Region 28	NRPS-like , NRPS	7,429,859	7,496,532	JBIR-126	NRP	92%
Region 29	T2PKS	7,929,435	8,001,929	spore pigment	Polyketide	58%
Region 30	NRPS	8,491,088	8,548,503	vazabitide A	NRP	30%
Region 31	siderophore , butyrolactone	8,577,649	8,595,787	leinamycin	NRP + Polyketide:Modular type I + Polyketide:Trans-AT type I	2%

Figure 3.7 – antiSMASH output displaying hits present in the A11 hybrid assembly. Colours in the left-hand column are generated by antiSMASH and are related to the ‘type’ of BGC, as listed in the second column.

3.3.2 Antimicrobial Screening

Strain A11 was tested for antimicrobial activity against *M. luteus,* MRSA NCTC12493 and *E. coli* NCTC10418 using the agar-plug method. Zones of inhibition were measured as 3mm against *M. luteus*, 3mm against MRSA and 1mm against *E. coli*. The antimicrobial activity of A11 in liquid culture was assessed using Marine Broth, ½ Marine Broth, TSB and LB. Antimicrobial activity was detected after 72 hours of growth in both LB and TSB media (**Figure 3.8)**. Zone sizes were recorded as 1mm for both media. No antimicrobial activity was detected in either broth after a further day of incubation. LB broth was selected for scale-up and downstream purification due to its low complexity.

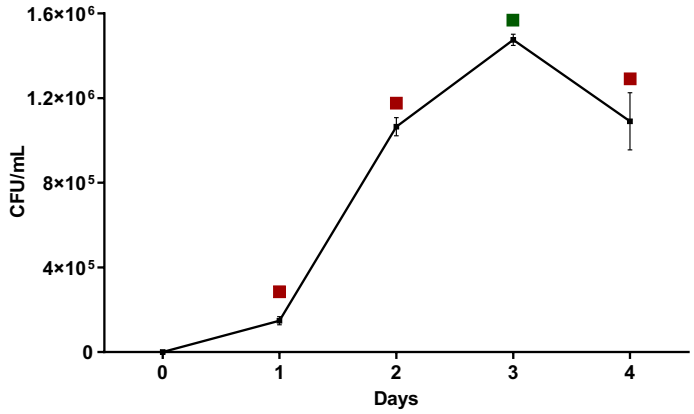

Figure 3.8 – Growth curve of isolate A11 in LB broth. Detection of antimicrobial activity against *Escherichia coli* NCTC 10418 in liquid culture indicated by coloured squares. Red: no activity detected. Green: activity detected.

3.3.3 Purification and LC/MS of C-A11

A 500 mL 3 day LB culture of A11 was fractionated using a combination of reverse-phase C18 and size exclusion column chromatography. Presence of antimicrobial activity in the eluted fractions was assessed by well-diffusion. The presence of antimicrobial activity (designated **C-A11**) was detected in SNAP Ultra C18 column

fractions eluted between 14-21% ACN+0.01% TFA. These active fractions were injected into the Äkta pure system and eluted from a 10/300 GL Size Exclusion Column with a retention time of 20.60m. The active fraction was re-injected for 2 subsequent rounds of size exclusion purification in order to remove impurities (**Figure 3.9, next page**).

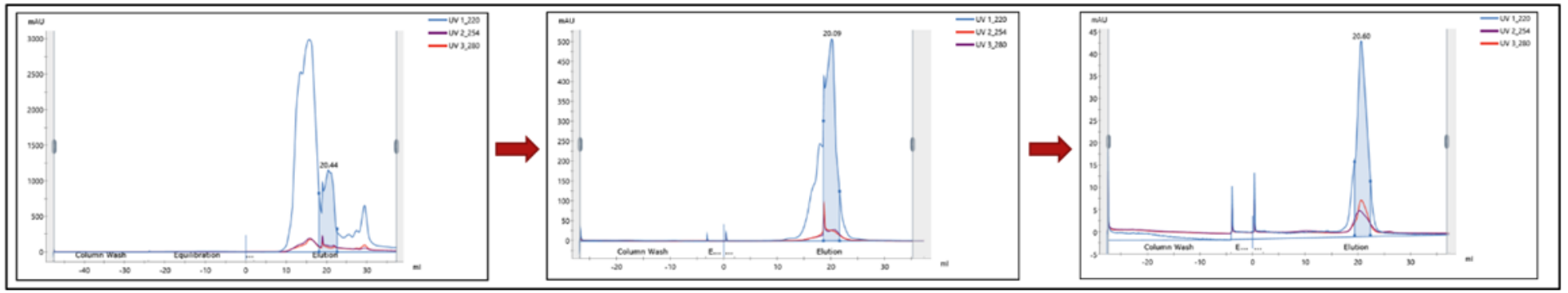

Figure 3.9 – Subsequent rounds of injection of the strain A11 active fractions into the Akta pure system for size exclusion chromatography. Highlighted blue section represents the antimicrobial containing fraction as confirmed by well diffusion assays, measured at a UV wavelength of 220 nm.

The purified agent obtained from FPLC was suspected to be proteinaceous in nature due to the absorbance spectra as measured at 280, 254 and 220 nm. The active fraction obtained after FPLC purification was analysed using LC/MS (**Figure 3.10**).

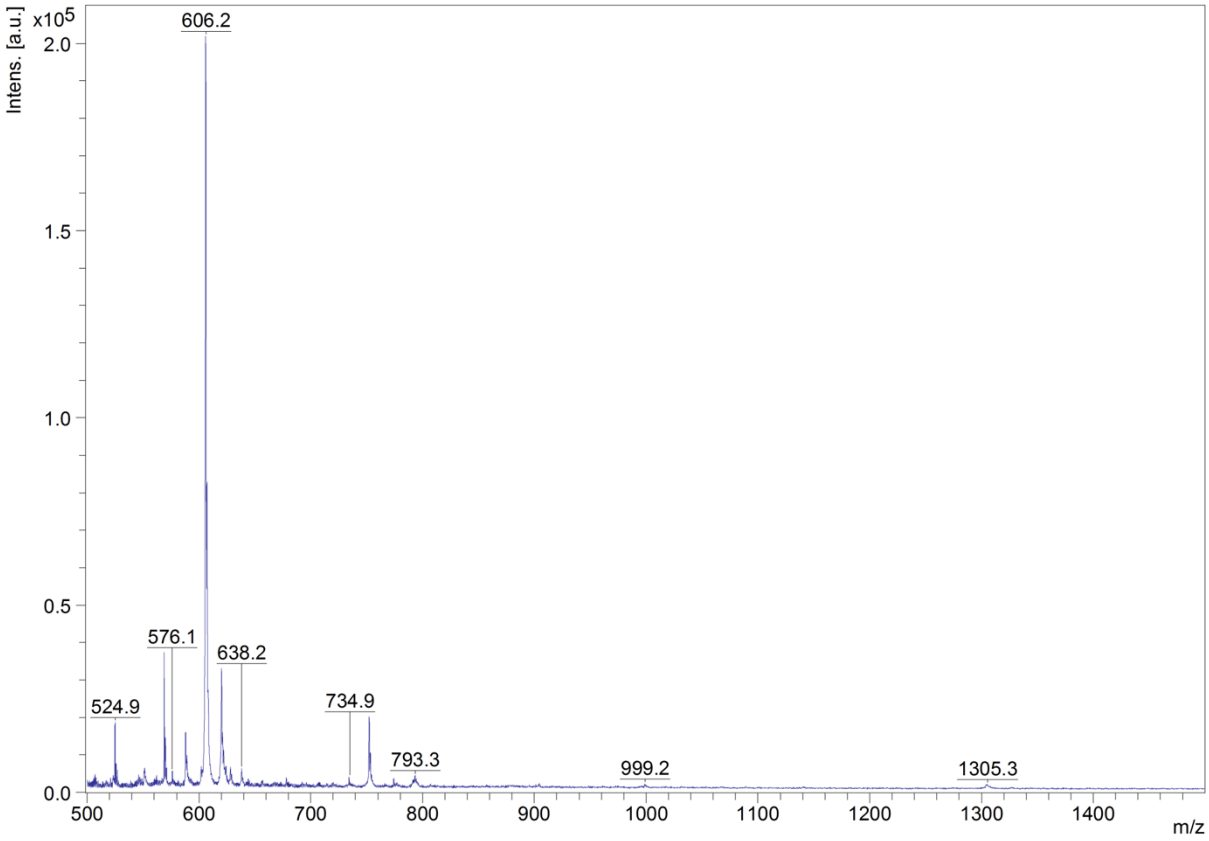

Figure 3.10 – LC/MS absorbance spectra for **C-A11**. Numbers above peaks represent *m/z* values.

The major component present in the LC/MS sample was determined to have an *m/z* of 606.2.

The concentration of **C-A11** in the purified fraction was determined to be 90 µg/mL using a Pierce BCA Protein Quantification Assay.

3.3.4 Inhibitory Concentration Testing

The MIC and Minimum Bactericidal Concentration (MBC) for **C-A11** were determined according to Weigand, Hilpert & Hancock (160) (**Figure 3.11, next page**). MIC values are given as the well treated with the lowest concentration of C-A11 (μg/mL) that differed significantly from the growth control when measured at OD_{600} as measured by t-test. MBC values are given as the well treated with the lowest concentration that did not produce any CFU when plated onto solid growth media after 20hrs of incubation. The MIC for **C-A11** was demonstrated to be between 2-16 μg/mL, with the lowest MIC against *Pseudomonas aeruginosa* PA01 (2 μg/mL). The MBC for **C-A11** was demonstrated to be 16 μg/mL for all indicator strains tested.

A

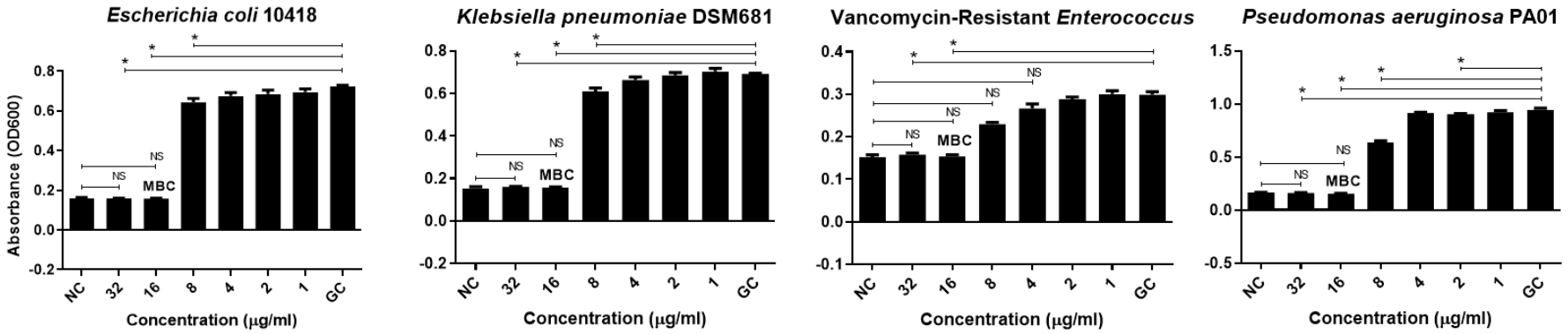

B

MHB	*E. coli* 10418	*K. pneumonia* 681	VRE	*P. aeruginosa* PA01
MIC (µg/mL)	8	8	16	2
MBC (µg/mL)	16	16	16	16

Figure 3.11 – A) Graphs displaying OD_{600} of cultures treated with C-A11. MIC and MBC indicated on graph**. B)** Table of C-A11 MIC/MBC figures. Bars represent Standard Error. Significance determined by t-test. GC refers to Growth Control (no inhibition). NC refers to Negative Control (no cells).

3.3.5 *Galleria mellonella* Toxicity Assay

An *in vivo* concentration of 160 μg/mL **C-A11** was injected into 10 *Galleria mellonella* wax moth larvae. Larvae were monitored for signs of melanisation and/or death over a 5 day period, with the test group displaying 80% survival compared to the control group, which were injected with 10μL PBS in order to account for the trauma of injection (**Figure 3.12**). This indicates that at *in vivo* concentration of 10-20 x MIC, the LD_{50} was not reached.

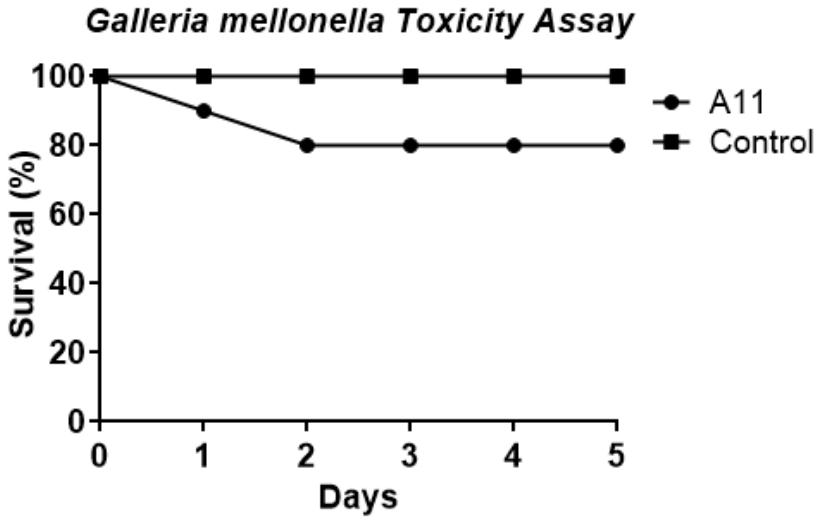

Figure 3.12 – *In vivo* toxicity assay for **C-A11**.

3.3.6 C-A11 Identity Prediction

A literature search was performed in order to cross-reference compounds present in the A11 antiSMASH analysis with the *m/z* value and antimicrobial activity data obtained for **C-A11**.

A total of 2 of the 31 products listed in the antiSMASH analysis had previously been described as having an antimicrobial effect against both Gram-positive and Gram-negative organisms. A third product had no previously reported antimicrobial activity yet had a highly similar *m/z* value. The 3 agents are listed in **Table 3.2** along with their described *m/z* values.

Table 3.2 – Cross-referencing antiSMASH analysis for stain A11 vs. literature-derived information for similarly sized compounds.

antiSMASH ID	*m/z*	Activity	Organism	Reference
Deimino-Antipain	606.3	NA	*Streptomyces albulus* NRRL B3066	(6)
BE-43547 A1-C2	607.4	G+/G-	*Streptomyces arenicola* CNR107	(168)
Kosinostatin	617	G+/G-	*Micromonospora* sp. TP-A0468	(169)

The similarity of the *m/z* value of **C-A11** (606.2) to that of deimino-antipain (6), provided the basis for further investigation of **C-A11**, and its potential bioactivity as a protease inhibitor.

Of the 31 BGCs detected in A11, 5 were also present in the genome of *Streptomyces albulus* NRRL B-3066 (**Table 3.3**). The strain *S. albulus* NRRL B-3066, as will be discussed, is the isolate from which the closest homologue to **C-A11** is suspected to have been first identified in (6).

Table 3.3 – BGCs present in the genomes of both A11 and *S. albulus* NRRL B-3066, detected by AntiSMASH.

BGC	Type	Length (bp)	Conserved Regions
Istamycin	Melanin	26,953	4%
Desferrioxamin B/E	Siderophore	10,880	100%
Hopene	Terpene	26,516	61%
Alkylresorcinol	Type 3 PKS	40,930	100%
Deimino-antipain	NRPS-Like	42355	33%

The identities of ORFs identified by antiSMASH as encoding deimino-antipain were confirmed using BLASTp. The co-occurrence of these regions in the genomes most similar to A11 were also explored (**Figure 3.13**). Information on the third most similar genome (*Streptomyces venezuelae* ATCC 21018) is not displayed as the cluster encoding deimino-antipain was not detected by antiSMASH in that strain.

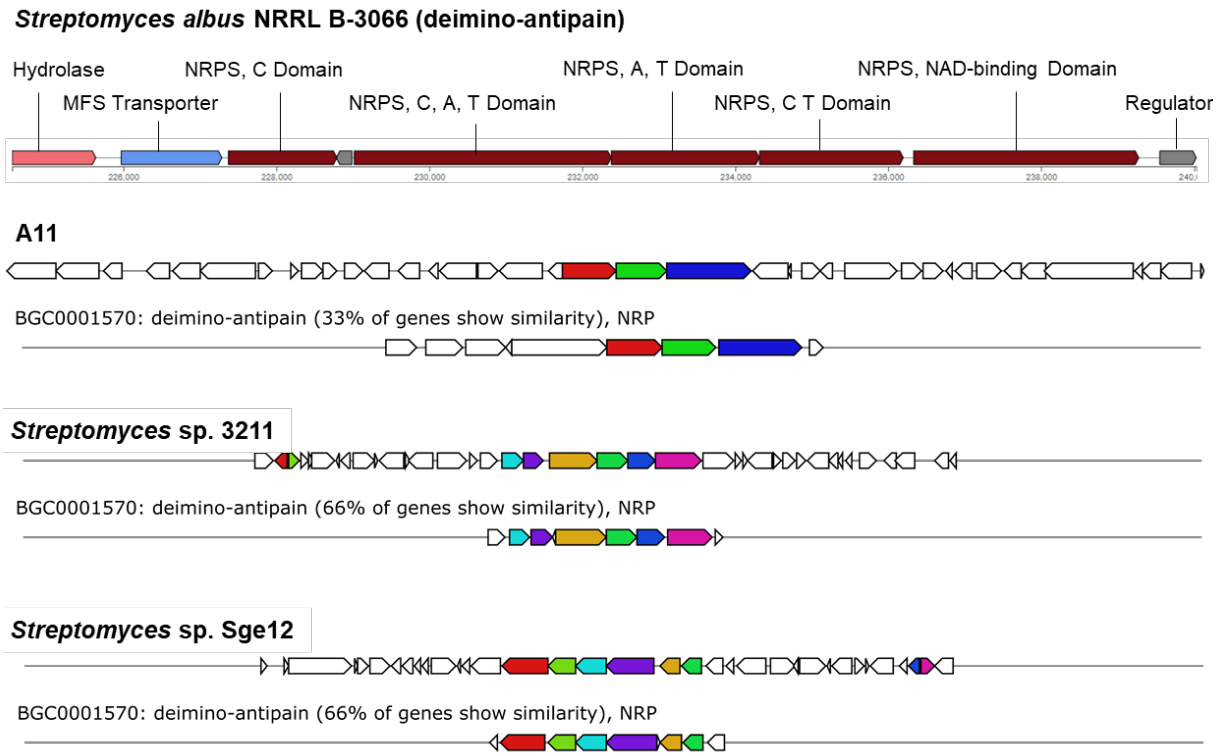

Figure 3.13 – Genomic regions in the deimino-antipain cluster (*S. albulus* NRRL B-3066) with the clusters from the 2 most similar genomes to A11. In each panel, the coloured sections represent the deimino-antipain cluster regions/proteins identified by antiSMASH that are also present in those clusters. Colouring of regions is arbitrary and does not represent function/identity. The identity of regions in the deimino-antipain cluster (top panel) are scaled separately and are taken from the original research article detailing functional assignment (6).

Regions that were given a specific function (using BLASTp) are included in **Table 3.4**. Regions identified as 'hypothetical protein' or which provided no significant similarity have been omitted. A total of 6 of the 23 annotated regions were also present in the cluster of *S. albulus* NRRL B-3066. Three NRPS domains identified by antiSMASH, as well as an additional 3 proteins were present in both clusters. Of the 23 proteins identified, several have uses as polyketide synthases. Other keys functions are the

production of proteases and the cellular differentiation of *Streptomyces*, as will be discussed later.

Table 3.4 – Annotated regions the Biosynthetic Gene Cluster (BGC) responsible for deimino-antipain production in the A11 genome. QC: Query Cover (%) score from BLASTp result. Identity: identical base matches from BLASTp result.

Top BLASTp Hit	**QC**	**Identity**	**In *S. albulus* NRRL B-3066**
PoxB2 Pyruvate dehydrogenase [ubiquinone]	99%	91.90%	N
GltA3 Glutamate Synthase (NADPH) large chain	99%	91.33%	N
SAM-dependent methyltransferase	98%	88.68%	Y
Phosphatase PAP2 family protein	88%	85.19%	N
YihY/virulence factor BrkB family protein	100%	86.56%	N
Acetyltranferase	99%	88.82%	N
Arginase	98%	85.34%	N
Cell filamentation protein Fic	96%	78.32%	N
MFS Transporter	100%	94.13%	Y
Polyketide cyclase /reductase	91%	85.56%	N
Nrps5	95%	94.22%	Y
Nrps4	100%	95.21%	Y
NRPS/polyketide synthase	95%	86.10%	Y
Cytochrome p450 107B1	99%	93.83%	N
Copper transport protein YcnJ precursor	97%	76.47%	N
AMP-dependent synthetase	100%	87.02%	N
GlcNAc-PI de-N-acetylase	99%	92.42%	N
GAF domain protein	97%	92.57%	Y
Subtilisin DY	99%	94.84%	N
CyaB adenylate cyclase 2	100%	92.63%	N
7-carboxy-7-deazaguanine synthase	100%	92.91%	N
Glycosyltransferase	96%	92.11%	N
Molybdenum cofactor biosynthesis protein A	94%	93.78%	N

3.3.7 Protease Inhibition Activity

In order to confirm the identity of **C-A11** as deimino-antipain, or a homologue, the protease inhibitory activity of **C-A11** was first assessed using the skim milk agar assay (170). **C-A11** was shown to prevent the formation of a zone of casein degradation caused by trypsin at a concentration of 45 µg/mL (**Figure 3.14A)**.

At a concentration of 45 µg/mL, **C-A11** was determined to inhibit the proteolytic activity of trypsin by 99.76% (**Figure 3.14C**) using a microtitre-plate assay. This concentration was selected as the highest possible given the amount of compound retrieved from purification experiments. Antipain (45 µg/mL), used as a control, was determined to inhibit the proteolytic activity of trypsin by 76.25%. Epidermicin (45 µg/mL), used as an internal negative control antimicrobial peptide, did not significantly inhibit the proteolytic activity of trypsin (13.09%). The inhibitory effect of **C-A11** was further tested at a series of concentrations (**Figure 3.14D**). **C-A11** did not inhibit the proteolytic activity of trypsin at concentrations lower than 45 µg/mL. Antipain appeared to inhibit trypsination in a dose-dependent fashion, whilst **C-A11** did not at the concentrations tested. Epidermicin did not significantly inhibit the trypsination of BAPNA at the concentrations tested.

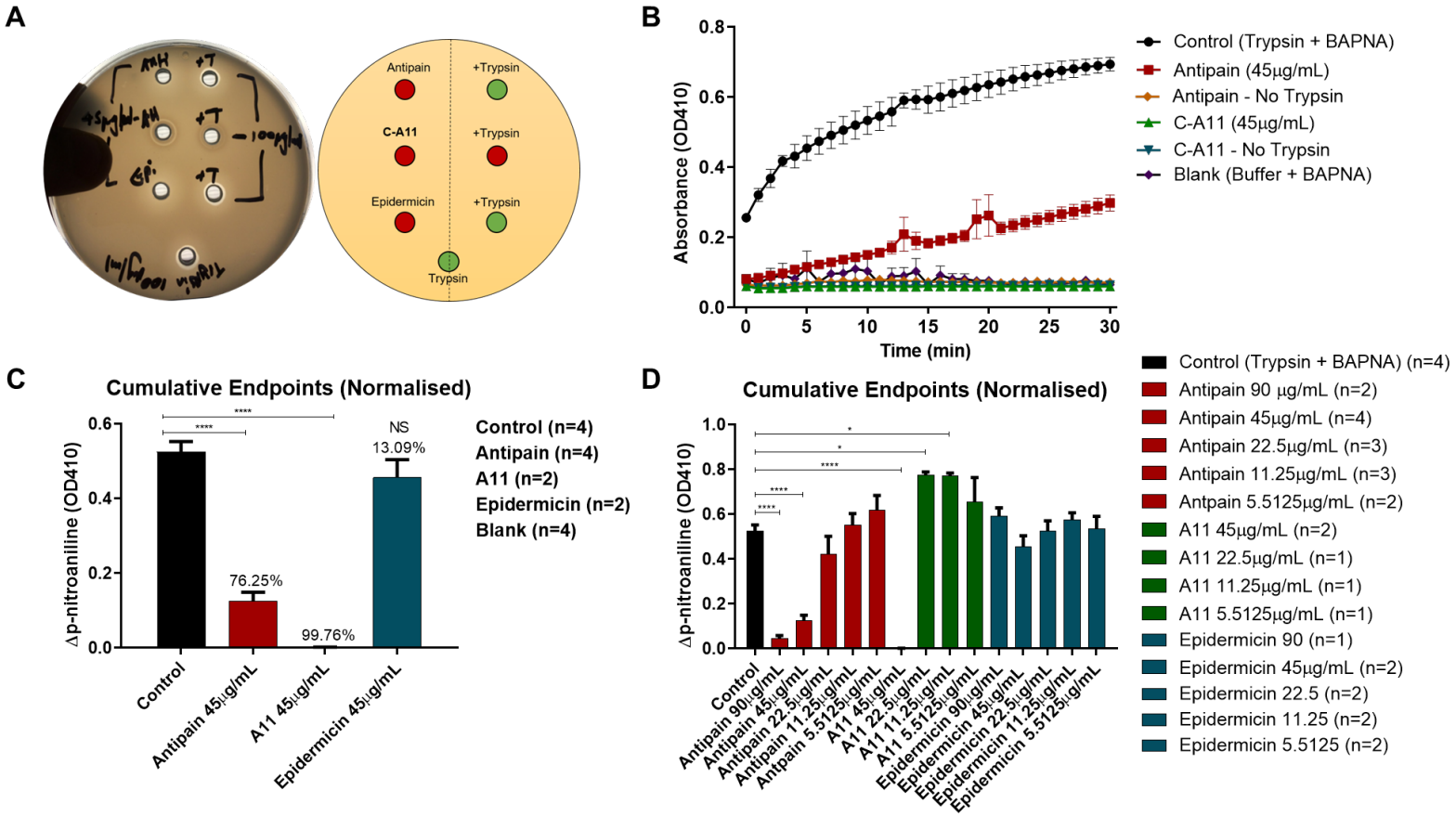

Figure 3.14 – A) Skim milk agar assay. **B)** Measurement of trypsination of BAPNA over time. **C)** Endpoints for BAPNA assay. Values indicate the percentage inhibition relative to control (Trypsin + BAPNA). **D)** Endpoints for BAPNA assay over further concentrations Bars: Standard Error. Significance measured by t-test. '*' represents p-value of <0.05, '**' represents p-value of <0.01, '***' represents p-value of <0.001.

3.4 Discussion & Conclusions

Numerous studies have sought to isolate *Actinobacteria* from sponge hosts (23,29–35) owing to their propensity for the production of antimicrobial and bioactive agents. The majority of antibacterial agents obtained from sponge-associated bacteria have been derived from bacteria belonging to the Phylum of *Actinobacteria* (1). Similarly, the *Streptomyces sp*. represent a genus of the *Actinobacteria* most often submitted to the NCBI from sponge-specific studies.

The draft genome sequence of strain A11 was obtained using a combination of Illumina and Oxford Nanopore sequencing. The consensus sequence obtained indicated that isolate A11 is a potentially novel strain, or perhaps species of *Streptomyces sp.* obtained from culture of bacteria from the previously uncharacterised deep-sea Hexactinellid sponge *Pheronema carpenteri*. Whilst being obtained from the culture of bacteria from a sponge host, A11 did not require seawater for its growth - suggesting that A11 is not an obligate marine species (171). The sequence obtained for isolate A11 is most similar to *Streptomyces* sp. strain 3211, a strain isolated from disease-suppressive soil (172). Isolate 3211 has been previously submitted to antiSMASH for biosynthetic gene cluster analysis revealing the presence of 36 BGCs (173), which is the similar to the number present in *S. albulus* NRRL B-3066. Isolate 3211 also contains the core biosynthetic genes responsible for the production of deimino-antipain. A11 was submitted to antiSMASH and contained a total of 31 BGCs, 5 of which were also present in the *S. albulus* NRRL B-3066. Of the 5 BGCs that were shared, 4 have also been identified as being generally conserved within the genomes of both acidophilic and non-acidophilic *Streptomyces* species (174). In addition, the BGCs were more highly conserved within the genomes of 5

acidophilic *Streptomyces*, i.e. those that grow in media with a pH between 4.5-7.5 (175). The pH of deep water in the North Atlantic has been reported at values between 7.91-8.14 (176). The ability of A11 to grow at a range of pH was not tested and is therefore unknown whether it is acidophilic or non-acidophilic. Interestingly, the BGC that was not conserved within other *Streptomyces* genomes was the one encoding deimino-antipain. A separate study also characterised similarities in the BGC profiles of 8 *Streptomyces* strains, finding an average BGC count of 32, and also the shared presence of 4 of the 5 BGCs shared between A11 and *S. albulus* NRRL B-3066 (177). Again, deimino-antipain was present but only in 1 of the 8 strains. A BLASTn search of the BGC for deimino-antipain taken from *S. albulus* NRRL B-3066 reveals its presence in only 100 submitted sequences, of a total of 1,381,686 listed as *Streptomyces* in the nr/nt database. The Genbank and Refseq databases that the NCBI nt is comprised of together contain around 232 million sequences. Together, this potentially suggests that the production of deimino-antipain within *Streptomyces* is not particularly widespread. This perhaps is exemplified by the fact that prior to 2016 (6), deimino-antipain had not been isolated.

A11 exhibited antimicrobial activity against both Gram-positive and Gram-negative organisms using agar plug diffusion, and simultaneous antagonism assays – and was selected for downstream analysis on this basis. Antimicrobial activity was detected in liquid culture after 3 days of incubation, coinciding with the end of log phase growth. The production of secondary metabolites by *Streptomyces* sp. is a highly regulated process most commonly associated with the transition from the vegetative phase to the formation of aerial hyphae and sporulation - as a result of nutrient limitation (149). This information combined with mass Spectrometry analysis and information obtained

from genome mining suggested **C-A11** to be most similar to deimino-antipain, a protease inhibitor previously isolated from *Streptomyces albulus* NRRL B-3066 as a result of bacterial extract screening (6). Deimino-antipain was not investigated by Maxson et al. (6) on the basis of antimicrobial activity, however was considered in light of its similarity to antipain, which has widespread use as a protease inhibitor in industry and research (178). The authors do however indicate the diverse uses for peptides containing aldehydes (such as deimino-antipain), including drugs such as streptomycin that act through non-covalent mechanisms and those produced via polyketide synthases.

Whilst **C-A11** was investigated further on the basis of its similarity to deimino-antipain, it is perhaps relevant to note that the two other most similar compounds in terms of size and antimicrobial activity were obtained from marine isolates (168,179,180). The differences in *m/z* values from that of **C-A11** meant that they were considered less likely to be identical, or highly similar matches. The decision to investigate **C-A11** on the basis of its similarity to antipain, rather than to all 3 compounds was also taken in part due to the amount of **C-A11** that could be purified, which restricted a wider examination of activity.

Deimino-antipain is a derivative of the protease inhibitor antipain (178). Extensive efforts have been made in order isolate and categorise protease inhibitors from bacteria, with numerous examples being obtained from *Streptomyces* sp. (167,181–183). Protease inhibitors play roles in a wide range of biological and biotechnological processes. Their production in *Streptomyces* sp. is associated with a reduction in biomass in liquid culture and has been shown to be involved in the formation of aerial hyphae on solid media (155). It is interesting to note that the majority of *Streptomyces* sp. do not form aerial hyphae nor sporulate in liquid culture, however they can form

early substrate-like mycelium and antibiotic-producing hyphae (184). In the case of *Streptomyces exfoliatus*, the protease inhibitor leupeptin is produced as part of a cascade of trypsin-like protease, leupeptin and leupeptin-inactivating-enzyme – each part of the cascade responsible for inhibiting the activity of the preceding molecule (154,155). The disappearance of antimicrobial activity after day 4 of liquid culture may also therefore be a potential indication that **C-A11** is most similar to deimino-antipain. The biosynthetic gene cluster responsible for deimino-antipain production in the A11 genome also contained ORFs for the production of the serine protease subtilisin, and may therefore be involved in a similar signalling cascade in A11.

The BGC encoding deimino-antipain production in *S. albulus* NRRL B-3066 contained ORFs that include a hydrolase, transporter, central NRPS/PKS biosynthesis modules and a regulatory protein (6). The A11 BGC included regions that correspond to the central NRPS/PKS modules as well as the MFS-type transporter. However, the production of deimino-antipain in both strains appears to be under the control of a different regulator, as different regulatory proteins were present in the BGCs from each cluster. The A11 BGC also contained numerous other regions that were not present in the *S. albulus* NRRL B-3066 cluster. The presence of these regions may mean that the final product is distinct from the previously characterised version of deimino-antipain, and indicate that it is produced via a distinct biosynthetic pathway. Differences in the BGCs may also be the result of inaccuracies in the sequencing of either A11 of *S. albulus* NRRL B-3066.

Protease inhibition can be monitored by measuring the change in release of trypsin-induced p-nitroanilide from benzoyl-Arg p-nitroanilide (BAPNA) as a result of co-incubation with a protease inhibitor (185). In an attempt to confirm the identity of **C-**

A11, the ability of **C-A11** to inhibit trypsination was measured. **C-A11** exhibited stronger protease inhibitory activity when compared to antipain (99.76% inhibition compared to 76.25%). Whilst antipain exhibited a dose-dependent inhibition of trypsin, **C-A11** appeared only to inhibit trypsin at a concentration of 45 μg/mL. A dose-dependent inhibition may however have been observed if tested between the concentrations of 22.5-45 μg/mL. Epidermicin, an antimicrobial peptide used as an internal/laboratory negative control did not significantly inhibit the trypsination of BAPNA across a series of replicates. A slight difference in endpoint absorbance was observed, and is suspected to be due to competition with BAPNA for substrate-binding of trypsin, preventing some release of p-nitroanilide.

C-A11 exhibited antimicrobial activity against both Gram-positive and Gram-negative bacteria. Protease inhibitors are widely used as antiviral therapeutics, most commonly for HIV/AIDS (186) and Hepatitis C (187). There are currently no clinically approved protease inhibitors for use in treating bacterial infection. It has been suggested however that this could be due to the use of screening methods based largely on the substrate-binding specificity of synthetic small molecules (188). It is possible that screening for inhibitors against specific bacterial proteases may provide an interesting avenue of development for novel antibacterial agents. The agent **C-A11** was also demonstrated to not display *in vivo* toxicity when tested at 10-20x MIC, which provides at least a preliminary indication of low-toxicity associated with its use as a therapeutic agent.

The culture of bacteria from the previously uncharacterised Hexactinellid sponge *P. carpenteri* led to the isolation of a potentially novel *Streptomyces* species. Isolate A11

displayed antimicrobial activity against both Gram-positive and Gram-negative organisms. An antimicrobial agent was purified from culture of A11 and is suspected to be a protease inhibitor most similar to deimino-antipain (6). The low yield, and inability to produce higher quantities of **C-A11** imposed a limitation on continued characterisation. Higher quantities would perhaps have provided the opportunity to determine the peptide sequence, and in doing so determine the similarity to deimino-antipain. The genome of A11 was sequenced, which revealed the presence of numerous biosynthetic gene clusters, indicating that A11 has the capacity for diverse production of antimicrobial and bioactive agents.

Chapter 4

Culture-Independent characterisation of the *Pheronema carpenteri* microbiota and a comparison with sediment and seawater.

4.1 Introduction

4.1.1 The Hexactinellid Microbiota

The composition of the sponge microbiota has been characterised for numerous sponge species (43), owing in part to their propensity for the production of novel antimicrobials and biologics (21,41) (see also **Chapter 3, Section 1.1**) The sponge microbiota has been found, in general, to be shared across species (43), display stability over time (48,52) and consist of 'core' and 'non-core' organisms (49,51). The vast majority of studies to date have focused on the Demosponges, and those that can be obtained from shallow waters (43,47,189).

The most comprehensive analysis of the Hexactinellid microbiota to date consisted of an analysis of the 16S rDNA profile for 7 different species. The Hexactinellid microbiota was reported to have a marked increase in abundance of reads attributed to the Proteobacteria, Bacteroidetes, Nitrospinae, Patescibacteria and Planctomycetes relative to Demosponge populations that were characterised at the same time (87). The Hexactinellid microbiota has also been shown to possess a higher number of unique amplicon sequence variants (ASVs) (122) when compared to both Demosponges and seawater. The Hexactinellid microbiota also shared a higher number of variants with seawater than it did with Demosponges. Hexactinellid sponges studied were dominated largely by the Proteobacteria, specifically by Alpha- and -Gamma-proteobacteria. Sponge-specific differences were also observed between the individual sponge species. The presence of *Nitrospinae* and *Patescibacteria* is almost exclusively associated with Hexactinellid sponges, with the *Planctomycetes* displaying a higher tendency to be associated with Hexactinellid sponges than Demosponges (122). Whether these trends are consistent with other members of the Hexactinellid Class remains to be fully explored and was the rationale for the current work.

With regards to the ‘High Microbial Abundance’ – ‘Low Microbial Abundance’ (HMA-LMA) dichotomy that has become apparent in sponge taxonomy (91–93) it has been proposed that all deep-sea sponges may in fact be Low Microbial Abundance (LMA) sponges ($1x10^{5-6}$ bacterial cells/g wet-weight of sponge tissue) (94). Such claims have not yet been fully explored however, due to the paucity of studies focused specifically on the characterisation of deep-sea, and Hexactinellid sponge microbiota.

4.1.2 Differences in the microbiota of sponges, sediment and seawater

The sediment microbiota is of interest due in part to the biology and life cycle of Hexactinellid sponges. The filter-feeding nature of sponges means large quantities of seawater and planktonic bacteria come into contact with sponge tissue (2,42). Glass sponges have been shown to demonstrate extremely efficient filtration, in some cases removing up to 95% of bacteria from seawater (190). Glass sponges that sit on ocean shelves, such as those collected in this study are affected by ‘sediment slumps’ twice a year (191), indicating transfer of high suspended sediment concentrations (SSC) to the sponge tissue. Numerous species of Hexactinellid sponge display ‘anchoring’ in soft-substrate environments such as sediment, whereby the feeding, or basket-like portion of the sponge is raised above the sea floor and attached by an ‘anchor’ made of siliceous spicules. This ‘sponge-sediment’ relationship is thought to be in part to prevent the large transfer of particulate material such as sediment, that may be disturbed (192). Neither *Pheronema carpenteri* nor *Hertwigia* sp. attach to the seabed by an anchor however. The main body of the sponge is situated on the seafloor and is attached by shorter root spicules (90). This morphological trait may have a part to play in determining the acquisition and crossover of microbes from the seabed. Th

The acquisition of microbial inhabitants from the surrounding environment, otherwise known as horizontal transmission, is an important means by which the microbiota of organisms is shaped (193). The importance of horizontal transmission in determining sponge microbiota varies between sponge species (194) however, and the extent to which this may impact the microbiota of *P. carpenteri*, or Hexactinellid sponges in general, is relatively unknown.

Upon contact with SSC above 10mg/L^{-1}, Hexactinellid sponges are known to undergo feeding arrests, characterised by a reduction in pumping rates (195). This behaviour is distinct from that of some Demosponges, which have been shown to contract in order to expel particles, a process that has been referred to as ‘sneezing’ (196). It has been suggested therefore that sediment ‘smothering’, as is seen with Demosponges is less of an issue for Hexactinellid sponges (191). However, it may be the case that cessation of filtration leads to a less efficient removal of sediment-derived microbes. There is some evidence to suggest that removal rates of bacterial cells may be slower for Hexactinellid sponges than for Demosponges (197). Previous studies have examined the difference in sponge and sediment microbiota, as well as transfer caused by specific SSC events. At both Phylum and OTU level, no significant transmission of bacteria between sediment and seawater samples was shown to occur in several species of Demosponge, when exposed to elevated SSC (198). The microbiota of one sponge however, displayed a significant shift, with the recruitment of 3 OTUs from the Cyanobacteria. Whether this would be the same for Hexactinellid sponges, and for *P. carpenteri* in particular is unknown.

The rationale for the current study was based on the knowledge gaps outlined above concerning the Hexactinellid, Pheronema and sediment microbiota. Next-Generation Sequencing (NGS) 16S rDNA community profiling was conducted in order to characterise each microbiota and facilitate determination of taxonomic and structural differences. This study aims to provide the first molecular characterisation of the *Pheronema carpenteri* microbiota, using NGS 16S rDNA community profiling. *Pheronema carpenteri* was selected for characterisation only, as insufficient DNA yield could be obtained from samples of *Hertwigia* sp. to proceed with sequencing library preparation. The study will also determine the suitability of the chosen sequencing technology and analysis pipeline and use statistical methods to determine taxonomic and structural differences between the sponge, sediment and seawater microbiota collected at two separate sampling sites (transects). This information will also will be used to determine the degree of intra-species dissimilarity between biological replicate samples as well as identify the presence and relative abundance of isolates cultivated from *Pheronema carpenteri* (see **Chapter 2**) within the microbiota.

4.2. Methods

4.2.1 Sample Collection

Sponge, seawater and sediment samples were collected from two separate sampling sites (transects) in the North Atlantic deep sea in 2019 (CE19 Research Cruise) (**Figure 4.1**). *P. carpenteri* sponges were collected using ROVs and photographed in situ before removal. Sediment core samples were collected using sediment corers and transferred to sterile 50 mL tubes aboard the cruise vessel. Samples were collected from each transect within 10m distance of each other, providing biological replicates.

All samples were frozen at -20°C upon collection and transferred to the laboratory under dry ice.

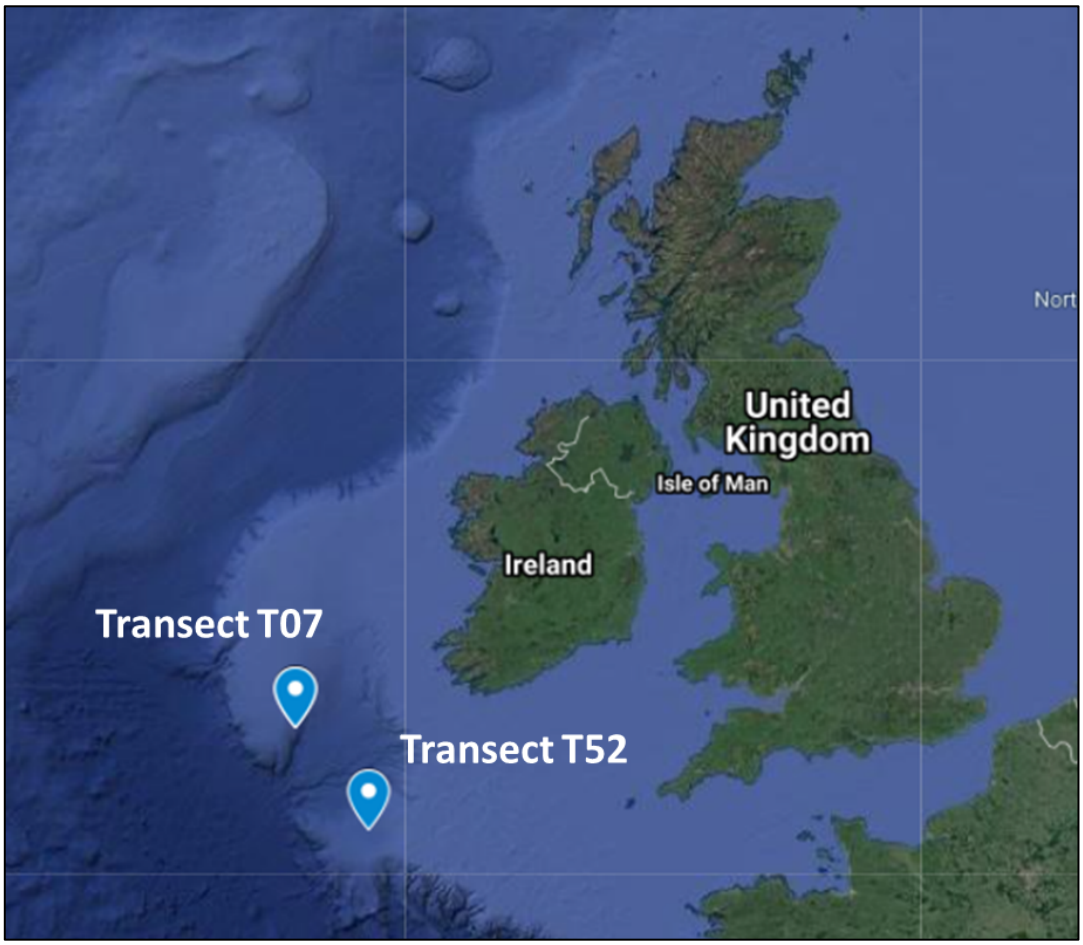

Figure 4.1 – Sampling sites of sponge, seawater and sediment samples used in this study.

Three replicates of each sponge were collected, along with sediment samples from the base of each sponge. A list of sample ID's used in the text, along with relevant information is displayed in **Table 4.1**.

Table 4.7 – Sample information for sponge, sediment and seawater samples collected in this study.

Sponge ID	Sample Site (Transect)	Depth (m)
Sponge_009	T52	1208
Sponge_010	T52	1208
Sponge_011	T52	1208
Sediment_009	T52	1207
Sediment_010	T52	1208
Sediment_011	T52	1208
Seawater_011	T52	Not taken at collection (>1000m)
Sponge_027	T07	Not taken at collection (>1000m)
Sponge_028	T07	Not taken at collection (>1000m)
Sponge_029	T07	Not taken at collection (>1000m)
Sediment_027	T07	Not taken at collection (>1000m)
Sediment_028	T07	Not taken at collection (>1000m)
Sediment_029	T07	Not taken at collection
Seawater_029	T07	Not taken at collection

* Sponge and sediment IDs with the same number represent where sediment samples were collected within 1m of the corresponding sponge i.e. Sponge_009 and Sediment_009. Samples with the same transect number (T52 or T07) were all collected from the same sampling site i.e. all within 10m distance of each other. The two transects were 120 miles apart. A single seawater sample was collected from each transect, i.e. within the same 10m distance as all sediment and sponge samples. Depth measurements were recorded at time of sampling.

4.2.2 DNA Extraction

Upon arrival in the laboratory, *P. carpenteri* sponges were cut into 0.5g (wet weight) tissue segments using a sterile scalpel. Tissue segments were taken from the inner surface of each sponge replicate. DNA was extracted from the inner sponge tissue segments (0.25g) using the DNeasy PowerSoil Kit (Qiagen) following the manufacturer's instructions. DNA was extracted from a total of 1g of each sponge in 4 separate extractions, was eluted in 100µL nuclease-free water and was combined after extraction using a Speedvac Concentrator (Thermofisher). DNA was extracted from 0.25g of each sediment core using the above methods. Filter paper, through which water samples were drawn, was cut into small fragments using sterile scissors and placed into individual Eppendorf tubes. Each filter paper fragment contained the biological material from 1.5L of seawater. All DNA was then quantified using a High Sensitivity Qubit Fluorometer (Thermofisher), prior to sequencing library preparation.

4.2.3. Library Preparation & Sequencing

Library preparation and DNA amplification of the full 16S rRNA genomic region was performed using the Oxford Nanopore 16S Barcoding Kit SQK-RAB204 **(primers: 27F:** 5′-AGAGTTTGGATCMTGGCTCAG-3′**, 1492r:** 5′-CGGTTACCTTGTTACGACTT-3′**)** (113–116) **(Eurofins Genomics)**. A total of 3 different sequencing libraries were constructed in order to obtain sufficient genomic material for sequencing, as well as sufficient sequencing output data. Library information is displayed in **Table 4.2**.

Table 4.8 – Sample and library information for MinION runs performed in this study.

Barcode	Sample	Barcoded DNA (ng)	PCR Amplifications	Library
1	Sediment_009	10	1	1
2	Sediment_010	10	1	1
3	Sediment_011	10	1	1
6	Sponge_011	10	1	1
8	Sediment_027	10	1	1
9	Sediment_028	10	1	1
10	Sediment_029	10	1	1
11	Sponge_027	10	1	1
12	Sponge_028	10	1	1
2	Water_029	20*	1	2
4	Sponge_009	20*	1	2
5	Sponge_010	20*	1	2
1	Sponge_029	10	2**	3
2	Water_029	10	2**	3
4	Sponge_009	10	2**	3
5	Sponge_010	10	2**	3
7	Water_009	10	2**	3

*20ng DNA was used due to low yield from the extraction procedure.

**2 PCR amplifications were performed in order to increase the amount of DNA available for sequencing. The use of 20ng DNA in the previous barcoding library (see Table) did not produce a significantly higher amount of genomic material for sequencing and did not produce as many sequencing reads.

DNA libraries were loaded onto the MinION sequencer and sequenced according to the manufacturer's instructions (**Protocol ID: SQK-RAB204**). Individual sequencing runs were allowed to sequence for a total of 48hr run time before being stopped manually. Pore occupancy and sequencing output was monitored using the MinKNOW software (199).

4.2.4.1 Bioinformatic Analysis

Sequenced reads were outputted in the fast5 format. Reads were base-called using Guppy Basecaller (200), demultiplexed using Porechop (https://github.com/rrwick/Porechop) prior to downstream bioinformatics analysis using Mothur v1.44.3. An overview of the pipeline used to process the raw fastq reads is provided in the sections below.

4.2.4.2 Data Processing, Alignment and Quality Control

Bioinformatic analysis was carried out using Mothur v1.44.3 (201) using the recommended pipeline (202).

- All bioinformatic tools are given in *italics*. All tools belong to Mothur v1.44.3 unless otherwise specified.
- All FASTQ files corresponding to the samples in each sequencing library were processed at the same time.

FASTQ reads were converted to FASTA format using *FASTQtoFASTA* v.1.1.5 (Galaxy). Group files were generated for each file using *make.group.* Sequences were screened using *screen.seqs* to a maximum length of 1500bp, with a maximum number of ambiguous bases of 0. Unique sequences were obtained using *unique.seqs*, outputting the data in name file format. Sequences represented by each unique

sequence in the name file were counted using *count.seqs*, with group information provided by the group file from *make.group*.

4.2.4.3 Sequence Alignment

FASTA sequences were aligned using the silva.nr_138.align (full-length 16S rRNA gene) database (obtained from https://mothur.s3.us-east-2.amazonaws.com/wiki/silva.nr_v138.tgz) using *align.seqs.* Aligned sequences were screened again using *screen.seqs* (minimum length: ***see note**, maximum homopolymers: 22). ***NB:** This number was selected based on the lowest number of bases contained within the 97.5th percentile of the data for all FASTA files in the library. Maximum homopolymer number was set using the maximum homopolymer length present in the reference database, as recommended in the literature (202,203). The alignments were trimmed to the regions containing the aligned genomic information using *filter.seqs* (trump character: .). As the screening, alignment and filtration steps may have led to certain sequences no longer being unique, representative sequences were re-obtained using *unique.seqs.*

4.2.4.4 Dereplication

Aligned FASTA sequences that differed by <5% sequence similarity were grouped together using *pre.cluster (diffs: 70)* in order to account for sequencing error. This step assumes a 95% sequencing accuracy for the MinION platform (16). Chimera identification (*de novo)* was performed using *chimera.vsearch* and chimeric sequences were removed from the FASTA file using *remove.seqs*, specifying the 'accnos' output from *chimera.vsearch*.

4.2.5.5 Taxonomic Assignment

Taxonomy was assigned to sequences with *classify.seqs*, using the silva.nr_138.tax reference database for reference taxonomy (obtained from https://mothur.s3.us-east-2.amazonaws.com/wiki/silva.nr_v138.tgz). Non-bacterial sequences were removed from the FASTA file using *remove.lineage*, by specifying the removal of 'Chloroplast-Mitochondria-unknown-Archaea-Eukaryota'. Consensus taxonomy for each OTU was assigned using *classify.otu*. Mothur taxonomy files were combined.

4.2.4.6 Phylotyping & Rarefaction Analysis

Phylotype (Mothur) was used in order to group sequences into OTUs based on taxonomy. Phylotyping was performed at taxonomic levels from Genus to Phylum, in order to assess the number of different taxons present in the dataset at each taxonomic level. Rarefaction curves were generated from this phylotyping data rather than FASTA-based OTU-clustering, as the high number of 'singleton' reads generated by Oxford Nanopore sequencing prevents realistic rarefaction of OTUs based on sequence similarity (16). Rarefaction of taxon counts was performed using *rarefaction.single*.

4.2.4.7 OTU Clustering

FASTA sequences were clustered into OTUs using *cluster.split*. Sequences were clustered using cutoff values of 0.05, corresponding to a percentage similarity of 95%*****. *****Conventionally, OTUs may be clustered at the 97% similarity for genus-level clustering (204). The *pre.cluster* step previously employed to account for sequencing error (*see **4.3**)* however nullifies the effect of clustering MinION sequences at ≥95% similarity.

4.2.5 Data Visualisation

Statistical analyses and data visualisation were performed using Graphpad Prism 9 and R using the phyloseq package (https://joey711.github.io/phyloseq/). All figures were produced in Graphpad Prism 8 excluding PCoA plotting and Alpha diversity measurements. Principal Co-ordinate Analysis ordination was performed on OTU data using Bray-Curtis dissimilarity in R using phyloseq. The pipeline for analyses and functions performed in R can be viewed at https://vaulot.github.io/tutorials/Phyloseq_tutorial.html#gettin-started.

4.3 Results

4.3.1 16S rDNA sequence data was obtained using the MinION sequencing platform

Sequence data was obtained for sponge, sediment and seawater samples recovered from two different sampling sites. Information pertaining to the raw, demultiplexed reads obtained from sequencing is contained within **Table 4.3**. Sponge samples from Library 3 had a higher number of reads per sample than sponges from other libraries. Samples from Library 1 had in general a lower maximum read length, with and average read length that was closest to that of the full length 16S rRNA gene (~1500bp). An additional PCR step (Library 3) appeared to have a greater impact on the number of reads obtained for each sample than for the addition of 20ng template DNA (Library 2).

Table 4.9 – Sequence read information for all samples sequenced in this study.

Barcode	Sample	Library	num_seqs	sum_len	min_len	avg_len	max_len
1	Sediment_009	1	334,367	475,389,160	4	1,421.8	6,648
2	Sediment_010	1	251,043	360,967,326	5	1,437.9	9,722
3	Sediment_011	1	467,297	654,581,123	8	1,400.8	5,126
6	Sponge_011	1	140,200	201,231,631	56	1,435.3	13,232
8	Sediment_027	1	485,413	696,722,707	48	1,435.3	6,895
9	Sediment_028	1	430,123	612,383,474	45	1,423.7	6,192
10	Sediment_029	1	345,327	496,715,685	43	1,438.4	15,070
11	Sponge_027	1	13,069	18,510,281	3	1,416.4	40,293
12	Sponge_028	1	16,585	23,783,944	32	1,434.1	8,273
2	Water_029	2	16,052	2,519,577	1	157	30,235
4	Sponge_009	2	86,571	110,831,359	2	1,280.2	68,812
5	Sponge_010	2	6,828	7,860,180	2	1,151.2	4,570
1	Sponge_029	3	557,852	206,256,999	1	369.7	108,627
2	Water_029	3	174,539	21,658,338	1	124.1	114,610
4	Sponge_009	3	691,278	399,475,562	1	577.9	134,490
5	Sponge_010	3	631,991	371,415,673	1	587.7	77,838
7	Water_011	3	568,084	191,388,833	1	336.9	242,311

*Num_seqs represents total number of sequences obtained. Sum_len is the summative length in nucleotide bases obtained for each sample. Min_len is the shortest read length. Avg_len is the average read length. Max_len is the longest read length. All lengths are given in number of nucleotide bases.

4.3.1 Sequencing across two MinION runs does not impact taxonomic classification

In order to address the degree of difference that may have been caused by Oxford Nanopore sequencing inaccuracy, the 16S rDNA amplicons from library 3 were sequenced twice, over two separate 48hr runs and compared. Sequences obtained from each sequencing run are those referred to in tables and figures as 'L3' and 'L32'. For each of the three sponge samples outlined, Sponge_009 produced the highest combined number of reads (68,260), Sponge_010 produced the second highest (65,477) and Sponge_029 produced the least (28,115). Water_011 produced a combined total of 23 reads, and water_029 produced a combined total of 14 reads. Information for each barcoded, post-mothur sample is displayed in **Table 4.4**.

Table 4.10 – Sample information for classified reads obtained from samples over two separate MinION runs. Sample ID denotes library, run and barcode information i.e. L3B1 denotes library 3, barcode 1. L32B1 denotes library 3, run 2, barcode 1.

Sponge (Lib)	Sponge_029 (L3B1/L32B1)	Sponge_009 (L3B4/L32B4	Sponge_010 (L3B5/L32B5)	Water 029 (L3B2/L32B2)	Water 011 (L3B7/L32B7)
Run 1	17154	41933	43152	5	13
Run 2	**10961**	**26327**	**26360**	**9**	**10**
Total	**28115**	**68260**	**69512**	**14**	**23**

*****The low number of quality-filtered reads obtained from water samples was judged to prevent a more meaningful analysis. Reads were retained in figures for reference purposes. This sample was analysed in order to represent an environmental control.

For Sponge_009 and Sponge_010, all differences in relative abundance of each phylum represented a <1% difference between the two sequencing runs. For

Sponge_029, all differences were <1% excluding; reads that were ‘Unclassified’ i.e. those that were classified as bacteria at kingdom level but could not be assigned a phylum (2.2% difference), and reads classified as Dependentiae (1.4% difference).

For Sponge_009 the order of phyla in terms of relative abundance (%) was identical for both sequencing runs, except for Cyanobacter and Chloroflexi, which were each one of the two least abundant phyla in each sequencing run (along with Nitrospinae) (**Figure 4.2**). Cyanobacter made up 0.01% of reads from the first run but was absent in the second. Chloroflexi made up 0.004% of reads from the first and 0.003% in the second. For Sponge_010 the order of phylum in terms of relative abundance (%) was identical for both sequencing runs.

For Sponge_029 the order of phyla in terms of relative abundance (%) was almost identical for both sequencing runs, excluding several phyla for which differences in relative abundance were negligible.

Water samples displayed a higher difference in phylum relative abundance between the two samples, as well as in phylum order when compared to sponge samples (**Figure 4.2**). This is thought to be due to the low number of sequences obtained for water samples. It should also be noted that all Library 3 samples were subjected to two PCR amplifications which may have reduced differences between separate runs, as will be discussed in detail later on.

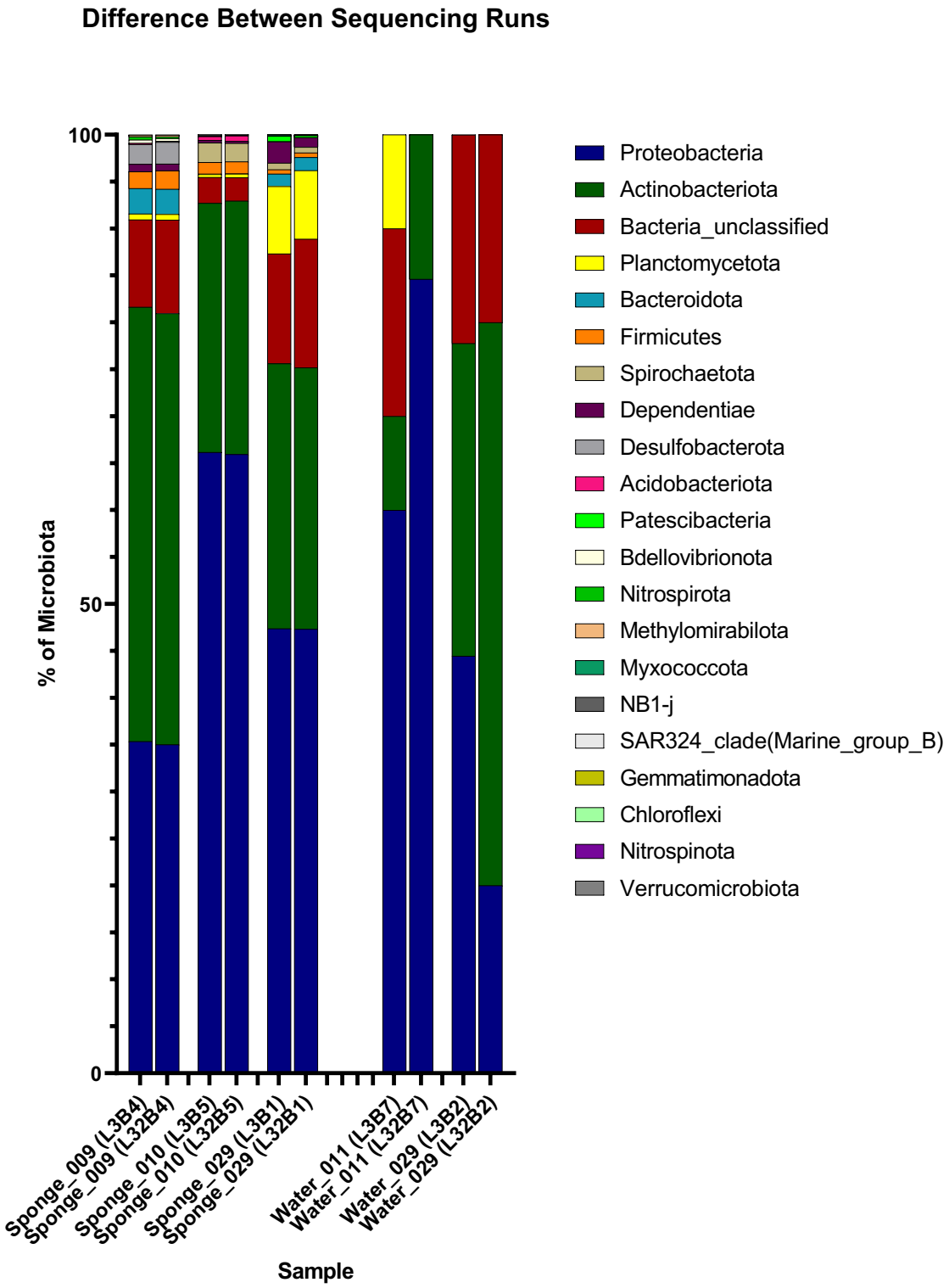

Figure 4.2 – Comparison of taxonomic classification for samples sequenced across two separate MinION runs. Sample ID denotes library, run and barcode information i.e. L3B1 denotes library 3, barcode 1. L32B1 denotes library 3, run 2, barcode 1.

4.3.2 An additional PCR step in library preparation impacts taxonomic classification, when using the MinION sequencing platform

Reads from both sequencing runs analysed above were combined, in order to compare them to reads that were generated after only a single amplification step during library 2 preparation (**Figure 4.3**).

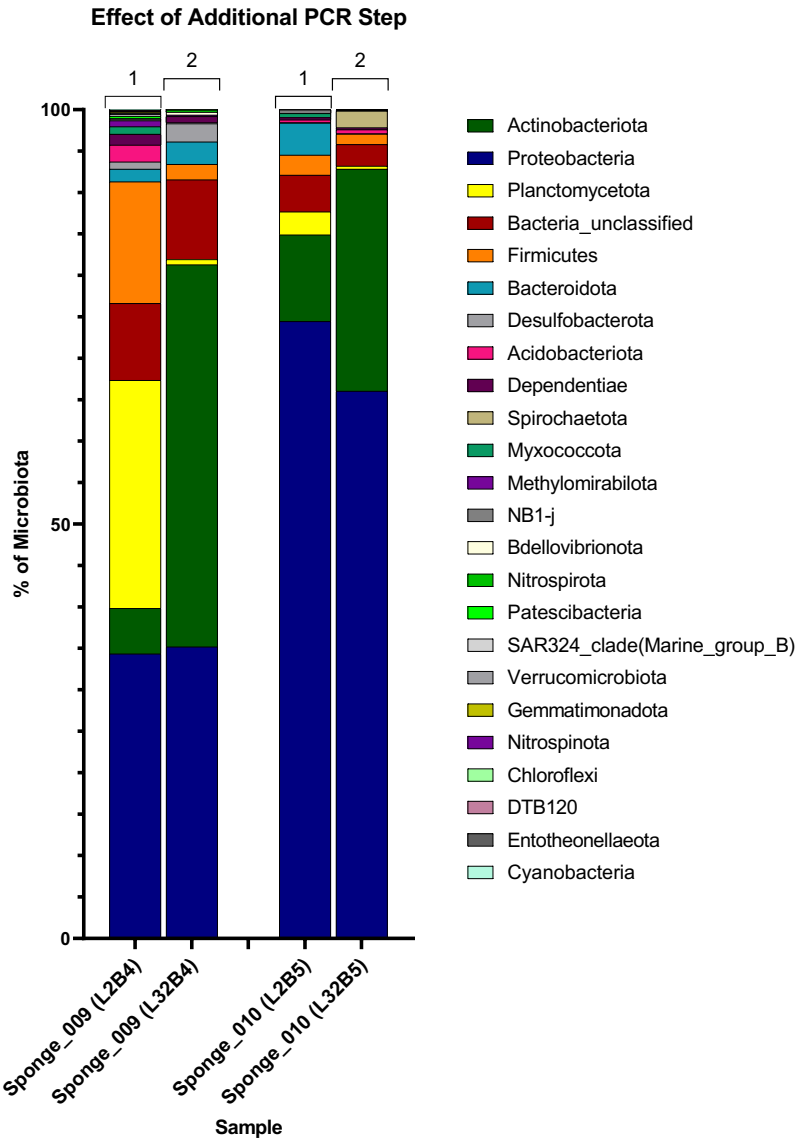

Figure 4.3 – Comparison of taxonomic classification for samples sequenced after one or two amplification steps. Numbers above bars denote number of PCR amplification steps used in library preparation. Sample ID denotes library, run and barcode

information i.e. L2B4 denotes library 3, barcode 4. L32B4 denotes library 3, run 2, barcode 4.

For Sponge_009, the largest difference in phyla attributed to an additional PCR step was observed in the Actinobacteria (40.6%; range = 46.1–5.5%), Planctomycetes (26.9%; range =27.5–0.6%), Firmicutes (12.8%; range = 14.7–1.9%) and Bacteroidota (1.2%; range = 2.7–1.1%) (**Figure 4.4**). The difference in all other phyla was <1%.
For Sponge_010, the largest difference in phyla attributed to an additional PCR step was observed in the Actinobacteria (16.3%; range = 26.8-10.4%), Proteobacteria (8.4%; range =74.5-66.1%), Bacteroidetes (3.8%; range =3.9-0.04%), Planctomycetes (2.4%; range =2.7-0.4%), Spirochataetes (2%; range = 2-0%), Unclassified (1.8%; range =4.4-2.6%) and Firmicutes (1.2%; range = 2.4-1.2%). The difference in all other phyla was a <1%. The differences observed for Sponge_010 were lower than those observed for the same phyla in Sponge_009, excluding the Bacteroidetes. More phyla showed a >1% difference in Sponge_010 than in Sponge_009. The Actinobacteria showed the biggest difference caused by PCR step for both sponges.

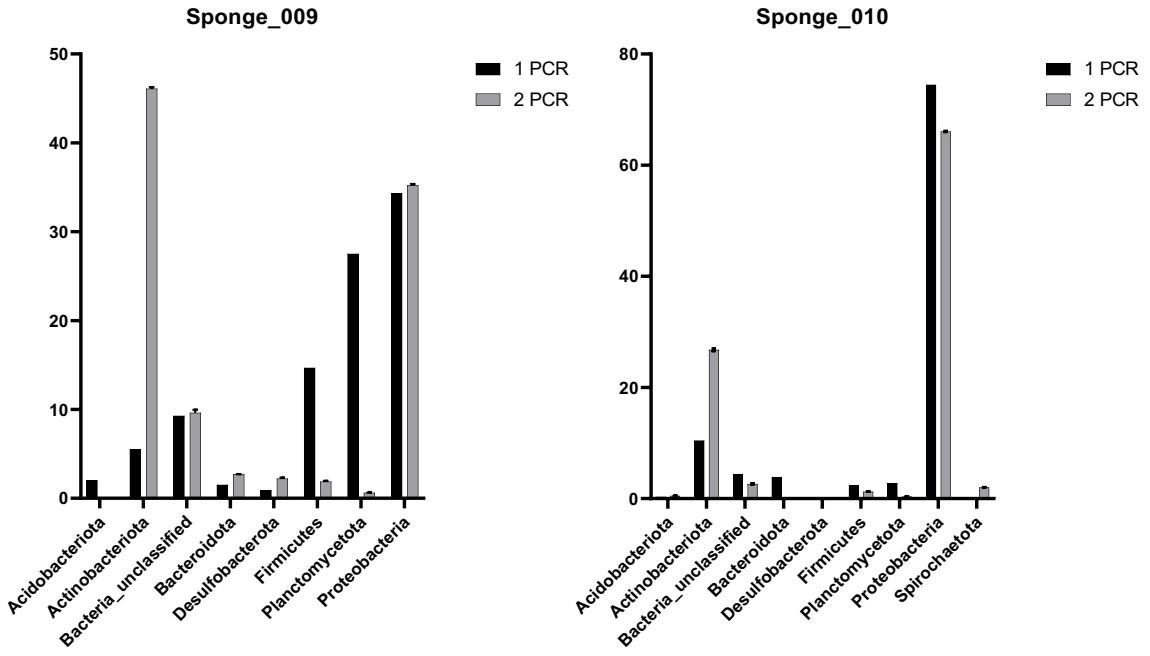

Figure 4.4 – Range in relative abundance of each phylum, in sponge samples (009 and 010) that were sequenced after one or two amplification steps. Bars represent mean abundance. Lines represent range (minimum to maximum).

The same OTUs were not altered by ≥1% in each sponge after a second amplification The difference in relative abundance caused by additional amplification was also compared at OTU level (**Figure 4.5**). The OTUs in each sponge for which relative abundance changed by >1% were analysed. For Sponge_009, 10 OTUs were increased by >1% after an additional amplification (**Figure 4.5A**). Two of these OTUs increased by >10%, making up 31.95% of the microbiota after two rounds of amplification. Of the 10 OTUs, 5 were Actinobacteria, 4 were Proteobacteria and 1 was Bacteroidota. All of the 10 OTUs that were increased by >1% were also present in the top 19 most abundant OTUs i.e. those with >1% relative abundance. The relative abundance of 10 different OTUs decreased by >1% (**Figure 4.5B**). A single OTU

decreased by over >10%, representing a 23% change. Of the 10 OTUs, 5 were Firmicutes, 3 were Proteobacteria and 2 were Planctomycetota.

For Sponge_010, 6 OTUs increased by >1% after an additional amplification (**Figure 4.5A**). Of the 6 OTUs, 3 were Actinobacteria, 2 were Proteobacteria and 1 was Spirochaetota. A total of 3 were also present in the 10 OTUs from Sponge_009 that showed the highest increase (Actinobacteriota, Actinobacteria, Gammaproteobacteria). Increases in relative abundance caused by additional amplification were lower for Sponge_010 than for Sponge_009, with the largest increase in relative abundance being 8.24% for Sponge_010, compared to 21% for Sponge_009. The relative abundance of 9 OTUs decreased by >1% (**Figure 4.5B**). Of the 9 OTUs, 6 were Proteobacteria, 1 was Planctomycetota, 1 was 'Bacteria_unclassified' and 1 was Bacteroidota. Of the 9 OTUs, 2 were also present in the OTUs decreased by >1% in Sponge_009 (Pirellulaceae, Alphaproteobacteria).

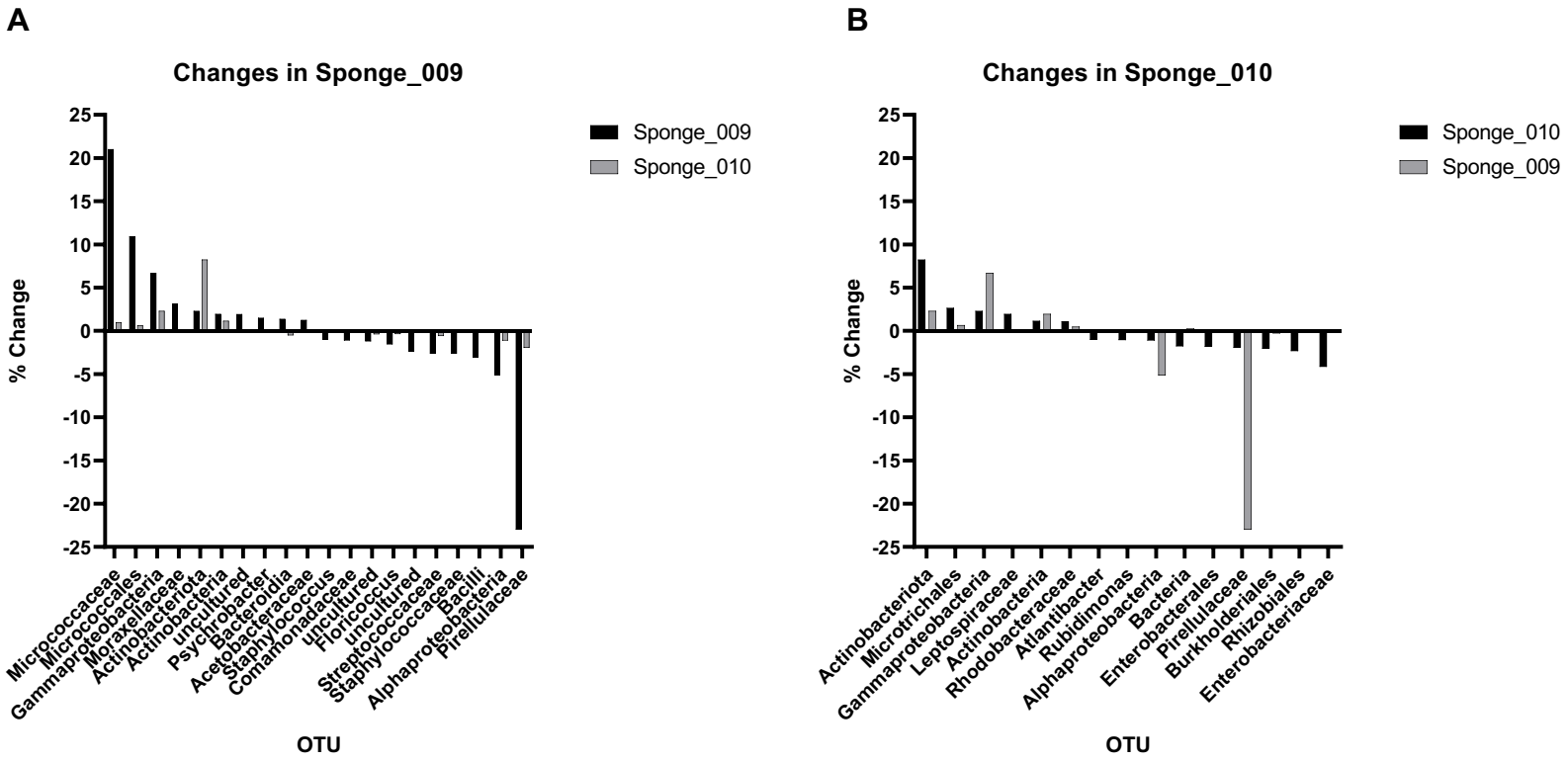

Figure 4.5 – Overview of OTUs that had a change in relative abundance of ≥1% after a second amplification step. **A)** OTUs that were changed by ≥1% after a second amplification in Sponge_009, compared to the amount by which they were altered in Sponge_010. **B)** OTUs that were changed by ≥1% after a second amplification in Sponge_010, compared to the amount by which they were altered in Sponge_009.

Due to the high similarity between bacterial composition at phylum level, reads from separate sequencing runs were combined for downstream analysis. Due to the differences in bacterial composition attributed to an additional PCR step at both phylum and OTU level, reads obtained for each sample using a single amplification were not combined with those obtained using a second amplification. The combination of sequencing reads prior to downstream analysis is depicted in **Figure 4.6.**

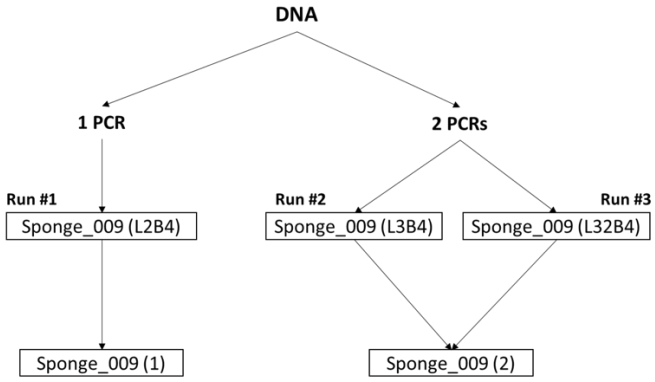

Figure 4.6 – Graphical representation of the combination of reads from samples determined to be sufficiently similar.

4.3.3 Pheronema carpenteri and sediment display distinct microbiota at phylum level.

Replicate sponge and sediment samples were collected from two sites (transects T07 and T52). The words ‘transect’ and ‘sample site’ will be used here interchangeably. Reads obtained from sponges that were amplified once (from Sponge_009, Sponge_010 and Sponge_029) were compared alongside sponge and sediment reads amplified once obtained from sequencing library 1 (Samples 011, 027 and 028). In order to provide a direct comparison, samples that were amplified twice were omitted from downstream analyses here.

A total of 31 different phyla were identified in at least one sponge sample, and a total of 54 phyla were identified in at least one sediment sample (**Figure 4.7**). In sponge samples, Proteobacteria was the most abundant phylum in 4 of 5 sponges. Planctomycetes was the most abundant phylum in Sponge_028. In sediment samples, Proteobacteria was the most abundant phylum in 5 of 6 samples. Reads categorised as ‘Bacteria_unclassified’ were the most abundant phylum-level assignment in Sediment_010.

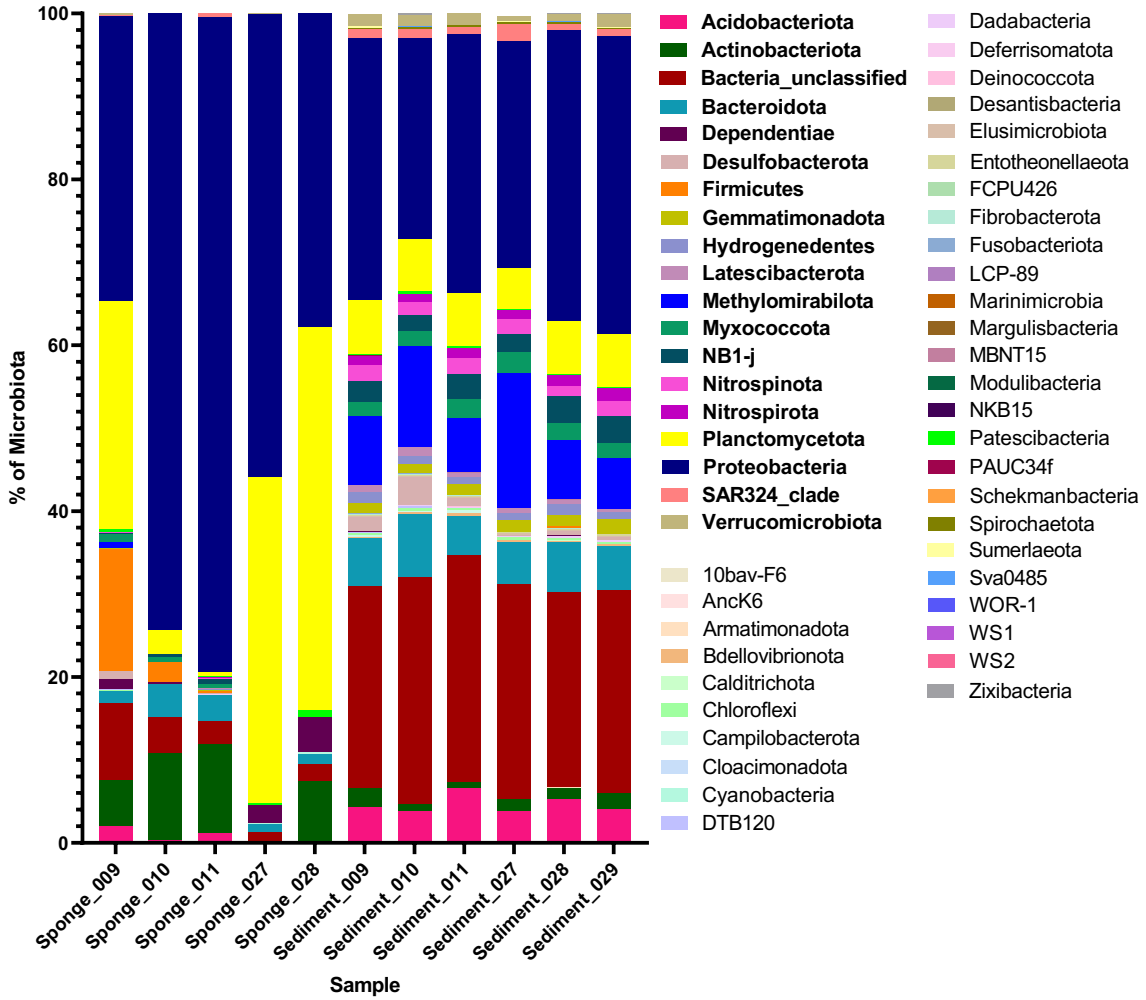

Figure 4.7 – Taxonomic composition of all sponge and sediment samples at phylum level. Phyla for which the relative abundance in at least one sample was ≥1% are displayed in the legend in bold font.

4.3.4 Pheronema carpenteri microbiota display enrichment of particular phyla

The extent to which particular phyla are enriched in either sponge or sediment samples is displayed in **Figure 4.8**. Phyla for which the relative abundance was higher in *P. carpenteri* samples than in sediment (by ≥1%) were Proteobacteria, Planctomycetota, Actinobacteria, Firmicutes and Dependentiae. Patescibacteria, Cyanobacteria, Margulisbacteria, 10bav-F6 and Marinimicrobia (SAR406_clade) were also enriched, but by <1%.

Phyla for which the relative abundance was higher in sediment samples compared to sponge (by ≥1%) were Methylomirabilota, Acidobacteria, NB1-J, Nitrospinota, Gemmatimonadota, Myxococcota, Verrucomicrobiota, Nitrospirota. All other phyla (n=35) were enriched by <1%. A comparison of which phyla had a higher relative abundance in either sponge or sediment samples is displayed in **Figure 4.8**.

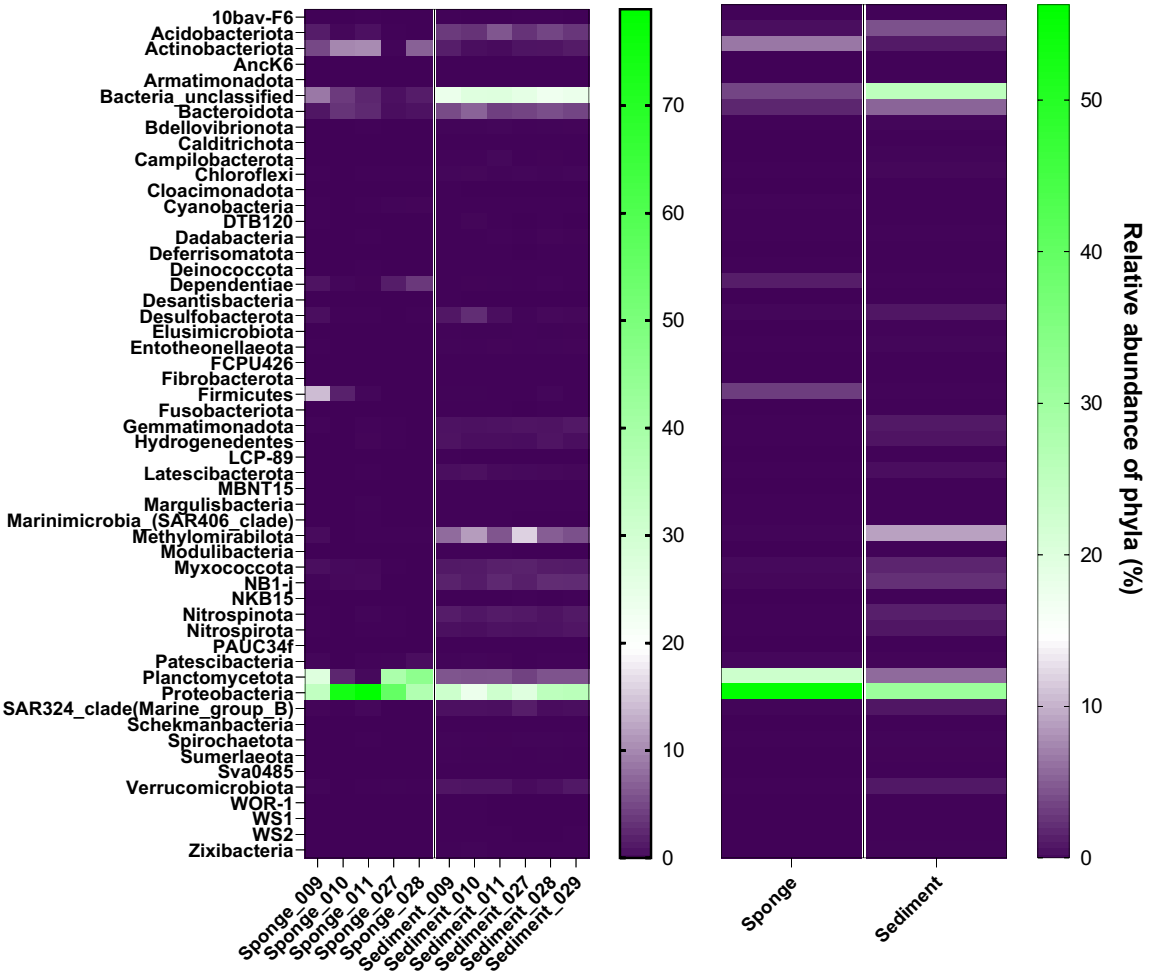

Figure 4.8 – Relative abundance of all phyla in sponge and sediment samples. Left panel: Phylum level abundance in each sample. Right panel: Average phylum abundance in sponge and sediment microbiota as a whole. Phyla which have a higher relative abundance appear towards the green end of the spectrum.

4.3.5 Pheronema carpenteri displays higher intra-sample dissimilarity than sediment

A 2-way ANOVA test was performed in order to assess the difference in mean abundance of each phylum between sponge samples at each transect. The abundance of *Proteobacteria* was significantly different between the two transect sites

(mean difference=16.37%; p-value=0.0001, 95% confidence interval). The abundance of *Planctomycetota* was also significantly different between the two transect sites (mean difference=32.47%; p-value=<0.0001, 95% confidence interval). The abundance of all other phyla was not significantly different between the two transect sites. At OTU level, the relative abundance of 10 OTUs were statistically different as measured by 2-way ANOVA (all p-values=<0.0001, 95% confidence interval). Statistically different OTUs were comprised of Mitrotrichales_unclassified, Bacteria_unclassified, Pirellulaceae_unclassified, Alphaproteobacteria_unclassified, Arenicellaceae_ge, Arenicellaceae_unclassified, Coxiella, Gammaproteobacteria_unclassified, an 'uncultured' OTU belonging to the Gimesiaceae family and an uncultured OTU belonging to the Legionellaceae family. Similar analyses were conducted at phylum and OTU level between sediment samples from each transect. At phylum level, only the presence of Proteobacteria was significantly different between the two transect sites (mean difference=4.347%, p-value=<0.0001, 95% confidence interval). At OTU level, the relative abundance of 3 OTUs were statistically different as measured by 2-way ANOVA (all p-values=<0.0001, 95% confidence interval). Statistically different OTUs were comprised of Bacteria_unclassified, wb1-A12 and Alphaproteobacteria_unclassified.

A Principal Co-ordinate Analysis (PCoA) based on Bray-Curtis distance was performed for relative abundance data obtained from sponge and sediment OTUs (**Figure 4.9A**). A total of 87.2% of the difference between samples could be displayed on two axes. A further 7.4% could be explained by a third axis, bringing the total to 94.6% of the difference. A scree plot for the ordination is included in **Appendix, Figure S7**. Sediment samples clustered together more closely with each other than with a

single sponge sample from either transect. Sponge_010 and Sponge_011 clustered more closely than with Sponge_009, or with sponges from transect T07. Sponge_027 and Sponge_028 clustered together more closely with each other than with sponges from transect T52, excluding Sponge_009. Sponge_009 clustered more closely with sponges from transect T07.

Estimates of samples richness and diversity were carried out on abundance data for sponge and sediment samples. Sediment samples from both transects displayed higher species richness, as estimated by Chao1 Index (**Figure 4.9B, Left**). Sediment samples from T07 displayed a higher range in Chao1 richness than sediment from T52. Sponges from T52 displayed a higher range in Chao1 richness than sponges from T07.

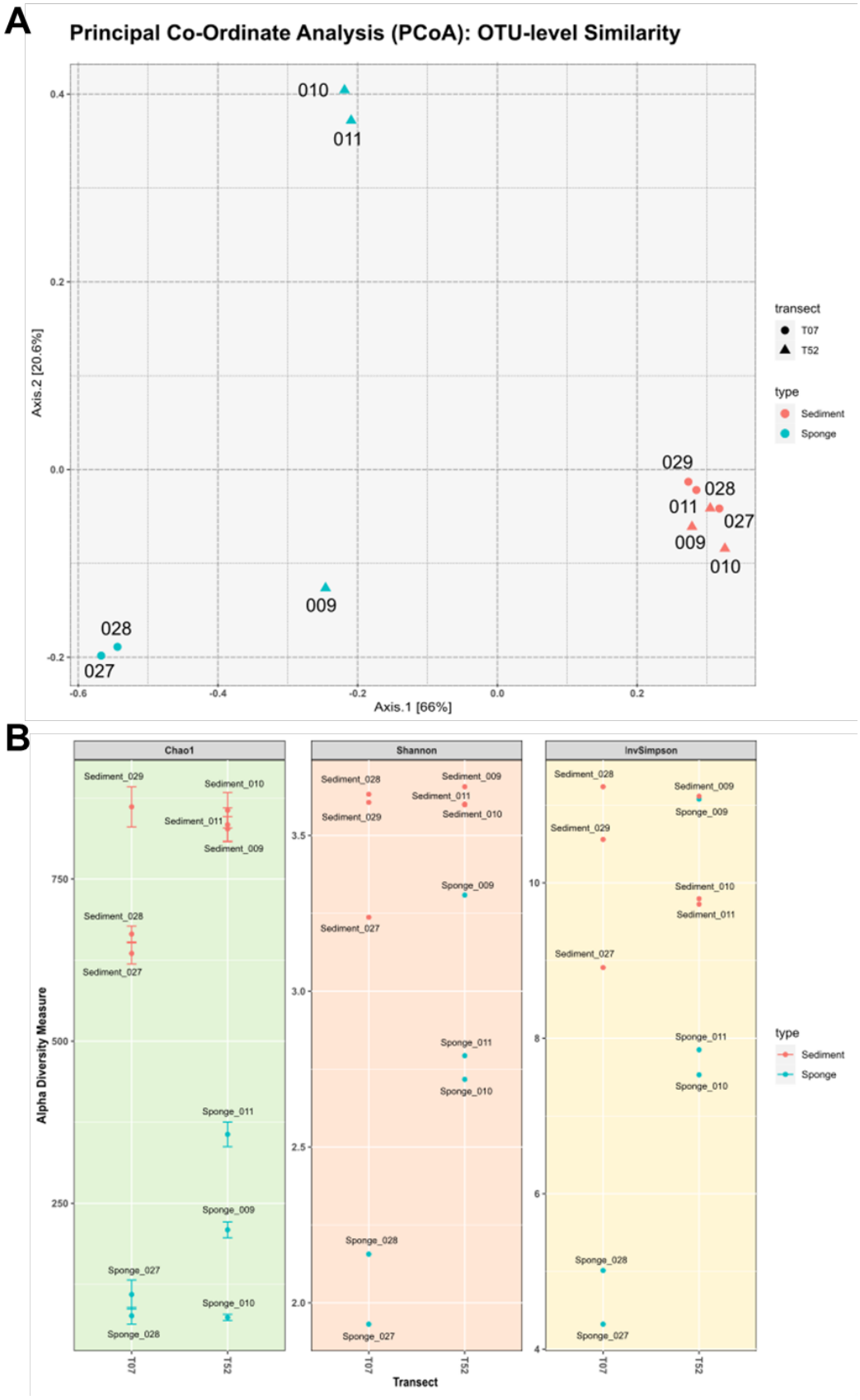

Figure 4.9 – A) Principal Co-Ordinate Analysis Plot based on the relative abundance of all OTUs in each sponge and sediment sample community. Numbers on graph refer

to the ID for each sample. Colour depicts sample type (sponge; sediment). Shape depicts sample site (T07; T52). **B)** Alpha Diversity (Chao1; Shannon; Inverse-Simpson) indices based on true (non-relative) abundance values of each sample. All plots were constructed using in R using the phyloseq package.

When less statistical weight was given to rare taxa (as in Chao1), all sponges from T52 displayed a higher richness than sponges from T07, as measured by Shannon Index (**Figure 4.9B, Middle**). Sponge_009 displayed a higher richness than Sediment_027. When more weight was given to dominant OTUs (InvSimpson), Sponge_009 displayed a higher richness than Sediment_010 and Sediment_011 from the same transect (**Figure 4.9B, Right**). Higher InvSimpson values are also associated with lower evenness scores and therefore Sponge_009 displays much lower community evenness than Sponge_010 and Sponge_11. In general, sediment samples displayed a higher species richness than sponge samples, across all diversity indices.

4.3.6 Sponge samples contain 'core' and sample-specific microbiota

Characterisation of the 'core' microbiota was compared using replicate thresholds (100% and 80%) and relative abundance thresholds. The replicate threshold percentage represents the percentage of sponge replicates that an OTU must be present in to be considered part of the core microbiota. The relative abundance threshold represents the average relative abundance of a particular OTU within the microbiota of all samples. Core and sponge-specific OTU analyses were performed on reads obtained after a single amplification, in order to provide a direct comparison to sediment samples collected from the same sites.

At a 100% replicate threshold, 17 of 406 OTUs (4.2%) occurred in all sponge samples, representing the 'core' microbiota. At an 80% replicate threshold, the sponge core microbiota was comprised of 32 OTUs (7.9%). Details of these OTUs are contained within **Appendix, Table S4**. Core OTUs at both replicate thresholds were made up of 5 different phyla (Actinobacteria, Bacteroidota, Dependentiae, Planctomycetota, Proteobacteria) and one OTU classified as 'Bacteria_unclassified'. Of the 17 OTUs, 9 were also included in the OTUs for which relative abundance differed significantly between the two transects. At the 100% replicate threshold, the relative abundance of the core microbiota as a whole made up between 62.1 - 93.6% of their respective microbiota. At an 80% replicate threshold, core OTUs made up between 65.8 – 95.4%. Individual core OTUs had an average relative abundance of between 0.005 - 35.4% in their respective microbiota (at both replicate thresholds). Altering the replicate threshold from 100% to 80% did not have an impact on the number of phyla that comprised the core OTUs (**Figure 4.10A**). Two core OTUs (Cyclobacteriaceae_unclassified; Planctomycetota_unclassified) had an average relative abundance of <0.1% in at least one sponge. The number of OTUs that had a relative abundance of either ≥10%, ≥1%, ≥0.1% or ≥0.01% are displayed in **Figure 4.10B**. Only 3 core OTUs had an average relative abundance of ≥10% (Pirellulaceae_unclassified; Alphaproteobacteria_unclassified; Gammaproteobacteria_unclassified).

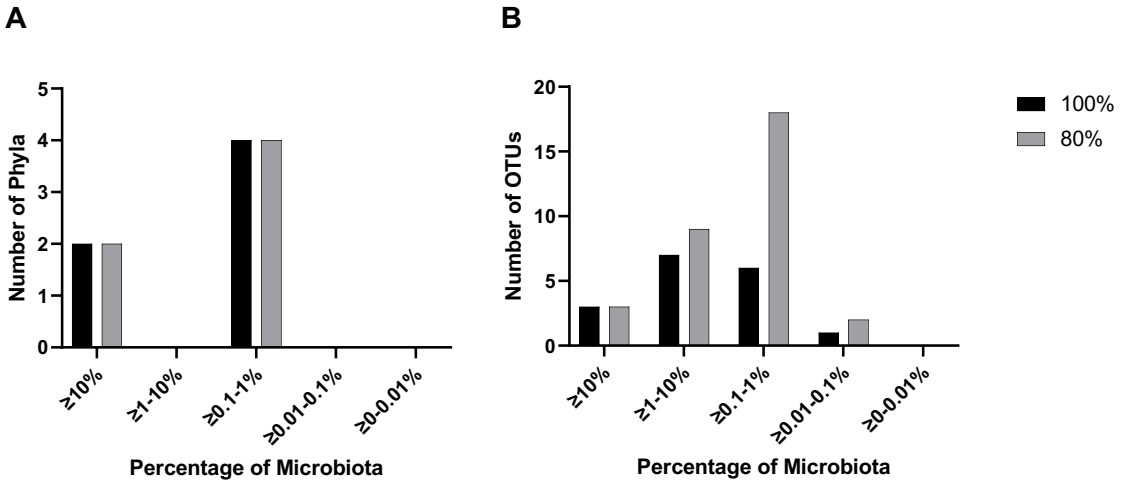

Figure 4.10 – The *Pheronema carpenteri* core microbiota. **A)** Number of phyla in the core microbiota that were represented by OTUs at various relative abundance thresholds. **B)** Number of OTUs in the core microbiota that had relative abundances above various thresholds. Abundance thresholds represent average abundance for each OTU across all samples.

There were 51 of 406 OTUs (12.6%) that did not occur in water and sediment samples that occurred in at least one sponge sample, representing 'sponge-specific' OTUs. The combined relative abundance of sponge-specific OTUs made up between 0.03 - 6.3% of their respective microbiota. There were no core OTUs at either 100% or 80% replicate threshold that did not also occur in at least one sediment or water sample. This demonstrates that no members of the core microbiota were sponge-specific OTUs. Sponge-specific OTUs were members of 8 different phyla (Actinobacteria, Bacteroidota, Cyanobacteria, Firmicutes, Patescibacteria, Planctomycetota, Proteobacteria, Verrucomicrobia). Of these phyla, none were found exclusively in sponges. The number of phyla and individual OTUs that had an average relative abundance of either ≥10%, ≥1%, ≥0.1% or ≥0.01% are displayed in **Figure 4.11A** and

Figure 4.11B, respectively. The majority of sponge-specific OTUs (82.4%) had an average relative abundance of <0.1%. Only 2 sponge-specific OTUs had an average relative abundance of ≥1% (Cutibacterium; Enterobacteriaceae_unclassified). No sponge-specific OTUs had an average relative abundance of ≥10%.

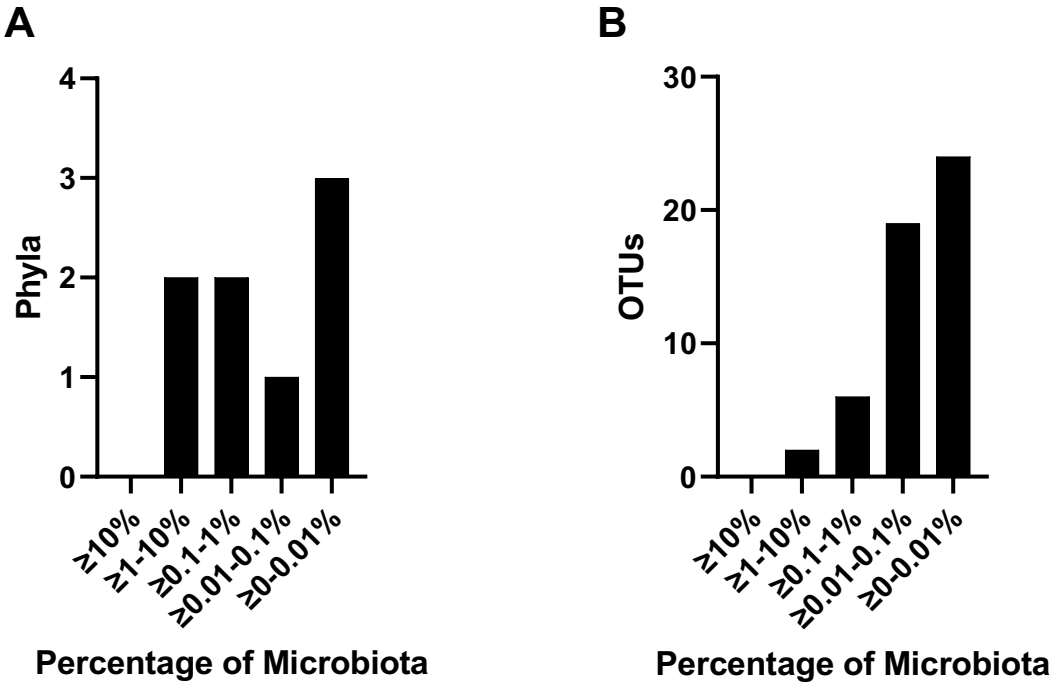

Figure 4.11 – The *Pheronema carpenteri* (sponge)-specific microbiota. No phyla were observed to be sponge-specific. **A)** Number of phyla that were represented by sponge-specific OTUs at various relative abundance thresholds. **B)** Number of sponge-specific OTUs that had relative abundances above various thresholds. Abundance thresholds represent average abundance for each OTU across all samples.

4.3.7 Sediment samples contain 'core' and sample-specific microbiota

The sediment core and sediment-specific microbiota was analysed in the same way as sponge samples. The replicate thresholds for core OTUs however were set at 100%

and 83.33% due to the inclusion of an additional sediment sample (Sediment_029), providing a total of six samples.

At the 100% replicate threshold the sediment core microbiota was composed of 41 phyla, and 451 of the 1014 OTUs (44.5%) were detected in sediment samples. At the 83.33% threshold it was comprised of 555 OTUs and 43 phyla (**Figure 4.12**). The change in replicate threshold had an effect on the number of phyla present in the core microbiota, however only at the abundance threshold of <0.01%. An additional 104 OTUs were included in the core microbiota at the 83.33% replicate threshold. The 451 core OTUs also contained the 3 OTUs for which relative abundance was significantly different at each transect site. The majority (80%) of sediment core OTUs had an average relative abundance of <0.1% at the 100% replicate threshold level. At the 83.33% replicate threshold this percentage was increased to 83.8%, 47.7% of which had an average relative abundance of <0.01%. Only 2 OTUs had an average relative abundance of >10% at either replicate threshold (Actinobacteria_unclassified and Bacteria_unclassified). The sediment core microbiota as a whole made up between 98.7 – 99.8% and 99.2 – 99.9% of the sediment microbiota, at 100% and 80% replicate thresholds, respectively.

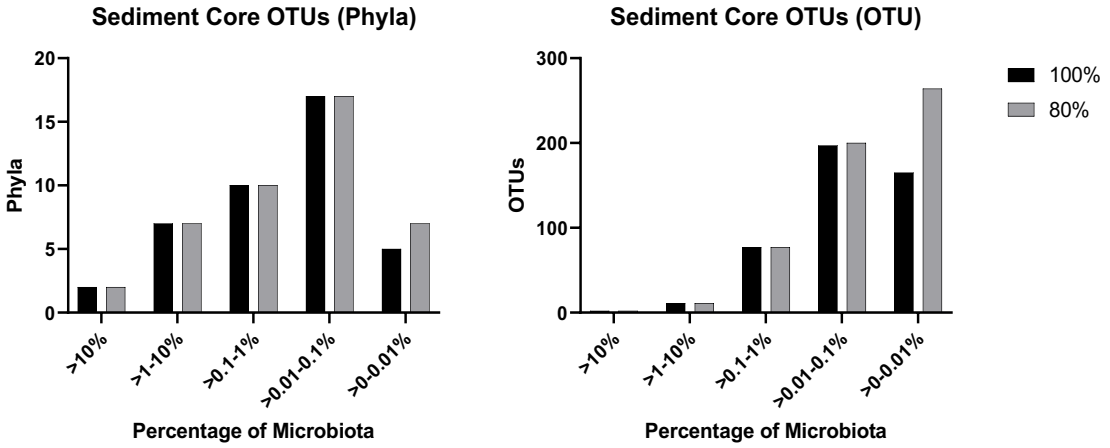

Figure 4.12 – Sediment core microbiota. **A)** Number of phyla in the core microbiota that were represented by OTUs at various relative abundance thresholds. **B)** Number of OTUs in the core microbiota that had relative abundances above various thresholds. Abundance thresholds represent average abundance for each OTU across all samples.

There were 659 of 1014 OTUs (65%) that were found in at least one sediment sample, that did not occur in sponges, representing the sediment-specific microbiota (**Figure 4.13**). The combined relative abundance of sediment-specific OTUs was between 3.4 – 5.4% of their respective microbiota. There were 193 OTUs that were sediment-specific OTUs that were also part of the core microbiota. This demonstrates that 42.8% of the core microbiota are also part of the sediment-specific microbiota. The majority (98.9%) of sediment-specific phyla were represented by OTUs that had an average relative abundance of <0.1%. In addition, 85.7% of these had an average relative abundance of <0.01%. No sediment-specific OTUs had an average relative abundance of ≥1%. There were 7 OTUs that had an average relative abundance of ≥0.1%. Individual sediment-specific OTUs made up between 0.0003 - 0.37% of their respective microbiota.

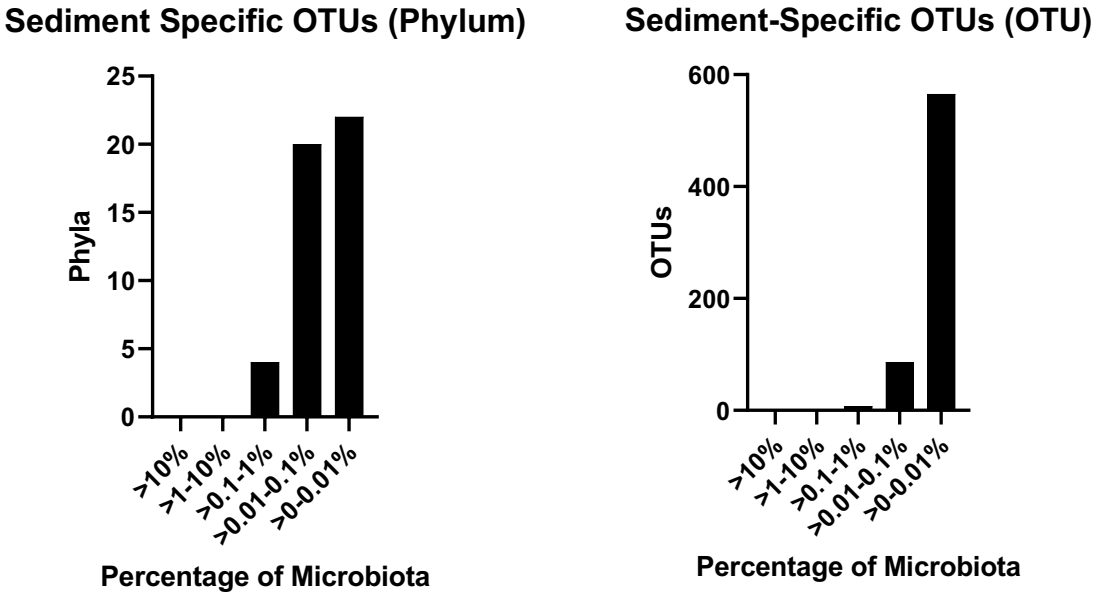

Figure 4.13 – The Sediment-specific microbiota. **A)** Number of phyla that were represented by sediment-specific OTUs at various relative abundance thresholds. **B)** Number of sediment-specific OTUs that had relative abundances above various thresholds. Abundance thresholds represent average abundance for each OTU across all samples.

There were 14 OTUs that were shared between the core microbiota of both sponge and sediment, indicating that they were present in every sample. A total of 6 of these OTUs were Proteobacteria, 3 were Planctomycetota, 2 were Actinobacteria, 1 was Dependentiae, 1 was Bacteroidota and 1 was designated as ‘Bacteria_unclassified’. There were 355 OTUs that were present in at least one sponge and one sediment sample, representing shared taxa. Shared taxa comprised between 94.6 - 99.96% of their respective microbiota. The names of all 51 OTUs present in the sponge-specific microbiota are contained within **Appendix, Table S4**.

4.3.8 Whole, core and sample-specific microbiota display different relative abundance distribution

The distribution of the average relative abundance of all sponge and sediment OTUs was explored, and is displayed in **Figure 4.14**. The sponge microbiota contained less OTUs than the sediment microbiota (406 OTUs compared to 1014)**.** The sponge microbiota had a higher mean OTU abundance (0.3% compared to 0.1%). The sponge core microbiota was comprised of a smaller percentage of the overall microbiota than the sediment core (4.2% compared to 44.5%). The sponge core microbiota had a higher mean average OTU abundance than the sediment core microbiota (4.5% compared to 0.2%). Both core microbiota contained the most abundant OTUs in their respective sample microbiota. The sponge-specific microbiota was comprised of a lower percentage of the total microbiota than the sediment-specific microbiota (12.6% compared to 65%). For both sponge and sediment, the core microbiota was comprised of less OTUs than the specific microbiota. In both cases, the core microbiota had a higher maximum, minimum and mean OTU abundance than the specific microbiota. In both cases, the core microbiota had a higher mean OTU abundance than the overall microbiota.

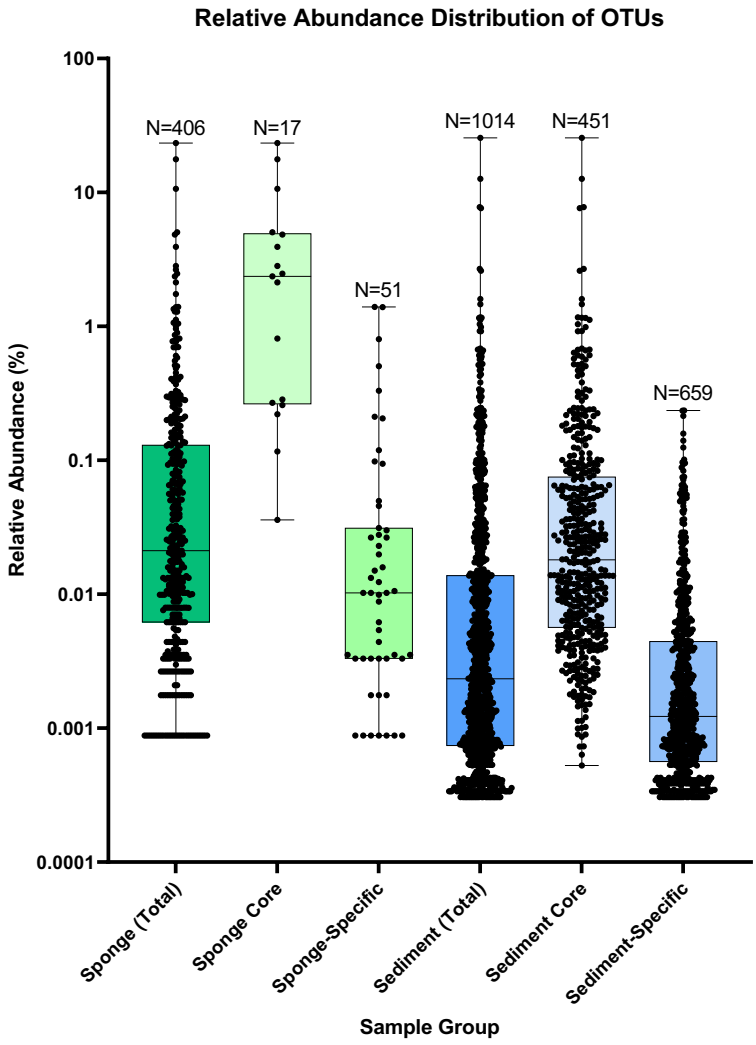

Figure 4.14 – Histogram to display the relative abundance distribution of OTUs in samples subsets (Total, Core, Specific). Box limits represent upper and lower quartiles. Middle line represents mean. Lines represent minimum and maximum. Core microbiota is given at a 100% replicate threshold.

4.3.9 Isolates from culture-based experiments are present in the *Pheronema carpenteri* and sediment metagenome datasets

The presence and relative abundance of bacterial genera cultured in **Chapter 2** within the *Pheronema carpenteri* microbiota was assessed (**Figure 4.15**). The presence of *Streptomyces* specific reads was also assessed in order to represent isolate A11 from **Chapter 3**. Where the presence of a particular genus was not detected in any sample, the lowest taxonomic level detected that the isolate belonged to was also included.

Of the 13 distinct cultured isolate genera, 7 were present in at least one sponge or sediment sample. A total of 5 were present in sponge samples, whereas 4 were present in sediment samples. The genera *Micrococcus, Dermacoccus* and *Kocuria* were present in sponges but not sediment samples. The most abundant cultured genera in any one sponge sample was *Psychrobacter* (0.68%). Reads pertaining to *Streptomyces* spp. were not detected in either sponge or sediment samples. The most abundant OTU in any one sediment sample was also *Pseudomonas* (0.003%). The cumulative percentage of OTUs that were represented by cultured isolates was between 0 – 0.72% for sponges and 0 – 0.0031% for sediment. When the presence of the closest taxonomic ranks to cultured isolates was considered, both Alphaproteobacteria_unclassified and Actinobacteria_unclassified were present in all samples. Bervibacteriaceae_unclassified were present in sponge samples but not sediment.

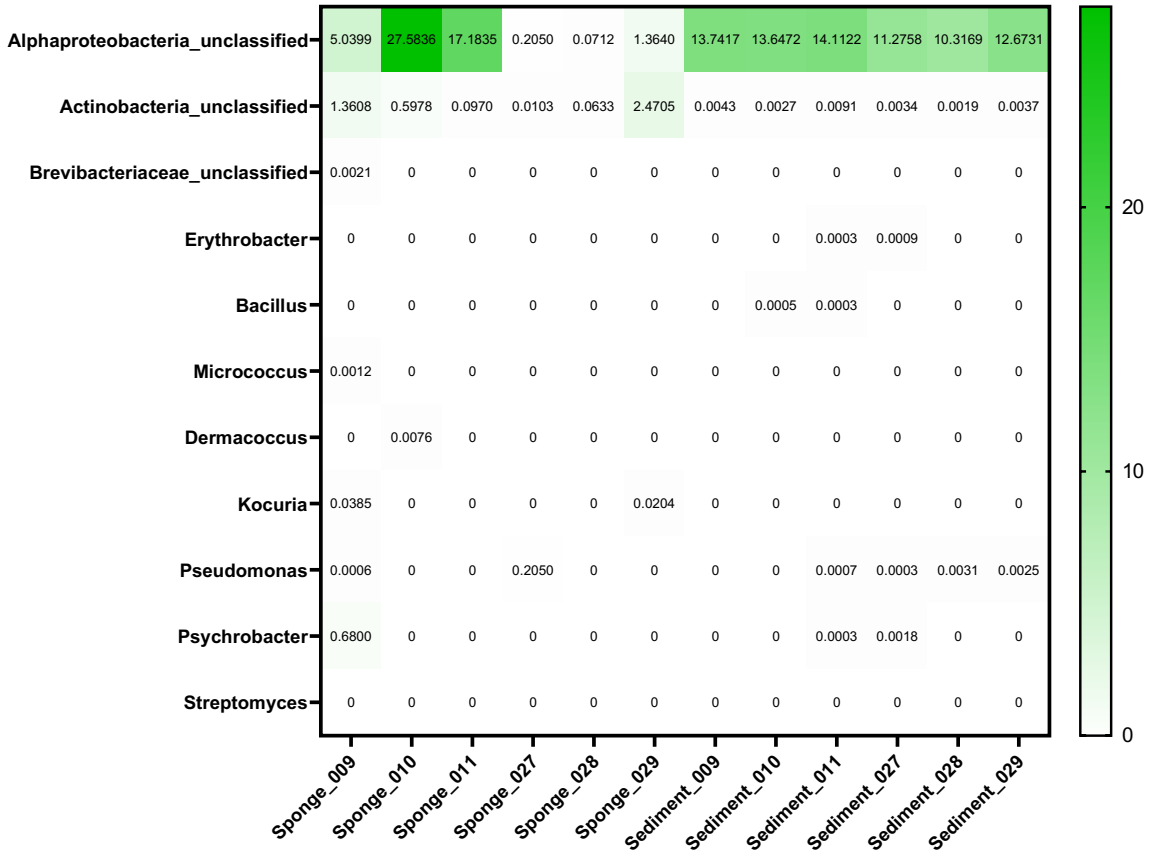

Figure 4.15 – Relative abundance of isolates cultured from *Pheronema carpenteri* within the sediment and sponge metagenome determined microbiota.

4.2 Discussion & Conclusions

Whilst the microbiota of many sponges of the Demosponge class have been characterised (43,189), only a handful of characterisations of the Hexactinellid microbiota have been carried out (86–88). In each case however, sequencing was performed using the Illumina platform (205). In this study, the first survey of the bacterial 16S rRNA gene associated with samples of the deep sea Hexactinellid sponge *Pheronema carpenteri* was carried out using the MinION sequencing platform (16,206).

The conversion of electronic signals into nucleotide bases has been shown to lead to an increased error rate for the MinION sequencing platform (~5%), when compared to other currently available sequencing technologies (16). A report from 2015 stated that error rates for sequences derived from Nanopore sequencing at the time were between 5-40% (207), which demonstrates the ongoing improvement in sequence classification over the last 5 years. Improvements in the conversion of electrical signals, as well as in the alignment of longer reads continue to lead to improved sequence classification (200), and may allow retrospective analyses of data currently being obtained. Questions still exist however concerning the accuracy of base-calling using the MinION platform. In this study, reads from several samples were obtained over multiple sequencing runs. In order to identify where differences in sequence classification may have been caused by the choice of sequencing platform, the taxonomic classification of the same sponge sample sequenced across two sequencing runs was compared. Current estimated error rates for the MinION sequencing platform are ~5% (16).

In general, differences attributed to the sequencing run were relatively small. For two of three sponges, all differences in phylum-level classification were <1%. For the third

sponge, all differences were <1%, excluding the Dependentiae and reads that were 'Unclassified' (i.e. those that were classified as bacteria at kingdom level but could not be assigned a phylum). These two groups differed by 1.4% and 2.2%, respectively. Sponge_029, for which marginally higher differences in taxonomic classification were observed, was collected from a different sample site than the other two sponges. It therefore appears that reads from samples generated over two MinION sequencing runs can be considered similar enough to combine them for downstream analyses. General differences between the composition of the sponge microbiota at each site may also have a part to play in affecting the accuracy of classification over runs, which will be discussed in more depth later. It should also be noted that of the three sponges, the lowest number of reads was obtained for Sponge_029, which may in part have lowered the accuracy of the overall microbiota classification. Whilst the analysis of MinION sequencing accuracy here was not based on classification of a mock microbiota of known sequences or through reference to a dataset generated using an additional platform, the results obtained help provide some information as to the reproducibility in sequence classification over several runs. The overall similarity in taxonomic outcome for each run was judged sufficiently close for reads from each run to be combined for downstream analysis, providing one set of reads for each sponge.

The reads compared above were derived from DNA samples amplified twice prior to sequencing. Reads were also obtained from DNA templates that were amplified only once, providing an opportunity to compare the effect of an additional PCR step on taxonomic classification. Difference in relative abundance at phylum level could be traced to particular OTUs, with the OTUs that were changed by ≥1% following a second amplification being representative of the phyla that were also changed. It is

interesting however that the particular OTUs that were increased or decreased by ≥1% were not, in general, the same for both sponge replicates.

For both sponges, half the OTUs that were amplified by ≥1% after a second PCR were not present in the sample after only a single amplification. In addition, the majority of the same OTUs could not be classified more accurately than at Class level. Preferentially amplified sequences did not display a significantly high, or low GC-content, or represent the most abundant OTUs in the sample after a single amplification. Sequence processing also contained a chimera identification and removal step. Therefore, whilst steps were taken to remove the presence of spurious sequences it is possible that the over-represented sequences may not represent true taxa present in the sponge microbiota. Alternatively, it may be the case that a high number of 'unclassified' sequences represent rare taxa within the microbiota that are the result of poor coverage within reference databases (208). This may also explain why such OTUs were not identified after only a single amplification step.

The use of a second amplification also reduced differences observed between the microbiota of sponge replicates, making the taxonomic outcome more similar. Given the proposed amplification of 'junk' sequences outlined above, it was judged that the microbiota obtained after a single PCR amplification was a more accurate representation of the true flora. Further analysis of the differences between sponge and sediment microbiota was therefore based on reads obtained after a single amplification.

The data for the microbiota determined by 16S rRNA gene sequencing in this study were obtained from sponge tissue taken from the inner chamber of *P. carpenteri*, as it was hypothesised that this would represent the more stable, or less 'transient'

microbiota. The large amount of marine debris present on the outside of the sponge sample was assumed to be made up in part of SSC and other debris. Whilst microbial 16S rRNA information was not obtained for the outer layer of *P*. *carpenteri*, a comparison between the sediment and inner layer microbiota will help to distinguish the overlap between the sediment microbiota and sponge resident microbiota. The efficient filtration rates mentioned above suggest that there may be a low overlap between sediment microbiota and that of the inner sponge membrane.

The *P. carpenteri* microbiota was found to contain fewer OTUs than the sediment microbiota (406 compared to 1014). A higher intra-sample diversity was observed in sponge species, however, with a larger difference between the relative abundance of OTUs present in each sample. The sediment microbiota displayed an overall higher similarity between the presence and relative abundance of each phyla in each sample, as measured by Pearson's Correlation Co-efficient and 2-way ANOVA testing. In a comparison of the microbiota of the deep-sea Hexactinellid sponge *Vazella pourtalesii* and a sediment microbiota, *V. pourtalesii* was also found to display a much wider intra-species dissimilarity than the sediment microbiota (88). Several other studies, whilst not looking at intra-species dissimilarity as directly have documented a higher intra-species dissimilarity for Hexactinellid sponges in general, when compared to Demosponges (43,87).

In comparing the specific phyla that were more prevalent in the sediment microbiota, similarities with those demonstrated by Busch *et al*. in sponges obtained from the Scotian Shelf (Canada) can be observed (88). Several phyla, including Acidobacteria, Bacteroidota, Chloroflexi, Gemmatimonadetes, Latescibacteria, Nitrospirae and Nitrospinae were enriched in sediment samples, compared to sponges. The sediment samples analysed by Busch *et al*. (88) show remarkable overlap with those analysed

here, in which the majority of the same phyla were also enriched. The most notable discrepancy however was in the presence of Chloroflexi, which whilst being one of the most abundant phyla in the Busch sediment samples was not observed in sediment samples analysed here. The Chloroflexi have also been reported to be abundant and diverse members of the Demosponge microbiota (209) as well as being considered an indicator taxa for HMA sponges (93) with a potential role in the degradation of organic matter (210). The observation that they were not abundant members of the microbiota of the samples analysed here may suggest that this role is performed by an alternate microbial symbiont. Without a further functional analysis of these microbiota however, this is currently unknown. In each case, Proteobacteria was the most abundant phyla in both sponge and sediment samples – a trend that has been reported for sponge microbiota in general (43,189). The composition of the *P. carpenteri* microbiota also shows similarity to that of 7 other Hexactinellid species previously analysed (87). Whilst there were differences between each microbiota characterised, the major phyla that were enriched in Hexactinellida (compared to Demosponges) were Proteobacteria, Bacteroidota, Nitrospinae and Planctomycetota. In general, the major phyla present in the *P. carpenteri* microbiota, from most to least abundant were Proteobacteria, Planctomycetota, Actinobacteria, Bacteroidota and Acidobacteriota. Firmicutes also made up 14% of the microbiota of Sponge_009, but made up only 0-2.4% of the other sponges analysed. This may be a result of differentiation between the microbiota of *P. carpenteri* replicates in general, however may also be attributed to sample contamination. The variable presence of Planctomycetes within the *P. carpenteri* microbiota is of particular note, as it has been identified as one of three ‘indicator taxa’ that are associated with the microbial abundance of the sponge host (189). Planctomycetes, along with Proteobacteria and

Bacteroidetes were associated with Low Microbial Abundance (LMA) sponges and were also the second most dominant phylum in the Hexactinellid sponge *Inflatella pellicula* (211). Interestingly, Actinobacteria have been associated with HMA sponges (93). Actinobacteria was one of the phyla that also featured prominently in the *P. carpenteri* microbiota, yet it also displayed a higher variation in intra-sample relative abundance. Actinobacteria is also not a phylum seen in as high abundance in other Hexactinellid sponges (87,88), and may be a factor associated with *Pheronema* sponges. It may also help to explain why *P. carpenteri* has produced more 'active' isolates in this study than the *Hertwigia* sp. samples. Actinobacteria derived from soil have been a historic source of novel antimicrobial agents (14) and comparisons may be made here with the global soil microbiota, in which Actinobacteria are a major constituent (212). A finding from this study that potentially supports this is the number of isolates belonging to the phylum Actinobacteria that were recovered in **Chapter 2**, with demonstrated antimicrobial activity in several of these isolates. Such claims are inconclusive however, as not all isolates grown in the course of this research were identified by 16S rRNA profiling.

By comparing community overlap between the *P. carpenteri* and sediment microbiota at OTU level it is possible to determine which OTUs represent sponge-, or sediment-specific microbiota. Additionally, it is possible to determine which taxa represent the sponge, or sediment 'core' microbiota. The core sponge microbiota has been previously analysed using several descriptions: OTUs which occur in 66% of sponge replicates that also have a relative abundance of >0.01% (51); OTUs that occur in either 70% (49), or 85% (43) of sponge replicates; and OTUs that occur across all sponge replicates (213). Changing the definition of the core microbiota has been found

to significantly alter the number of OTUs that comprise it (214), but not necessarily the taxonomic composition at phylum level (215). When considering the effect of sponge species, altering the threshold for the percentage of replicates in which an OTU must be present was found to impact the number of OTUs in the core microbiota, only when the definition was changed to require 90-100% (215).

The *P. carpenteri* core microbiota was comprised of 17 OTUs that occurred across all 5 replicates. Of these OTUs only a handful were classified down to genus level, indicating that they may not represent true bacterial species, or potentially that they represent unknown microbial taxa for which there is no current classification (216). This observation also applies to the classification of microbiota as a whole. Relaxing the threshold to OTUs that occurred in at least 80% of replicates increased the number of core OTUs by 15, but did not increase the number of phyla included in the core microbiota, which is congruent with previous findings (215). The sponge core microbiota was much smaller than that of the sediment in terms of number of taxa, which accounted for 44.5% of all sediment OTUs. The sponge core microbiota is generally not considered to contribute significantly to the sponge microbiota as a whole (43), which also appears to apply for *P. carpenteri.* The size of the core microbiota has also been found to be inversely correlated with the degree of overall intra-species community dissimilarity (217). The increased intra-species dissimilarity that has been reported for several Hexactinellid sponges (87) may, therefore, mean that Hexactinellid sponges have smaller core microbiota. The small size of the *P. carpenteri* core, as well as the high degree of intra-species dissimilarity appears to support this proposal. The inverse correlation of intra-species dissimilarity and core microbiota size also appears to hold true for the sediment samples analysed in this

study, as sediment microbiota displayed a notable similarity, and also had much larger core microbiota.

The *P. carpenteri* core microbiota had only a 0.73% overlap with seawater and 3.4% with sediment. A high overlap (50%) between the core microbiota of several shallow-water sponge species with that of seawater has previously been reported (213) a figure that is much higher than that observed here. For both 80% and 100% replicate thresholds, only a small number of the OTUs that comprise the *P. carpenteri* core microbiota are 'rare taxa' (<0.01% abundance) (83). This was distinct from the sediment core microbiota, in which the relative abundance of OTUs was increased for lower abundance/rare taxa. Members of the rare sponge taxa have previously been found to make up over 90% of all OTUs identified in *Hexadella* and *Mycale* sponges (83). Here however, the percentage of rare taxa was much smaller, with the percentage of rare taxa being between 0 – 35.7%. It should be noted however that sponges for which the number of rare taxa was 0% were also the samples which had a lower number of reads, which may have impacted the detection of rare taxa. Rare taxa in sponges have previously been observed to show high host-specificity (83). Comparison with other sponge species was not carried out for the *P. carpenteri* microbiota, however the majority of sponge-specific OTUs were also found to be rare taxa, for both sponge and sediment samples in this study.

The *P. carpenteri*-specific microbiota made up only 12.6% of the overall microbiota. The sponge-specific microbiota is thought to comprise the majority of each of sponge microbiota in general (43), with previous reports showing that 70 - 90% of taxa were sponge-specific (49,218). The same has also been reported for several species of

Hexactinellid sponge (87). The results here potentially suggest that *P. carpenteri* does not follow the same trend, however it may display a higher proportion of specific microbiota when directly compared to other sponge species, rather than sediment. The number of OTUs shared between sponge and sediment samples was much higher than the number of sponge-specific OTUs. A possibility may be that these shared OTUs are the result of horizontal transfer (219), whereas the sponge-specific microbiota are the result of vertical transfer (220). Sample-specific microbiota however may also be the result of acquisition of low abundance OTUs from seawater that were not detected due to poor DNA recovery or sequencing depth (213). The high percentage of sponge OTUs that were shared with sediment may also be a result of the facets of Hexactinellid biology, sediment slumps and pumping rate cessation outlined above. A direct comparison between hexactinellid sponges that display anchoring to the sediment floor with those that do not would be a potential way to further explore this hypothesis.

The lack of overlap between core and sponge-specific OTUs in the *P. carpenteri* microbiota is perhaps at odds with previous research that has detailed the high overlap apparent in the microbiota of *Cliona delitrix* (221)**.** Sponge core OTUs in general however are comprised overall of 'generalist' or non-sponge specific OTUs (43).

The inclusion of sponge and sediment samples from two sample sites allowed investigation of whether the microbial communities differed at each site. Whilst the *P. carpenteri* microbiota was not statistically different at each transect, there were several OTUs for which the relative abundance was significantly different at each site. Interestingly, the majority (9/10) of the OTUs that were different were also present in the core microbiota. The same trend was also observable for the sediment microbiota,

albeit with fewer statistically different OTUs. All 3 different OTUs were also present in the core microbiota. Several of the statistically different OTUs could be classified to genus level, however the majority could not. It may be the case that genomic library quality has a part to play in determining the number of reads that could not be classified and these figures, therefore, may not represent true differences in microbiota at each transect site. The use of 'relative abundance' reduces the statistical bias caused by differences in DNA quantity (i.e. by ignoring the number of passed-reads for each sample), however it cannot completely compensate for differences in sample quality (222). It is feasible however that differences in the composition of the microbiota of each sponge replicate would influence the rate and quality of DNA retrieval and, therefore, differences may also be a reflection of this. This however is highly speculative. In general, sponges from each transect grouped more closely with each than with other sponges (PCoA) and had higher correlation scores. The exception to this was Sponge_009, which displayed higher similarity to sponges from transect T52.

The *P. carpenteri* and sediment microbiota were screened for the presence of isolates obtained from culture-dependent studies (**Chapter 2 & 3**). When the sequence obtained for each isolate's 16S rRNA gene was classified using the same database as the *P. carpenteri* microbiota reads, 7 of the 13 different cultured OTUs were present in the *P. carpenteri* microbiota. The absence of 6 OTUs may be due to the fact that such isolates represent either extremely rare taxa that weren't detected in the microbiota, or contaminants that do not represent true sponge taxa (64).

The total relative abundance of isolates made up 0 – 0.72% of the *P. carpenteri* microbiota. Previous estimations of the cultivable portion of the host sponge microbiota have ranged from between 0 – 14% (57,60,81). The figures obtained here may serve

as an initial indication of the cultivable proportion of *P. carpenteri*, however taxonomic classification was not performed on all isolates obtained so this is therefore not an exhaustive study. Sequencing depth is also undoubtedly a factor in estimating this percentage. The presence and abundance of cultured OTUs was perhaps more consistent across replicate sediment samples and may be indicative of the higher intra-sample similarity of the sediment microbiota. The higher intra-species dissimilarity of *P. carpenteri* also perhaps suggests that different, or a higher diversity of isolates may be obtained from performing culture-dependent studies on multiple biological replicates of *P. carpenteri* sponges.

The presence of OTUs that correspond to isolate A11 (**Chapter 3**) was not detected in either the *P. carpenteri* or sediment microbiota; no reads from either sample were classified as *Streptomyces* at the genus level. In fact, the entire class of Actinomycetes was absent from the metagenome of all samples. This again may be due to such isolates representing rare or non-sponge/sediment taxa. Another reason may also be the bias implicit in PCR amplification against high and low GC-content sequences (223,224) - as *Streptomyces* are known and commonly-referred to as 'high GC-content' bacteria (225). *Streptomyces* are the most commonly cultured (and 'bioactive') members of the Actinobacteria from sponge-specific studies (1). Whilst the presence of Actinobacteria in the sponge microbiota in general is well documented (23), to the best of the author's knowledge, specific molecular studies detailing the presence of the *Streptomyces* genus within sponge microbiota are lacking (35).

This is the first study reporting the molecular profiling of the microbiota of *P. carpenteri*. Overall, *P. carpenteri* displays a microbiota that is congruent with that of the global sponge microbiome at phylum level (43), and with previous studies of Hexactinellid

sponges (87). The majority of the *P. carpenteri* microbiota consists of OTUs that are shared with sediment, however it has a distinct microbiota in terms of taxonomic composition, has a smaller core, and a smaller sponge-specific microbiota. The presence of cultivated isolates within the *P. carpenteri* microbiota was demonstrated, indicating that culture-dependent studies are to some extent successful in obtaining sponge-associated bacteria for the purposes of natural product discovery.

Chapter 5

Final Discussion & Conclusions

5.1 Discussion

Two species of Hexactinellid sponge were investigated in this work. The two sponges were initially assessed using a culture-dependent approach, revealing differences in cultivable bacteria and the presence of isolates with antimicrobial activity. In the case of *Pheronema carpenteri*, culture-independent approaches were also used in order to reveal the composition of the microbiota as a whole, as well as demonstrate a high intra-species dissimilarity, when compared to sediment microbiota. The sponge microbiota in general is thought to be shaped most strongly by a combination of host identity, geographic location and temperature (48–51). Differences in the overall sponge microbiota can be observed at a species level (43), as well as between sponges belonging to different classes (87,88). Intra-species dissimilarity with sponge microbiota was first revealed by large-scale studies characterising the microbiota of numerous sponge replicates (43). Studies characterising the Hexactinellid microbiota have also provided an early indication that intra-species dissimilarity may be more pronounced in glass sponges when compared to Demosponges (87).

The *Hertwigia* sp. and *P. carpenteri* samples used in this work displayed different cultivable microbes, with an overall low degree of overlap between the morphotypes obtained from sponge replicates of each sponge species. A higher number of bacteria was cultivated from *Hertwigia* sp., which also displayed a higher overlap in the morphotypes cultured. This overlap may be due to a more conserved microbiota overall, however may apply to just the portion of the microbiota that was capable of being cultured. The markedly low overlap in cultivable microbes from *P. carpenteri*, a finding which could be explored by further optimisation of culture parameters, provided a preliminary indication that *P. carpenteri* possesses a higher intra-species dissimilarity at microbiota level. This information, combined with the higher number of

active isolates from *P. carpenteri* also suggests that the microbiota of *Hertwigia* sp. and *P. carpenteri* are to a certain extent distinct.

The composition and intra-species dissimilarity inherent in the *P. carpenteri* microbiota was further explored using a culture-independent approach. *P. carpenteri* was found to possess a much higher intra-species dissimilarity than sediment samples collected from the same transect during the same sampling event. The high degree of intra-species dissimilarity, as well as the contrast between the *P. carpenteri* and sediment microbiota is thought to be due to a combination of glass sponge biology, sponge-sediment interactions, filtration and pumping habits (2,190,192).

In addition to the higher intra-species dissimilarity, *P. carpenteri* also contained a much smaller microbiota, core and sponge-specific microbiota than sediment. The core microbiota of *P. carpenteri* was comprised of a small number of OTUs, the majority of which had a relative abundance of >1%. This is in contrast to sediment, which had a larger core that was made up mainly of OTUs with a relative abundance of <0.1%. The high intra-species dissimilarity is consistent with reports that this may be a feature of Hexactinellid microbiota in general (87). The phyla for which *P. carpenteri* was enriched were also consistent with the phyla that were enriched in the *Vazella pourtalesii* microbiota when compared to sediment (88). These results indicate that the *P. carpenteri* microbiota is distinct in its structure from that of the surrounding environment, however it shows a degree of overlap with the sediment microbiota in terms of shared OTUs. The overlap in shared OTUs suggests that sediment microbiota may also be a potential reservoir of novel antimicrobial candidates. A culture-independent characterisation of the *Hertwigia* sp. microbiota was not carried out due to the inability to obtain sufficient quantities of DNA template. Whether the extremely low amount of genomic material obtained from *Hertwigia* sp. is reflective of a small or

low-microbial-abundance (LMA) microbiota (93) is unknown. It is also difficult to suggest whether *P. carpenteri* may be classified as an HMA or LMA sponge based on the data presented here, as bacterial concentration per sponge weight was not looked at specifically. In addition, the variable presence of the three taxa commonly indicative of LMA or HMA sponges prevents a definitive conclusion. Further work would be recommended in order to explore this.

Sponge-associated microbes have been targeted for characterisation owing in part to their importance in ecological processes (52), but also their ability to produce antimicrobial agents (41). Several isolates displaying antimicrobial activity were obtained from both *Hertwigia* sp. and *P. carpenteri*. Whilst a higher overall number of morphotypes were obtained from *Hertwigia* sp., a higher number of the morphotypes obtained from *P. carpenteri* displayed antimicrobial activity.

An isolate belonging to the *Streptomyces* genus was selected for downstream characterisation. The isolate was obtained from *P. carpenteri* and was selected on the basis of its antimicrobial production. Numerous studies have focused on cultivation of Actinobacteria from marine and freshwater sponges (23,31,35,54), as a means to identify isolates with antimicrobial activity (1). The Actinobacteria phylum, and in particular the *Streptomyces* genus are responsible for the highest number of antimicrobial candidates derived from sponge-associated bacteria (1). In addition, the second and third most prolific producers of antimicrobials from sponge-associated bacteria are the Firmicutes and Proteobacteria – which along with the Actinobacteria are the three most commonly cultivated phyla from sponges in general, and from *P. carpenteri* in this work. As further explored in **Chapter 4**, the presence of Actinobacteria within the *P. carpenteri* microbiota may also be indicative of further

general antimicrobial potential. In addition, numerous bacterial isolates were isolated that displayed antimicrobial activity, however were not followed owing to time and resource constraints.

The vast majority of bacterial isolates cultivated from *P. carpenteri* were found to be comprised of OTUs that had a relative abundance of <1% within the *P. carpenteri* microbiota. Some cultivable isolates represented OTUs that had a relative abundance of >0.1% as well as 0.001%. This suggests that cultivable isolates may be more likely to comprise members of the rare sponge biosphere (83). This phenomenon has been commented on previously (74). Members of the rare biosphere are thought to be those that play important 'supporting' roles in the essential ecological processes, and in maintaining the stability of microbiota in general (221). If this is true for the sponge microbiota then it may help towards explaining why sponge-associated bacteria have emerged as such a prolific source of antimicrobials in recent decades (41). Such claims may be expanded on with the use of metagenomic surveys attempting to localise the presence of biosynthetic gene clusters within the sponge microbiota as a whole. In addition, the fact that currently cultivable isolates represent such a small percentage of the overall microbial community, is perhaps promising. The same is true specifically for the sponges analysed in this study. The low percentage of cultured isolates as well as the high presence of Actinobacteria within the microbiota points towards their potential as promising sources of novel antimicrobial candidates for the future. The proposed undiscovered biological and chemical diversity in the deep sea (100) suggests that there is still a lot more to be discovered with regards to novel antimicrobial candidates.

With regards to the continuation of work presented herein, several opportunities exist to carry out further work. The preliminary work to assess the impact of pressure on the cultivability of sponge isolates presents a novel opportunity to further explore the presence of piezotolerant microbes and their biotechnological potential. The simulation of higher atmospheric pressures would presumably bring with it the potential to culture microbes adapted to life in the deep sea (226) and potentially reveal a new cultivable fraction of the true sponge-associated microbes (71). In order to generate pressures similar with that of the deep-sea sponge environment, work with researchers involved in industrial food processing may be a potential avenue for collaboration and would aid in the further exploration of expanding the cultivable portion of microbes from *Hertwigia* sp. and *Pheronema carpenteri* (227). Efforts at bacterial culture herein have led to the recovery and archiving of several strains with biotechnological potential. The further use of pressurised culture could be used to examine their ability to thrive in the deep-sea environment.

Additional work to explore the cultivable diversity of sponge-associated-microbes could also expand on the use of sponge-derived substrates in culture media, here investigated with the use of carnitine hydrochloride. The previous identification of adaptation by sponge microbes to utilise sponge-related factors (121) presents an interesting opportunity to retrieve microbes adapted to life in the sponge and deep-sea microenvironment. The ability of gut bacteria to utilise different metabolites, thereby reducing competition (228) raises questions as to whether this would be the same for the sponge microbiota.

The antimicrobial agent characterised herein is suspected to be a protease inhibitor with potential use as an antimicrobial as well as in biotechnological and industrial

processes. Low yield of the compound however prevented further *in vitro* characterisation. Further work that makes use of the OSMAC principle for optimising antimicrobial production (229,230) or bacterial cloning (231) may be of use in obtaining more material. With the availability of more antimicrobial agent, additional information regarding the cellular toxicity, haemolytic activity, chemical structure and full spectrum of use as a protease inhibitor could be explored. Nuclear Magnetic Resonance (NMR) would be recommended to identify the structure. Given that **C-A11** outperformed antipain, as well as appeared not to act in a dose-dependent manner potentially suggests that it acts by a separate mechanism. The differences between the genomic regions present in the A11 BGC and those present in the genome of *S. albulus* NRRL B-3066 also support this and suggest that it may be synthesised and exported from the cell in a different manner, providing the rationale for further investigation.

Further genomic analysis of strain A11 would also be recommended in order to explore the full range of antimicrobial metabolites it is capable of producing, as well as provide a more definite view on its status as a novel species.

The work conducted herein provided the first culture-independent look at the microbiota of *Pheronema carpenteri*. Future work to explore themes identified with the use of 16S rDNA community profiling could be used to provide a more comprehensive look at the sponge core and specific microbiota in comparison to other species of Hexactinellid sponge, as well as with other replicates of *P. carpenteri*. This would help to consolidate data obtained here and expand on current indications of a specific Hexactinellid, and deep-sea sponge microbiota (86–88,94).

Numerous 16S rDNA reads obtained for the *P. carpenteri* microbiota pertain to ‘uncultured’ and/or highly novel strains that are suspected to be marine-adapted. This

information could be used, alongside metagenomic sequencing for *in silico* mining of novel BGCs and ribosomally-encoded peptides that may be targeted for culture-independent synthesis and follow-up *in vitro* testing. Given the biotechnological potential of isolates identified herein, as well as in marine sponges in general, it is highly likely that metagenomic sequencing reads associated with *P. carpenteri* would contain regions encoding novel bioactive agents. Information obtained on the presence of BGCs within the microbiota could help to answer questions as to whether they are more likely to be found in certain OTUs in the *P. carpenteri* microbiota, and whether they occur in less, or more abundant OTUs. Such information could also help to inform future culture-dependent work as outlined above.

Overall, the two sponges explored in this work and their resident bacteria represent exciting repositories for the continued culture-dependent and culture-independent discovery of novel bioactive agents, as well as provide an opportunity to answer ecologically pertinent questions.

Bibliography

1. Indraningrat AAG, Smidt H, Sipkema D. Bioprospecting Sponge-Associated Microbes for Antimicrobial Compounds. Mar Drugs. 2016 May 2;14(5).
2. Leys SP, Mackie GO, Reiswig HM. The biology of glass sponges. Elsevier; 2007. p. 1–145.
3. Mangano S, Michaud L, Caruso C, Brilli M, Bruni V, Fani R, et al. Antagonistic interactions between psychrotrophic cultivable bacteria isolated from Antarctic sponges: a preliminary analysis. Res Microbiol. 2009 Feb;160(1):27–37.
4. Xin Y, Kanagasabhapathy M, Janussen D, Xue S, Zhang W. Phylogenetic diversity of Gram-positive bacteria cultured from Antarctic deep-sea sponges. Polar Biol. 2011 Oct;34(10):1501–12.
5. Jones SE, Elliot MA. “Exploring” the regulation of Streptomyces growth and development. Curr Opin Microbiol. 2018 Apr;42:25–30.
6. Maxson T, Tietz JI, Hudson GA, Guo XR, Tai H-C, Mitchell DA. Targeting reactive carbonyls for identifying natural products and their biosynthetic origins. J Am Chem Soc. 2016 Nov 23;138(46):15157–66.
7. O’Neill J. Tackling drug-resistant infections globally: final report and recommendations. 2016;
8. de Kraker MEA, Stewardson AJ, Harbarth S. Will 10 million people die a year due to antimicrobial resistance by 2050? PLoS Med. 2016 Nov 29;13(11):e1002184.
9. Ten threats to global health in 2019 [Internet]. [cited 2021 Sep 30]. Available from: https://www.who.int/news-room/spotlight/ten-threats-to-global-health-in-2019
10. Yong D, Toleman MA, Giske CG, Cho HS, Sundman K, Lee K, et al.

Characterization of a new metallo-beta-lactamase gene, bla(NDM-1), and a novel erythromycin esterase gene carried on a unique genetic structure in Klebsiella pneumoniae sequence type 14 from India. Antimicrob Agents Chemother. 2009 Dec;53(12):5046–54.

11. Liu Y-Y, Wang Y, Walsh TR, Yi L-X, Zhang R, Spencer J, et al. Emergence of plasmid-mediated colistin resistance mechanism MCR-1 in animals and human beings in China: a microbiological and molecular biological study. Lancet Infect Dis. 2016 Feb;16(2):161–8.
12. Karakonstantis S, Kritsotakis EI, Gikas A. Treatment options for K. pneumoniae, P. aeruginosa and A. baumannii co-resistant to carbapenems, aminoglycosides, polymyxins and tigecycline: an approach based on the mechanisms of resistance to carbapenems. Infection. 2020 Dec;48(6):835–51.
13. Chen L, Todd R, Kiehlbauch J, Walters M, Kallen A. Notes from the Field: Pan-Resistant New Delhi Metallo-Beta-Lactamase-Producing Klebsiella pneumoniae - Washoe County, Nevada, 2016. MMWR Morb Mortal Wkly Rep. 2017 Jan 13;66(1):33.
14. Lewis K. New approaches to antimicrobial discovery. Biochem Pharmacol. 2017 Jun 15;134:87–98.
15. World Health Organisation. 2020 antibacterial agents in clinical and preclinical development: an overview and analysis [Internet]. [cited 2021 Nov 19]. Available from: https://www.who.int/publications/i/item/9789240021303
16. Santos A, van Aerle R, Barrientos L, Martinez-Urtaza J. Computational methods for 16S metabarcoding studies using Nanopore sequencing data. Comput Struct Biotechnol J. 2020 Jan 31;18:296–305.
17. Solden L, Lloyd K, Wrighton K. The bright side of microbial dark matter: lessons

learned from the uncultivated majority. Curr Opin Microbiol. 2016 Jun;31:217–26.

18. Ling LL, Schneider T, Peoples AJ, Spoering AL, Engels I, Conlon BP, et al. A new antibiotic kills pathogens without detectable resistance. Nature. 2015 Jan 22;517(7535):455–9.

19. Tortorella E, Tedesco P, Palma Esposito F, January GG, Fani R, Jaspars M, et al. Antibiotics from Deep-Sea Microorganisms: Current Discoveries and Perspectives. Mar Drugs. 2018 Sep 29;16(10).

20. Mehbub MF, Lei J, Franco C, Zhang W. Marine sponge derived natural products between 2001 and 2010: trends and opportunities for discovery of bioactives. Mar Drugs. 2014 Aug 19;12(8):4539–77.

21. Blunt JW, Copp BR, Keyzers RA, Munro MHG, Prinsep MR. Marine natural products. Nat Prod Rep. 2017 Mar 17;34(3):235–94.

22. Santhi LS, Vssl PT, Sy N, Krishna E R. Bioactive Compounds from Marine Sponge Associates: Antibiotics from Bacillus Sp. Nat Prod Chem Res. 2017;05(06).

23. Abdelmohsen UR, Bayer K, Hentschel U. Diversity, abundance and natural products of marine sponge-associated actinomycetes. Nat Prod Rep. 2014 Mar;31(3):381–99.

24. Palomo S, González I, de la Cruz M, Martín J, Tormo JR, Anderson M, et al. Sponge-derived Kocuria and Micrococcus spp. as sources of the new thiazolyl peptide antibiotic kocurin. Mar Drugs. 2013 Mar 28;11(4):1071–86.

25. Just-Baringo X, Albericio F, Álvarez M. Thiopeptide engineering: a multidisciplinary effort towards future drugs. Angew Chem Int Ed Engl. 2014 Jun 23;53(26):6602–16.

26. Vinogradov AA, Suga H. Introduction to thiopeptides: biological activity, biosynthesis, and strategies for functional reprogramming. Cell Chem Biol. 2020 Aug 20;27(8):1032–51.

27. Nagai K, Kamigiri K, Arao N, Suzumura K, Kawano Y, Yamaoka M, et al. YM-266183 and YM-266184, novel thiopeptide antibiotics produced by Bacillus cereus isolated from a marine sponge. I. Taxonomy, fermentation, isolation, physico-chemical properties and biological properties. J Antibiot. 2003 Feb;56(2):123–8.

28. Schneemann I, Kajahn I, Ohlendorf B, Zinecker H, Erhard A, Nagel K, et al. Mayamycin, a cytotoxic polyketide from a Streptomyces strain isolated from the marine sponge Halichondria panicea. J Nat Prod. 2010 Jul 23;73(7):1309–12.

29. Zhang H, Zhang W, Jin Y, Jin M, Yu X. A comparative study on the phylogenetic diversity of culturable actinobacteria isolated from five marine sponge species. Antonie Van Leeuwenhoek. 2008 Mar;93(3):241–8.

30. Kim TK, Garson MJ, Fuerst JA. Marine actinomycetes related to the “Salinospora” group from the Great Barrier Reef sponge Pseudoceratina clavata. Environ Microbiol. 2005 Apr;7(4):509–18.

31. Li ZY, Liu Y. Marine sponge Craniella austrialiensis-associated bacterial diversity revelation based on 16S rDNA library and biologically active Actinomycetes screening, phylogenetic analysis. Lett Appl Microbiol. 2006 Oct;43(4):410–6.

32. Zhang H, Lee YK, Zhang W, Lee HK. Culturable actinobacteria from the marine sponge Hymeniacidon perleve: isolation and phylogenetic diversity by 16S rRNA gene-RFLP analysis. Antonie Van Leeuwenhoek. 2006 Aug;90(2):159–69.

33. Jiang S, Sun W, Chen M, Dai S, Zhang L, Liu Y, et al. Diversity of culturable actinobacteria isolated from marine sponge Haliclona sp. Antonie Van Leeuwenhoek. 2007 Nov;92(4):405–16.

34. Selvin J, Gandhimathi R, Kiran GS, Priya SS, Ravji TR, Hema TA. Culturable heterotrophic bacteria from the marine sponge Dendrilla nigra: isolation and phylogenetic diversity of actinobacteria. Helgol Mar Res. 2009 Sep;63(3):239–47.

35. Sun W, Dai S, Jiang S, Wang G, Liu G, Wu H, et al. Culture-dependent and culture-independent diversity of Actinobacteria associated with the marine sponge Hymeniacidon perleve from the South China Sea. Antonie Van Leeuwenhoek. 2010 Jun;98(1):65–75.

36. Back CR, Stennett HL, Williams SE, Wang L, Ojeda Gomez J, Abdulle OM, et al. A New Micromonospora Strain with Antibiotic Activity Isolated from the Microbiome of a Mid-Atlantic Deep-Sea Sponge. Mar Drugs. 2021 Feb 11;19(2).

37. Matroodi S, Siitonen V, Baral B, Yamada K, Akhgari A, Metsä-Ketelä M. Genotyping-Guided Discovery of Persiamycin A From Sponge-Associated Halophilic Streptomonospora sp. PA3. Front Microbiol. 2020 Jun 9;11:1237.

38. Cao DD, Do TQ, Doan Thi Mai H, Vu Thi Q, Nguyen MA, Le Thi HM, et al. Antimicrobial lavandulylated flavonoids from a sponge-derived actinomycete. Nat Prod Res. 2020 Feb;34(3):413–20.

39. Yin Z, Zhu M, Davidson EH, Bottjer DJ, Zhao F, Tafforeau P. Sponge grade body fossil with cellular resolution dating 60 Myr before the Cambrian. Proc Natl Acad Sci USA. 2015 Mar 24;112(12):E1453-60.

40. Love GD, Grosjean E, Stalvies C, Fike DA, Grotzinger JP, Bradley AS, et al. Fossil steroids record the appearance of Demospongiae during the Cryogenian

period. Nature. 2009 Feb 5;457(7230):718–21.

41. Blunt JW, Carroll AR, Copp BR, Davis RA, Keyzers RA, Prinsep MR. Marine natural products. Nat Prod Rep. 2018 Jan 16;35(1):8–53.

42. Weisz JB, Lindquist N, Martens CS. Do associated microbial abundances impact marine demosponge pumping rates and tissue densities? Oecologia. 2008 Mar;155(2):367–76.

43. Thomas T, Moitinho-Silva L, Lurgi M, Björk JR, Easson C, Astudillo-García C, et al. Diversity, structure and convergent evolution of the global sponge microbiome. Nat Commun. 2016 Jun 16;7:11870.

44. Chaib De Mares M, Jiménez DJ, Palladino G, Gutleben J, Lebrun LA, Muller EEL, et al. Expressed protein profile of a Tectomicrobium and other microbial symbionts in the marine sponge Aplysina aerophoba as evidenced by metaproteomics. Sci Rep. 2018 Aug 7;8(1):11795.

45. Fieseler L, Horn M, Wagner M, Hentschel U. Discovery of the novel candidate phylum “Poribacteria” in marine sponges. Appl Environ Microbiol. 2004 Jun;70(6):3724–32.

46. Schmidt EW, Obraztsova AY, Davidson SK, Faulkner DJ, Haygood MG. Identification of the antifungal peptide-containing symbiont of the marine sponge Theonella swinhoei as a novel δ-proteobacterium, “ Candidatus Entotheonella palauensis.” Mar Biol. 2000 Jul 17;136(6):969–77.

47. Steinert G, Rohde S, Janussen D, Blaurock C, Schupp PJ. Host-specific assembly of sponge-associated prokaryotes at high taxonomic ranks. Sci Rep. 2017 May 31;7(1):2542.

48. Griffiths SM, Antwis RE, Lenzi L, Lucaci A, Behringer DC, Butler MJ, et al. Host genetics and geography influence microbiome composition in the sponge Ircinia

campana. J Anim Ecol. 2019 Nov;88(11):1684–95.

49. Schmitt S, Tsai P, Bell J, Fromont J, Ilan M, Lindquist N, et al. Assessing the complex sponge microbiota: core, variable and species-specific bacterial communities in marine sponges. ISME J. 2012 Mar;6(3):564–76.

50. Hentschel U, Hopke J, Horn M, Friedrich AB, Wagner M, Hacker J, et al. Molecular evidence for a uniform microbial community in sponges from different oceans. Appl Environ Microbiol. 2002 Sep;68(9):4431–40.

51. Lurgi M, Thomas T, Wemheuer B, Webster NS, Montoya JM. Modularity and predicted functions of the global sponge-microbiome network. Nat Commun. 2019 Mar 1;10(1):992.

52. Pita L, Rix L, Slaby BM, Franke A, Hentschel U. The sponge holobiont in a changing ocean: from microbes to ecosystems. Microbiome. 2018 Mar 9;6(1):46.

53. Saurav K, Borbone N, Burgsdorf I, Teta R, Caso A, Bar-Shalom R, et al. Identification of Quorum Sensing Activators and Inhibitors in The Marine Sponge Sarcotragus spinosulus. Mar Drugs. 2020 Feb 20;18(2).

54. Kiran GS, Thomas TA, Selvin J. Production of a new glycolipid biosurfactant from marine Nocardiopsis lucentensis MSA04 in solid-state cultivation. Colloids Surf B, Biointerfaces. 2010 Jun 15;78(1):8–16.

55. Luter HM, Whalan S, Webster NS. Exploring the role of microorganisms in the disease-like syndrome affecting the sponge Ianthella basta. Appl Environ Microbiol. 2010 Sep;76(17):5736–44.

56. Bergman O, Haber M, Mayzel B, Anderson MA, Shpigel M, Hill RT, et al. Marine-based cultivation of diacarnus sponges and the bacterial community composition of wild and maricultured sponges and their larvae. Mar Biotechnol.

2011 Dec 1;13(6):1169–82.

57. Friedrich AB, Fischer I, Proksch P, Hacker J, Hentschel U. Temporal variation of the microbial community associated with the mediterranean sponge Aplysina aerophoba. FEMS Microbiol Ecol. 2001 Dec;38(2–3):105–15.

58. Webster NS, Hill RT. The culturable microbial community of the Great Barrier Reef sponge Rhopaloeides odorabile is dominated by an α-Proteobacterium. Mar Biol. 2001 Apr 23;138(4):843–51.

59. Webster NS, Wilson KJ, Blackall LL, Hill RT. Phylogenetic diversity of bacteria associated with the marine sponge Rhopaloeides odorabile. Appl Environ Microbiol. 2001 Jan;67(1):434–44.

60. Li C-Q, Liu W-C, Zhu P, Yang J-L, Cheng K-D. Phylogenetic diversity of bacteria associated with the marine sponge Gelliodes carnosa collected from the Hainan Island coastal waters of the South China Sea. Microb Ecol. 2011 Nov;62(4):800–12.

61. Brück WM, Reed JK, McCarthy PJ. The bacterial community of the lithistid sponge Discodermia spp. as determined by cultivation and culture-independent methods. Mar Biotechnol. 2012 Dec;14(6):762–73.

62. Montalvo NF, Davis J, Vicente J, Pittiglio R, Ravel J, Hill RT. Integration of culture-based and molecular analysis of a complex sponge-associated bacterial community. PLoS One. 2014 Mar 11;9(3):e90517.

63. Olson JB, Harmody DK, Bej AK, McCarthy PJ. Tsukamurella spongiae sp. nov., a novel actinomycete isolated from a deep-water marine sponge. Int J Syst Evol Microbiol. 2007 Jul;57(Pt 7):1478–81.

64. Sfanos K, Harmody D, Dang P, Ledger A, Pomponi S, McCarthy P, et al. A molecular systematic survey of cultured microbial associates of deep-water

marine invertebrates. Syst Appl Microbiol. 2005 Apr;28(3):242–64.

65. Romanenko LA, Uchino M, Falsen E, Frolova GM, Zhukova NV, Mikhailov VV. Pseudomonas pachastrellae sp. nov., isolated from a marine sponge. Int J Syst Evol Microbiol. 2005 Mar;55(Pt 2):919–24.

66. Romanenko LA, Uchino M, Tanaka N, Frolova GM, Mikhailov VV. Lysobacter spongiicola sp. nov., isolated from a deep-sea sponge. Int J Syst Evol Microbiol. 2008 Feb;58(Pt 2):370–4.

67. Robbins SJ, Song W, Engelberts JP, Glasl B, Slaby BM, Boyd J, et al. A genomic view of the microbiome of coral reef demosponges. ISME J. 2021 Jun;15(6):1641–54.

68. Thiel V, Imhoff JF. Phylogenetic identification of bacteria with antimicrobial activities isolated from Mediterranean sponges. Biomol Eng. 2003 Jul;20(4–6):421–3.

69. Kennedy J, Baker P, Piper C, Cotter PD, Walsh M, Mooij MJ, et al. Isolation and analysis of bacteria with antimicrobial activities from the marine sponge Haliclona simulans collected from Irish waters. Mar Biotechnol. 2009 Jun;11(3):384–96.

70. Olson JB, Lord CC, McCarthy PJ. Improved Recoverability of Microbial Colonies from Marine Sponge Samples. Microb Ecol. 2000 Aug;40(2):139–47.

71. Taylor MW, Radax R, Steger D, Wagner M. Sponge-associated microorganisms: evolution, ecology, and biotechnological potential. Microbiol Mol Biol Rev. 2007 Jun;71(2):295–347.

72. Lafi FF, Garson MJ, Fuerst JA. Culturable bacterial symbionts isolated from two distinct sponge species (Pseudoceratina clavata and Rhabdastrella globostellata) from the Great Barrier Reef display similar phylogenetic diversity.

Microb Ecol. 2005 Aug;50(2):213–20.

73. Kim TK, Fuerst JA. Diversity of polyketide synthase genes from bacteria associated with the marine sponge Pseudoceratina clavata: culture-dependent and culture-independent approaches. Environ Microbiol. 2006 Aug;8(8):1460–70.

74. Hardoim CCP, Cardinale M, Cúcio ACB, Esteves AIS, Berg G, Xavier JR, et al. Effects of sample handling and cultivation bias on the specificity of bacterial communities in keratose marine sponges. Front Microbiol. 2014 Nov 18;5:611.

75. Kennedy J, Codling CE, Jones BV, Dobson ADW, Marchesi JR. Diversity of microbes associated with the marine sponge, Haliclona simulans, isolated from Irish waters and identification of polyketide synthase genes from the sponge metagenome. Environ Microbiol. 2008 Jul 1;10(7):1888–902.

76. Muscholl-Silberhorn A, Thiel V, Imhoff JF. Abundance and bioactivity of cultured sponge-associated bacteria from the Mediterranean sea. Microb Ecol. 2008 Jan;55(1):94–106.

77. Phelan RW, O'Halloran JA, Kennedy J, Morrissey JP, Dobson ADW, O'Gara F, et al. Diversity and bioactive potential of endospore-forming bacteria cultured from the marine sponge Haliclona simulans. J Appl Microbiol. 2012 Jan;112(1):65–78.

78. Menezes CBA, Bonugli-Santos RC, Miqueletto PB, Passarini MRZ, Silva CHD, Justo MR, et al. Microbial diversity associated with algae, ascidians and sponges from the north coast of São Paulo state, Brazil. Microbiol Res. 2010 Aug 20;165(6):466–82.

79. Ettoumi B, Raddadi N, Borin S, Daffonchio D, Boudabous A, Cherif A. Diversity and phylogeny of culturable spore-forming Bacilli isolated from marine

sediments. J Basic Microbiol. 2009 Sep;49 Suppl 1:S13-23.

80. Liu Y, Lai Q, Dong C, Sun F, Wang L, Li G, et al. Phylogenetic diversity of the Bacillus pumilus group and the marine ecotype revealed by multilocus sequence analysis. PLoS One. 2013 Nov 11;8(11):e80097.

81. Sipkema D, Schippers K, Maalcke WJ, Yang Y, Salim S, Blanch HW. Multiple approaches to enhance the cultivability of bacteria associated with the marine sponge Haliclona (gellius) sp. Appl Environ Microbiol. 2011 Mar 1;77(6):2130–40.

82. Sogin ML, Morrison HG, Huber JA, Mark Welch D, Huse SM, Neal PR, et al. Microbial diversity in the deep sea and the underexplored “rare biosphere”. Proc Natl Acad Sci USA. 2006 Aug 8;103(32):12115–20.

83. Reveillaud J, Maignien L, Murat Eren A, Huber JA, Apprill A, Sogin ML, et al. Host-specificity among abundant and rare taxa in the sponge microbiome. ISME J. 2014 Jun;8(6):1198–209.

84. Hooper JNA, Van Soest RWM. Systema porifera. A guide to the classification of sponges. In: Hooper JNA, Van Soest RWM, Willenz P, editors. Systema Porifera. Boston, MA: Springer US; 2002. p. 1–7.

85. Morrow C, Cárdenas P. Proposal for a revised classification of the Demospongiae (Porifera). Front Zool. 2015 Apr 1;12:7.

86. Bayer K, Busch K, Kenchington E, Beazley L, Franzenburg S, Michels J, et al. Microbial Strategies for Survival in the Glass Sponge Vazella pourtalesii. mSystems. 2020 Aug 11;5(4).

87. Steinert G, Busch K, Bayer K, Kodami S, Arbizu PM, Kelly M, et al. Compositional and Quantitative Insights Into Bacterial and Archaeal Communities of South Pacific Deep-Sea Sponges (Demospongiae and

Hexactinellida). Front Microbiol. 2020 Apr 24;11:716.

88. Busch K, Beazley L, Kenchington E, Whoriskey F, Slaby BM, Hentschel U. Microbial diversity of the glass sponge Vazella pourtalesii in response to anthropogenic activities. Conserv Genet. 2020 Dec;21(6):1001–10.

89. Pisera A, Lévi C. 'Lithistid' Demospongiae. In: Hooper JNA, Van Soest RWM, Willenz P, editors. Systema Porifera. Boston, MA: Springer US; 2002. p. 299–301.

90. Barthel D. Tissue composition of sponges from the Weddell Sea, Antarctica:not much meat on the bones. Mar Ecol Prog Ser. 1995;123:149–53.

91. Hentschel U, Fieseler L, Wehrl M, Gernert C, Steinert M, Hacker J, et al. Microbial diversity of marine sponges. Prog Mol Subcell Biol. 2003;37:59–88.

92. Gloeckner V, Wehrl M, Moitinho-Silva L, Gernert C, Schupp P, Pawlik JR, et al. The HMA-LMA dichotomy revisited: an electron microscopical survey of 56 sponge species. Biol Bull. 2014 Aug;227(1):78–88.

93. Moitinho-Silva L, Steinert G, Nielsen S, Hardoim CCP, Wu Y-C, McCormack GP, et al. Predicting the HMA-LMA Status in Marine Sponges by Machine Learning. Front Microbiol. 2017 May 8;8:752.

94. Kennedy J, Flemer B, Jackson SA, Morrissey JP, O'Gara F, Dobson ADW. Evidence of a putative deep sea specific microbiome in marine sponges. PLoS One. 2014 Mar 26;9(3):e91092.

95. Sunagawa S, Coelho LP, Chaffron S, Kultima JR, Labadie K, Salazar G, et al. Structure and function of the global ocean microbiome. Science. 2015 May 22;348(6237):1261359.

96. Turk T, Ambrožič Avguštin J, Batista U, Strugar G, Kosmina R, Čivović S, et al. Biological activities of ethanolic extracts from deep-sea Antarctic marine

sponges. Mar Drugs. 2013 Apr 2;11(4):1126–39.

97. Wright AE, Killday KB, Chakrabarti D, Guzmán EA, Harmody D, McCarthy PJ, et al. Dragmacidin G, a Bioactive Bis-Indole Alkaloid from a Deep-Water Sponge of the Genus Spongosorites. Mar Drugs. 2017 Jan 11;15(1).

98. Crowley SP, O'Gara F, O'Sullivan O, Cotter PD, Dobson ADW. Marine Pseudovibrio sp. as a novel source of antimicrobials. Mar Drugs. 2014 Dec 9;12(12):5916–29.

99. Naughton LM, Romano S, O'Gara F, Dobson ADW. Identification of Secondary Metabolite Gene Clusters in the Pseudovibrio Genus Reveals Encouraging Biosynthetic Potential toward the Production of Novel Bioactive Compounds. Front Microbiol. 2017 Aug 18;8:1494.

100. Borchert E, Jackson SA, O'Gara F, Dobson ADW. Diversity of Natural Product Biosynthetic Genes in the Microbiome of the Deep Sea Sponges Inflatella pellicula, Poecillastra compressa, and Stelletta normani. Front Microbiol. 2016 Jun 29;7:1027.

101. Esteves AIS, Hardoim CCP, Xavier JR, Gonçalves JMS, Costa R. Molecular richness and biotechnological potential of bacteria cultured from Irciniidae sponges in the north-east Atlantic. FEMS Microbiol Ecol. 2013 Sep;85(3):519–36.

102. Staley JT, Konopka A. Measurement of in situ activities of nonphotosynthetic microorganisms in aquatic and terrestrial habitats. Annu Rev Microbiol. 1985;39:321–46.

103. Henson MW, Lanclos VC, Pitre DM, Weckhorst JL, Lucchesi AM, Cheng C, et al. Expanding the Diversity of Bacterioplankton Isolates and Modeling Isolation Efficacy with Large-Scale Dilution-to-Extinction Cultivation. Appl Environ

Microbiol. 2020 Aug 18;86(17).

104. Steinert G, Whitfield S, Taylor MW, Thoms C, Schupp PJ. Application of diffusion growth chambers for the cultivation of marine sponge-associated bacteria. Mar Biotechnol. 2014 Oct;16(5):594–603.

105. Tamburini C, Canals M, Durrieu de Madron X, Houpert L, Lefèvre D, Martini S, et al. Deep-sea bioluminescence blooms after dense water formation at the ocean surface. PLoS One. 2013 Jul 10;8(7):e67523.

106. Arístegui J, Gasol JM, Duarte CM, Herndld GJ. Microbial oceanography of the dark ocean's pelagic realm. Limnol Oceanogr. 2009 Sep;54(5):1501–29.

107. Wilkins LGE, Leray M, O'Dea A, Yuen B, Peixoto RS, Pereira TJ, et al. Host-associated microbiomes drive structure and function of marine ecosystems. PLoS Biol. 2019 Nov 11;17(11):e3000533.

108. Margassery LM, Kennedy J, O'Gara F, Dobson AD, Morrissey JP. Diversity and antibacterial activity of bacteria isolated from the coastal marine sponges Amphilectus fucorum and Eurypon major. Lett Appl Microbiol. 2012 Jul;55(1):2–8.

109. Kato S, Yamagishi A, Daimon S, Kawasaki K, Tamaki H, Kitagawa W, et al. Isolation of Previously Uncultured Slow-Growing Bacteria by Using a Simple Modification in the Preparation of Agar Media. Appl Environ Microbiol. 2018 Oct 1;84(19).

110. Tagg JR, Bannister LV. "Fingerprinting" beta-haemolytic streptococci by their production of and sensitivity to bacteriocine-like inhibitors. J Med Microbiol. 1979 Nov;12(4):397–411.

111. Connon SA, Giovannoni SJ. High-throughput methods for culturing microorganisms in very-low-nutrient media yield diverse new marine isolates.

Appl Environ Microbiol. 2002 Aug;68(8):3878–85.

112. Chen Y-L, Lee C-C, Lin Y-L, Yin K-M, Ho C-L, Liu T. Obtaining long 16S rDNA sequences using multiple primers and its application on dioxin-containing samples. BMC Bioinformatics. 2015 Dec 9;16 Suppl 18:S13.

113. Li Y, Zhang L, Xian H, Zhang X. Newly Isolated Cellulose-Degrading Bacterium Achromobacter xylosoxidans L2 Has Deinking Potential. BioResources. 2019 Feb 1;

114. Abell GCJ, McOrist AL. Assessment of the diversity and stability of faecal bacteria from healthy adults using molecular methods. Microb Ecol Health Dis. 2007 Jan;19(4):229–40.

115. Weisburg WG, Barns SM, Pelletier DA, Lane DJ. 16S ribosomal DNA amplification for phylogenetic study. J Bacteriol. 1991 Jan;173(2):697–703.

116. Tamura K, Nei M. Estimation of the number of nucleotide substitutions in the control region of mitochondrial DNA in humans and chimpanzees. Mol Biol Evol. 1993 May;10(3):512–26.

117. Button DK, Schut F, Quang P, Martin R, Robertson BR. Viability and isolation of marine bacteria by dilution culture: theory, procedures, and initial results. Appl Environ Microbiol. 1993 Mar;59(3):881–91.

118. Edgar RC. Updating the 97% identity threshold for 16S ribosomal RNA OTUs. Bioinformatics. 2018 Jul 15;34(14):2371–5.

119. Young M, Artsatbanov V, Beller HR, Chandra G, Chater KF, Dover LG, et al. Genome sequence of the Fleming strain of Micrococcus luteus, a simple free-living actinobacterium. J Bacteriol. 2010 Feb 1;192(3):841–60.

120. Slaby BM, Hackl T, Horn H, Bayer K, Hentschel U. Metagenomic binning of a marine sponge microbiome reveals unity in defense but metabolic

specialization. ISME J. 2017 Nov;11(11):2465–78.

121. Callahan BJ, McMurdie PJ, Holmes SP. Exact sequence variants should replace operational taxonomic units in marker-gene data analysis. ISME J. 2017 Dec;11(12):2639–43.

122. Cho J-C, Giovannoni SJ. Cultivation and growth characteristics of a diverse group of oligotrophic marine Gammaproteobacteria. Appl Environ Microbiol. 2004 Jan;70(1):432–40.

123. Zhou M, Dong B, Liu Q. Draft Genome Sequence of Psychrobacter piscatorii Strain LQ58, a Psychrotolerant Bacterium Isolated from a Deep-Sea Hydrothermal Vent. Genome Announc. 2016 Mar 3;4(2).

124. Yumoto I, Hirota K, Kimoto H, Nodasaka Y, Matsuyama H, Yoshimune K. Psychrobacter piscatorii sp. nov., a psychrotolerant bacterium exhibiting high catalase activity isolated from an oxidative environment. Int J Syst Evol Microbiol. 2010 Jan;60(Pt 1):205–8.

125. Oger PM, Jebbar M. The many ways of coping with pressure. Res Microbiol. 2010 Dec;161(10):799–809.

126. Riyanti, Balansa W, Liu Y, Sharma A, Mihajlovic S, Hartwig C, et al. Selection of sponge-associated bacteria with high potential for the production of antibacterial compounds. Sci Rep. 2020 Nov 12;10(1):19614.

127. Graça AP, Bondoso J, Gaspar H, Xavier JR, Monteiro MC, de la Cruz M, et al. Antimicrobial activity of heterotrophic bacterial communities from the marine sponge Erylus discophorus (Astrophorida, Geodiidae). PLoS One. 2013 Nov 13;8(11):e78992.

128. Anteneh YS, Yang Q, Brown MH, Franco CMM. Antimicrobial Activities of Marine Sponge-Associated Bacteria. Microorganisms. 2021 Jan 14;9(1).

129. Hamamoto H, Urai M, Ishii K, Yasukawa J, Paudel A, Murai M, et al. Lysocin E is a new antibiotic that targets menaquinone in the bacterial membrane. Nat Chem Biol. 2015 Feb;11(2):127–33.

130. Bano SA, Naz S, Uzair B, Hussain M, Khan MM, Bibi H, et al. Detection of microorganisms with antibacterial activities from different industrial wastes and GC-MS analysis of crude microbial extract. Braz J Biol. 2021 Sep 6;83:e245585.

131. Deblais L, Rajashekara G. Compound Prioritization through Meta-Analysis Enhances the Discovery of Antimicrobial Hits against Bacterial Pathogens. Antibiotics (Basel). 2021 Sep 2;10(9).

132. Imai Y, Meyer KJ, Iinishi A, Favre-Godal Q, Green R, Manuse S, et al. A new antibiotic selectively kills Gram-negative pathogens. Nature. 2019 Dec;576(7787):459–64.

133. Sathiyanarayanan G, Gandhimathi R, Sabarathnam B, Seghal Kiran G, Selvin J. Optimization and production of pyrrolidone antimicrobial agent from marine sponge-associated Streptomyces sp. MAPS15. Bioprocess Biosyst Eng. 2014 Mar;37(3):561–73.

134. Kunz AL, Labes A, Wiese J, Bruhn T, Bringmann G, Imhoff JF. Nature's lab for derivatization: new and revised structures of a variety of streptophenazines produced by a sponge-derived Streptomyces strain. Mar Drugs. 2014 Mar 25;12(4):1699–714.

135. Reimer A, Blohm A, Quack T, Grevelding CG, Kozjak-Pavlovic V, Rudel T, et al. Inhibitory activities of the marine streptomycete-derived compound SF2446A2 against Chlamydia trachomatis and Schistosoma mansoni. J Antibiot. 2015 Nov;68(11):674–9.

136. Viegelmann C, Margassery LM, Kennedy J, Zhang T, O'Brien C, O'Gara F, et

al. Metabolomic profiling and genomic study of a marine sponge-associated Streptomyces sp. Mar Drugs. 2014 Jun 2;12(6):3323–51.

137. Kaeberlein T, Lewis K, Epstein SS. Isolating “uncultivable” microorganisms in pure culture in a simulated natural environment. Science. 2002 May 10;296(5570):1127–9.

138. Lloyd KG, Steen AD, Ladau J, Yin J, Crosby L. Phylogenetically novel uncultured microbial cells dominate earth microbiomes. mSystems. 2018 Oct;3(5).

139. Amoutzias GD, Chaliotis A, Mossialos D. Discovery Strategies of Bioactive Compounds Synthesized by Nonribosomal Peptide Synthetases and Type-I Polyketide Synthases Derived from Marine Microbiomes. Mar Drugs. 2016 Apr 16;14(4).

140. Kumar PS, Dabdoub SM, Ganesan SM. Probing periodontal microbial dark matter using metataxonomics and metagenomics. Periodontol 2000. 2021 Feb;85(1):12–27.

141. Prihoda D, Maritz JM, Klempir O, Dzamba D, Woelk CH, Hazuda DJ, et al. The application potential of machine learning and genomics for understanding natural product diversity, chemistry, and therapeutic translatability. Nat Prod Rep. 2021 Jun 23;38(6):1100–8.

142. Rawlings ND, Tolle DP, Barrett AJ. Evolutionary families of peptidase inhibitors. Biochem J. 2004 Mar 15;378(Pt 3):705–16.

143. Koltai T. Nelfinavir and other protease inhibitors in cancer: mechanisms involved in anticancer activity. [version 2; peer review: 2 approved]. F1000Res. 2015 Jan 12;4:9.

144. Dabhade A, Patel P, Pati U. Proteinaceous protease inhibitor from Lawsonia

inermis: purification, characterization and antibacterial activity. Nat Prod Commun. 2013 Oct;8(10):1467–70.

145. Hulboy D. Protease inhibitors for the research market . Focus Biomolecules; 2015.

146. McKee DL, Sternberg A, Stange U, Laufer S, Naujokat C. Candidate drugs against SARS-CoV-2 and COVID-19. Pharmacol Res. 2020 Jul;157:104859.

147. Dimitrova-Stefanova DB, Gocheva BT. Screening for production of proteinase inhibitors by Antarctic Streptomycetes. J Basic Microbiol. 2018 Dec;58(12):1033–42.

148. McCormick JR, Flärdh K. Signals and regulators that govern Streptomyces development. FEMS Microbiol Rev. 2012 Jan;36(1):206–31.

149. Kim DW, Hesketh A, Kim ES, Song JY, Lee DH, Kim IS, et al. Complex extracellular interactions of proteases and a protease inhibitor influence multicellular development of Streptomyces coelicolor. Mol Microbiol. 2008 Dec 1;70(5):1180–93.

150. Chater KF, Biró S, Lee KJ, Palmer T, Schrempf H. The complex extracellular biology of Streptomyces. FEMS Microbiol Rev. 2010 Mar 1;34(2):171–98.

151. Claessen D, de Jong W, Dijkhuizen L, Wösten HAB. Regulation of Streptomyces development: reach for the sky! Trends Microbiol. 2006 Jul;14(7):313–9.

152. Hackl S, Bechthold A. The Gene bldA, a regulator of morphological differentiation and antibiotic production in streptomyces. Arch Pharm (Weinheim). 2015 Jul;348(7):455–62.

153. Kim IS, Lee KJ. Physiological roles of leupeptin and extracellular proteases in mycelium development of Streptomyces exfoliatus SMF13. Microbiology

(Reading, Engl). 1995 Apr;141 (Pt 4):1017–25.

154. Kim IS, Lee KJ. Trypsin-like protease of Streptomyces exfoliatus SMF13, a potential agent in mycelial differentiation. Microbiology (Reading, Engl). 1996 Jul;142 (Pt 7):1797–806.

155. Schmidt S, Adolf F, Fuchsbauer H-L. The transglutaminase activating metalloprotease inhibitor from Streptomyces mobaraensis is a glutamine and lysine donor substrate of the intrinsic transglutaminase. FEBS Lett. 2008 Sep 3;582(20):3132–8.

156. Kodani S, Hudson ME, Durrant MC, Buttner MJ, Nodwell JR, Willey JM. The SapB morphogen is a lantibiotic-like peptide derived from the product of the developmental gene ramS in Streptomyces coelicolor. Proc Natl Acad Sci USA. 2004 Aug 3;101(31):11448–53.

157. Balouiri M, Sadiki M, Ibnsouda SK. Methods for in vitro evaluating antimicrobial activity: A review. J Pharm Anal. 2016 Apr;6(2):71–9.

158. Miles AA, Misra SS, Irwin JO. The estimation of the bactericidal power of the blood. J Hyg (Lond). 1938 Nov;38(6):732–49.

159. Wiegand I, Hilpert K, Hancock REW. Agar and broth dilution methods to determine the minimal inhibitory concentration (MIC) of antimicrobial substances. Nat Protoc. 2008;3(2):163–75.

160. Hesketh-Best PJ, Mouritzen MV, Shandley-Edwards K, Billington RA, Upton M. Galleria mellonella larvae exhibit a weight-dependent lethal median dose when infected with methicillin-resistant Staphylococcus aureus. Pathog Dis. 2021 Feb 19;79(2).

161. Wick RR, Judd LM, Gorrie CL, Holt KE. Unicycler: Resolving bacterial genome assemblies from short and long sequencing reads. PLoS Comput Biol. 2017

Jun 8;13(6):e1005595.

162. Darling AE, Mau B, Perna NT. progressiveMauve: multiple genome alignment with gene gain, loss and rearrangement. PLoS One. 2010 Jun 25;5(6):e11147.

163. Blin K, Shaw S, Steinke K, Villebro R, Ziemert N, Lee SY, et al. antiSMASH 5.0: updates to the secondary metabolite genome mining pipeline. Nucleic Acids Res. 2019 Jul 2;47(W1):W81–7.

164. Cui H, Wang L, Yu Y. Production and Characterization of Alkaline Protease from a High Yielding and Moderately Halophilic Strain of SD11 Marine Bacteria. J Chem. 2015;2015:1–8.

165. Hockensmith K, Dillard K, Sanders B, Harville BA. Identification and characterization of a chymotrypsin-like serine protease from periodontal pathogen, Tannerella forsythia. Microb Pathog. 2016 Nov;100:37–42.

166. Sreedharan V, Bhaskara Rao KV. Efficacy of protease inhibitor from marine Streptomyces sp. VITBVK2 against Leishmania donovani - An in vitro study. Exp Parasitol. 2017 Mar;174:45–51.

167. Villadsen NL, Jacobsen KM, Keiding UB, Weibel ET, Christiansen B, Vosegaard T, et al. Synthesis of ent-BE-43547A1 reveals a potent hypoxia-selective anticancer agent and uncovers the biosynthetic origin of the APD-CLD natural products. Nat Chem. 2017 Mar;9(3):264–72.

168. Ma H-M, Zhou Q, Tang Y-M, Zhang Z, Chen Y-S, He H-Y, et al. Unconventional origin and hybrid system for construction of pyrrolopyrrole moiety in kosinostatin biosynthesis. Chem Biol. 2013 Jun 20;20(6):796–805.

169. Manorma K, Sharma S, Singla H, Kaundal K, Kaur M. Screening and Isolation of Protease Producing Bacteria from Rhizospheric Soil of Apple Orchards from Shimla District (HP), India. IntJCurrMicrobiolAppSci. 2017 May 20;6(5):249–55.

170. Claverías F, Gonzales-Siles L, Salvà-Serra F, Inganäs E, Molin K, Cumsille A, et al. Corynebacterium alimapuense sp. nov., an obligate marine actinomycete isolated from sediment of Valparaíso bay, Chile. Int J Syst Evol Microbiol. 2019 Mar;69(3):783–90.

171. Heinsch SC, Otto-Hanson L, Hsu S-Y, Kinkel L, Smanski MJ. Genome Sequences for Streptomyces spp. Isolated from Disease-Suppressive Soils and Long-Term Ecological Research Sites. Genome Announc. 2017 Jun 8;5(23).

172. Xu J, Xu M, Liu K, Peng Q, Tao M. Complete genome sequence of streptomyces sp. sge12, which produces antibacterial and fungicidal activities. Genome Announc. 2017 May 25;5(21).

173. Malik A, Kim YR, Jang IH, Hwang S, Oh D-C, Kim SB. Genome-based analysis for the bioactive potential of Streptomyces yeochonensis CN732, an acidophilic filamentous soil actinobacterium. BMC Genomics. 2020 Feb 3;21(1):118.

174. Poomthongdee N, Duangmal K, Pathom-aree W. Acidophilic actinomycetes from rhizosphere soil: diversity and properties beneficial to plants. J Antibiot. 2015 Feb;68(2):106–14.

175. Puerta P, Johnson C, Carreiro-Silva M, Henry L-A, Kenchington E, Morato T, et al. Influence of Water Masses on the Biodiversity and Biogeography of Deep-Sea Benthic Ecosystems in the North Atlantic. Front Mar Sci. 2020 Apr 21;7.

176. Nicault M, Tidjani A-R, Gauthier A, Dumarcay S, Gelhaye E, Bontemps C, et al. Mining the biosynthetic potential for specialized metabolism of a streptomyces soil community. Antibiotics (Basel). 2020 May 23;9(5).

177. Suda H, Aoyagi T, Hamada M, Takeuchi T, Umezawa H. Antipain, a new protease inhibitor isolated from actinomycetes. J Antibiot. 1972 Apr;25(4):263–6.

178. Furumai T, Igarashi Y, Higuchi H, Saito N, Oki T. Kosinostatin, a quinocycline antibiotic with antitumor activity from Micromonospora sp. TP-A0468. J Antibiot. 2002 Feb;55(2):128–33.

179. Maldonado LA, Fenical W, Jensen PR, Kauffman CA, Mincer TJ, Ward AC, et al. Salinispora arenicola gen. nov., sp. nov. and Salinispora tropica sp. nov., obligate marine actinomycetes belonging to the family Micromonosporaceae. Int J Syst Evol Microbiol. 2005 Sep;55(Pt 5):1759–66.

180. Bode W, Huber R. Natural protein proteinase inhibitors and their interaction with proteinases. Eur J Biochem. 1992 Mar 1;204(2):433–51.

181. Karthik L, Kumar G, Keswani T, Bhattacharyya A, Chandar SS, Bhaskara Rao KV. Protease inhibitors from marine actinobacteria as a potential source for antimalarial compound. PLoS One. 2014 Mar 11;9(3):e90972.

182. Kitani S, Yoshida M, Boonlucksanawong O, Panbangred W, Anuegoonpipat A, Kurosu T, et al. Cystargamide B, a cyclic lipodepsipeptide with protease inhibitory activity from Streptomyces sp. J Antibiot. 2018 Jul;71(7):662–6.

183. Manteca Á, Yagüe P. Streptomyces differentiation in liquid cultures as a trigger of secondary metabolism. Antibiotics (Basel). 2018 May 14;7(2).

184. Oliveira MGA, De Simone SG, Xavier LP, Guedes RNC. Partial purification and characterization of digestive trypsin-like proteases from the velvet bean caterpillar, Anticarsia gemmatalis. Comp Biochem Physiol B, Biochem Mol Biol. 2005 Mar;140(3):369–80.

185. Calza L, Manfredi R. Protease inhibitor monotherapy as maintenance regimen in patients with HIV infection. Curr HIV Res. 2012 Dec;10(8):661–72.

186. Pearlman BL. Protease inhibitors for the treatment of chronic hepatitis C genotype-1 infection: the new standard of care. Lancet Infect Dis. 2012

Sep;12(9):717–28.

187. Culp E, Wright GD. Bacterial proteases, untapped antimicrobial drug targets. J Antibiot. 2017 Apr;70(4):366–77.

188. Moitinho-Silva L, Nielsen S, Amir A, Gonzalez A, Ackermann GL, Cerrano C, et al. The sponge microbiome project. Gigascience. 2017 Oct 1;6(10):1–7.

189. Yahel G, Whitney F, Reiswig HM, Eerkes-Medrano DI, Leys SP. In situ feeding and metabolism of glass sponges (Hexactinellida, Porifera) studied in a deep temperate fjord with a remotely operated submersible. Limnol Oceanogr. 2007 Jan;52(1):428–40.

190. Region P, Leys S. Effects of Sediment on Glass Sponges (Porifera, Hexactinellida) and projected effects on Glass Sponge Reefs. undefined. 2013;

191. Schönberg CHL. Happy relationships between marine sponges and sediments – a review and some observations from Australia. J Mar Biol Ass. 2016 Mar;96(2):493–514.

192. Rosenberg E, Zilber-Rosenberg I. The hologenome concept of evolution after 10 years. Microbiome. 2018 Apr 25;6(1):78.

193. de Oliveira BFR, Freitas-Silva J, Sánchez-Robinet C, Laport MS. Transmission of the sponge microbiome: moving towards a unified model. Environ Microbiol Rep. 2020 Dec;12(6):619–38.

194. Grant N, Matveev E, Kahn AS, Leys SP. Suspended sediment causes feeding current arrests in situ in the glass sponge Aphrocallistes vastus. Mar Environ Res. 2018 Jun;137:111–20.

195. Elliott GRD, Leys SP. Coordinated contractions effectively expel water from the aquiferous system of a freshwater sponge. J Exp Biol. 2007 Nov;210(Pt 21):3736–48.

196. Kahn AS, Chu JWF, Leys SP. Trophic ecology of glass sponge reefs in the Strait of Georgia, British Columbia. Sci Rep. 2018 Jan 15;8(1):756.

197. Pineda M-C, Strehlow B, Sternel M, Duckworth A, Jones R, Webster NS. Effects of suspended sediments on the sponge holobiont with implications for dredging management. Sci Rep. 2017 Jul 10;7(1):4925.

198. Oxford Nanopore Technologies plc. New MinKNOW: software release makes nanopore sequencing better and easier [Internet]. [cited 2021 Nov 19]. Available from: https://nanoporetech.com/about-us/news/new-minknow-software-release-makes-nanopore-sequencing-better-and-easier

199. Wick RR, Judd LM, Holt KE. Performance of neural network basecalling tools for Oxford Nanopore sequencing. Genome Biol. 2019 Jun 24;20(1):129.

200. Schloss PD, Westcott SL, Ryabin T, Hall JR, Hartmann M, Hollister EB, et al. Introducing mothur: open-source, platform-independent, community-supported software for describing and comparing microbial communities. Appl Environ Microbiol. 2009 Dec;75(23):7537–41.

201. Hiltemann SD, Boers SA, van der Spek PJ, Jansen R, Hays JP, Stubbs AP. Galaxy mothur Toolset (GmT): a user-friendly application for 16S rRNA gene sequencing analysis using mothur. Gigascience. 2019 Feb 1;8(2).

202. Hiltemann S, Batut B, Clements D. 16S Microbial Analysis with mothur (extended) (Galaxy Training Materials) [Internet]. 2019 [cited 2021 Sep 28]. Available from: https://training.galaxyproject.org/training-material/topics/metagenomics/tutorials/mothur-miseq-sop/tutorial.html#overview

203. Henderson G, Yilmaz P, Kumar S, Forster RJ, Kelly WJ, Leahy SC, et al. Improved taxonomic assignment of rumen bacterial 16S rRNA sequences using

a revised SILVA taxonomic framework. PeerJ. 2019 Mar 5;7:e6496.

204. Bennett S. Solexa Ltd. Pharmacogenomics. 2004 Jun;5(4):433–8.

205. Mikheyev AS, Tin MMY. A first look at the Oxford Nanopore MinION sequencer. Mol Ecol Resour. 2014 Nov;14(6):1097–102.

206. Goodwin S, Gurtowski J, Ethe-Sayers S, Deshpande P, Schatz MC, McCombie WR. Oxford Nanopore sequencing, hybrid error correction, and de novo assembly of a eukaryotic genome. Genome Res. 2015 Nov;25(11):1750–6.

207. Calvo AY, Manrique JM, Jones LR. Rare unclassified 16S rRNA operational taxonomic units from the uncharted Engaño Bay (Argentinean Patagonia). Can J Microbiol. 2018 Jan;64(1):91–6.

208. Schmitt S, Deines P, Behnam F, Wagner M, Taylor MW. Chloroflexi bacteria are more diverse, abundant, and similar in high than in low microbial abundance sponges. FEMS Microbiol Ecol. 2011 Dec;78(3):497–510.

209. Bayer K, Jahn MT, Slaby BM, Moitinho-Silva L, Hentschel U. Marine Sponges as Chloroflexi Hot Spots: Genomic Insights and High-Resolution Visualization of an Abundant and Diverse Symbiotic Clade. mSystems. 2018 Dec 26;3(6).

210. Jackson SA, Flemer B, McCann A, Kennedy J, Morrissey JP, O'Gara F, et al. Archaea appear to dominate the microbiome of Inflatella pellicula deep sea sponges. PLoS One. 2013 Dec 30;8(12):e84438.

211. Delgado-Baquerizo M, Eldridge DJ, Liu Y-R, Sokoya B, Wang J-T, Hu H-W, et al. Global homogenization of the structure and function in the soil microbiome of urban greenspaces. Sci Adv. 2021 Jul 9;7(28).

212. Turon M, Cáliz J, Garate L, Casamayor EO, Uriz MJ. Showcasing the role of seawater in bacteria recruitment and microbiome stability in sponges. Sci Rep. 2018 Oct 12;8(1):15201.

213. Astudillo-García C, Bell JJ, Montoya JM, Moitinho-Silva L, Thomas T, Webster NS, et al. Assessing the strength and sensitivity of the core microbiota approach on a highly diverse sponge reef. Environ Microbiol. 2020 Sep 6;22(9):3985–99.

214. Astudillo-García C, Bell JJ, Webster NS, Glasl B, Jompa J, Montoya JM, et al. Evaluating the core microbiota in complex communities: A systematic investigation. Environ Microbiol. 2017 Apr;19(4):1450–62.

215. Dong Q, Brulc JM, Iovieno A, Bates B, Garoutte A, Miller D, et al. Diversity of bacteria at healthy human conjunctiva. Invest Ophthalmol Vis Sci. 2011 Jul 20;52(8):5408–13.

216. Turon M, Cáliz J, Triadó-Margarit X, Casamayor EO, Uriz MJ. Sponges and Their Microbiomes Show Similar Community Metrics Across Impacted and Well-Preserved Reefs. Front Microbiol. 2019 Aug 22;10:1961.

217. Taylor MW, Tsai P, Simister RL, Deines P, Botte E, Ericson G, et al. "Sponge-specific" bacteria are widespread (but rare) in diverse marine environments. ISME J. 2013 Feb;7(2):438–43.

218. Sipkema D, de Caralt S, Morillo JA, Al-Soud WA, Sørensen SJ, Smidt H, et al. Similar sponge-associated bacteria can be acquired via both vertical and horizontal transmission. Environ Microbiol. 2015 Oct;17(10):3807–21.

219. Webster NS, Taylor MW, Behnam F, Lücker S, Rattei T, Whalan S, et al. Deep sequencing reveals exceptional diversity and modes of transmission for bacterial sponge symbionts. Environ Microbiol. 2010 Aug;12(8):2070–82.

220. Easson CG, Chaves-Fonnegra A, Thacker RW, Lopez JV. Host population genetics and biogeography structure the microbiome of the sponge Cliona delitrix. Ecol Evol. 2020 Feb;10(4):2007–20.

221. Weiss S, Xu ZZ, Peddada S, Amir A, Bittinger K, Gonzalez A, et al.

Normalization and microbial differential abundance strategies depend upon data characteristics. Microbiome. 2017 Mar 3;5(1):27.

222. Browne PD, Nielsen TK, Kot W, Aggerholm A, Gilbert MTP, Puetz L, et al. GC bias affects genomic and metagenomic reconstructions, underrepresenting GC-poor organisms. Gigascience. 2020 Feb 1;9(2).

223. Farris MH, Olson JB. Detection of Actinobacteria cultivated from environmental samples reveals bias in universal primers. Lett Appl Microbiol. 2007 Oct;45(4):376–81.

224. Kirby R. Chromosome diversity and similarity within the Actinomycetales. FEMS Microbiol Lett. 2011 Jun;319(1):1–10.

225. Kirby R. Chromosome diversity and similarity within the Actinomycetales. FEMS Microbiol Lett. 2011 Jun;319(1):1–10.

226. Yu L, Jian H, Gai Y, Yi Z, Feng Y, Qiu X, et al. Characterization of two novel psychrophilic and piezotolerant strains, *Shewanella psychropiezotolerans* sp. nov. and *Shewanella eurypsychrophilus* sp. nov, adapted to an extreme deep-sea environment. Syst Appl Microbiol. 2021 Nov;44(6):126266.

227. Tsevdou M, Ouli-Rousi M, Soukoulis C, Taoukis P. Impact of High-Pressure Process on Probiotics: Viability Kinetics and Evaluation of the Quality Characteristics of Probiotic Yoghurt. Foods. 2020 Mar 19;9(3).

228. Louis P. Different substrate preferences help closely related bacteria to coexist in the gut. MBio. 2017 Nov 7;8(6).

229. Romano S, Jackson SA, Patry S, Dobson ADW. Extending the “one strain many compounds” (OSMAC) principle to marine microorganisms. Mar Drugs. 2018 Jul 23;16(7).

230. Pinedo-Rivilla C, Aleu J, Durán-Patrón R. Cryptic Metabolites from Marine-

Derived Microorganisms Using OSMAC and Epigenetic Approaches. Mar Drugs. 2022 Jan 18;20(2).

231. Chan EWL, Chin MY, Low YH, Tan HY, Ooi YS, Chong CW. The Antibacterial Agent Identified from *Acidocella* spp. in the Fluid of *Nepenthes gracilis* against Multidrug-Resistant *Klebsiella pneumoniae*: A Functional Metagenomic Approach. Microb Drug Resist. 2021 Aug;27(8):1018–28.

Appendix

Figure S1 – Chamber used to culture bacteria under increased atmospheric pressure

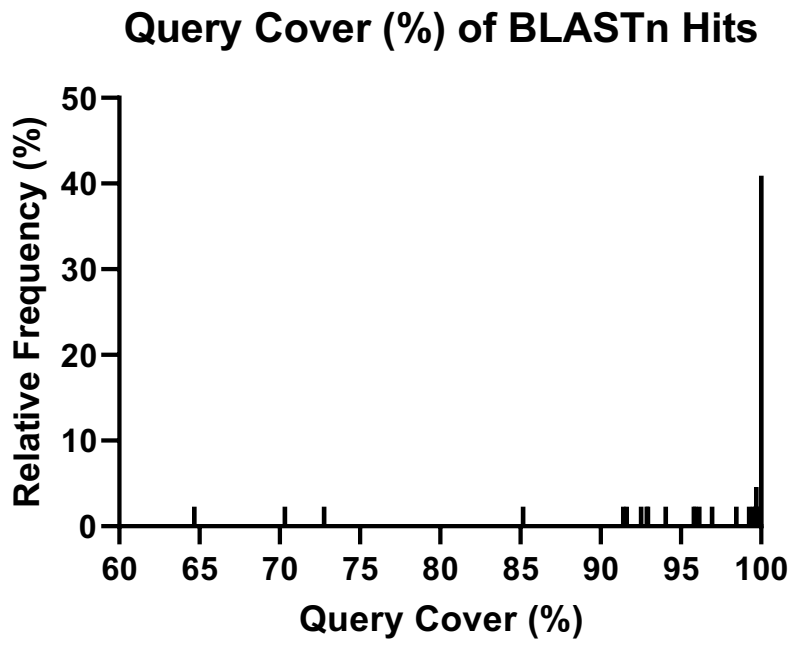

Figure S2 – Query Cover (%) matches for 16S rDNA sequences submitted to BLASTn

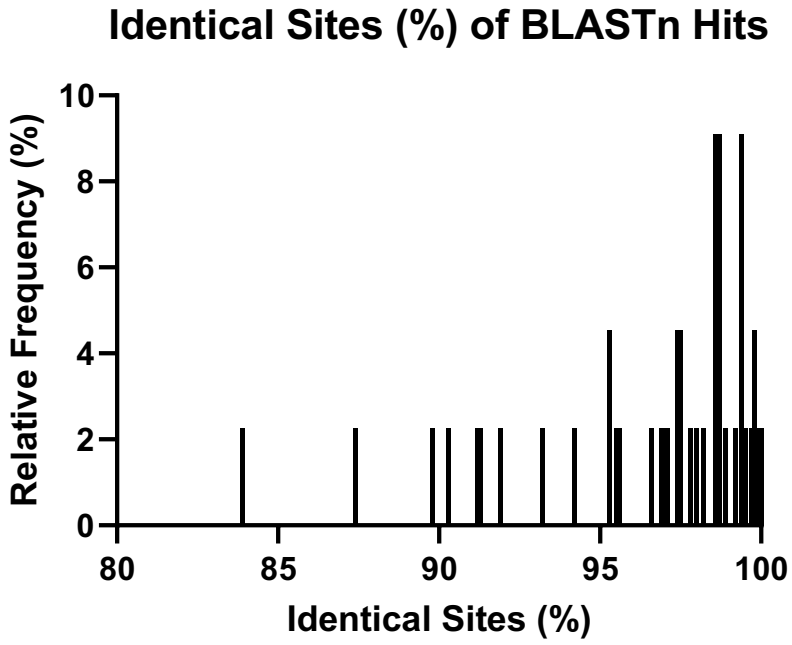

Figure S3 – Identical site (%) matches for 16S rDNA sequences submitted to BLASTn

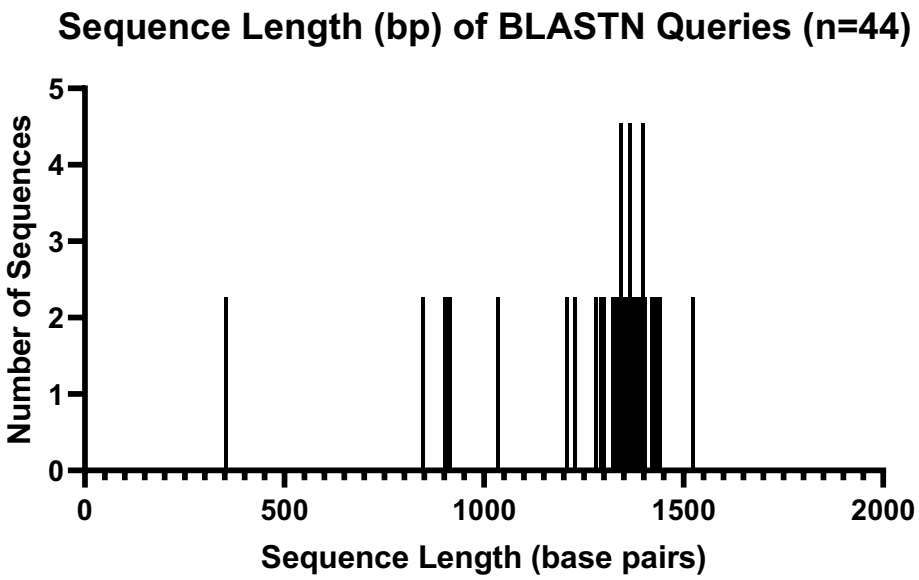

Figure S4 – Sequence length (base pairs) of 16S sequences submitted to BLASTn

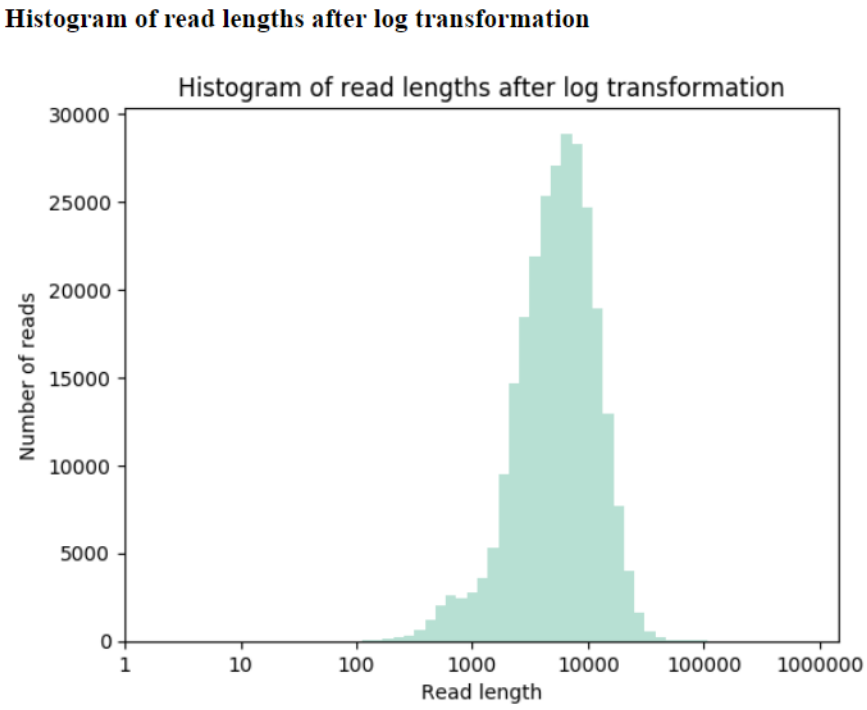

Figure S5 – Histogram of sequencing read lengths obtained after log transformation

Figure S6 – Read lengths vs. read quality for A11 Minion sequencing run

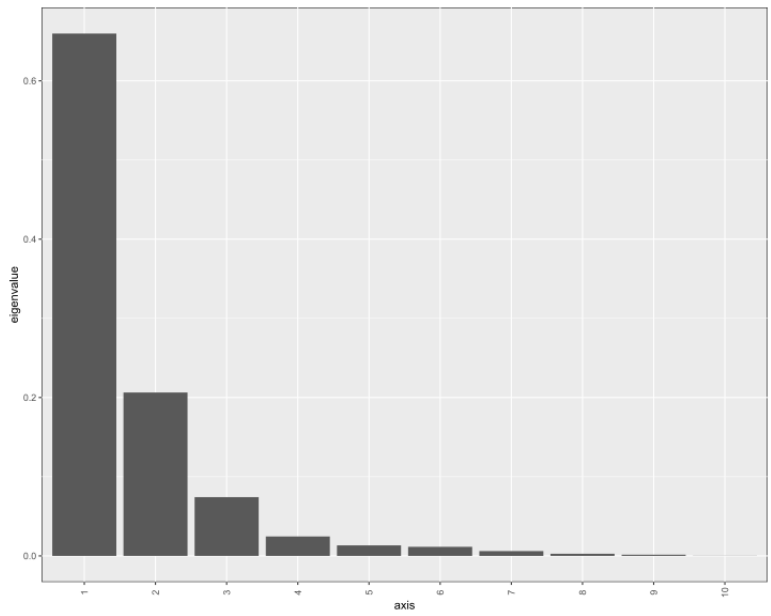

Figure S7 –Principal Co-ordinate Analysis Scree Plot

Table S11 – Media used for the culture of bacterial strains in this study

Media/Component	Code	Composition	Reference
ABC (Agar)	ABC	25g/L MgSO4·7H2O, 22.5g/L (NH4)2SO4, 7.5g/L Na2SO4·10H2O, 2.5g/L KH2PO4, 2.5g/L KCl, 0.7g/L Ca(NO3)2·4H2O, phosphate buffer (20mM final), 0.1g/L peptone, 0.1g/L yeast extract, 0.1 g/L glucose, ddH_2O, 1.5% agar (Sigma-Aldrich)	Kato et al., 2018
LB, Miller	LB/L	1.5% agar (Sigma-Aldrich), ddH_2O	-
LB, Miller + Carnitine	LC	1.5% agar (Sigma-Aldrich), ddH_2O, 0.2g/L Carnitine Hydrochloride	-
Low nutrient heterotrophic media	LNHM	1.0 µM NH_4Cl, 0.1 µM KH_2PO_4, and vitamin mix[(a)] at a 10^{-4} dilution of stock 1.5% agar (Sigma-Aldrich), ddH_2O	Cho and Giovannoni, 2004
Marine Agar	MA/M	37.4 g/L Marine Broth 2216 (BD Difco), 1.5% agar (Sigma-Aldrich), ddH_2O	-
Marine Agar + Carnitine	MC	37.4 g/L Marine Broth 2216 (BD Difco), 1.5% agar (Sigma-Aldrich), ddH_2O, 0.2g/L Carnitine Hydrochloride	-
Marine Broth	MB	37.4 g/L Marine Broth 2216 (BD Difco), ddH_2O	-
Oatmeal Agar	OM	72.5 g/L Oatmeal agar (Sigma), 33.3 g/L Instant Ocean™, ddH_2O	-
ABC, Broth	ABC	Basal salts, 1.5% agar (Sigma-Aldrich), phosphate buffer (20mM final), 0.1g/L peptone, 0.1g/L yeast extract , 0.1g/L glucose	Kato et al., 2018
R2a + Carnitine	RC	18.1 g/L R2a, 1.5% agar (Sigma-Aldrich), ddH_2O, 0.2g/L Carnitine Hydrochloride	-
Reasoner's 2A agar	R2a/R	18.1 g/L Reasoner's 2 agar (Oxoid), 33.3 g/L Instant Ocean™, ddH_2O	-
Starch-Yeast-Peptone-Seawater	SYP-SW	10g/L Starch, 4g/L Yeast Extract, 2g/L Peptone, Autoclaved Seawater	Margassery et al., 2012
Tryptic Soy Agar	TSA	1.5% agar (Sigma-Aldrich), ddH_2O	

[(a)] Thiamine HCl 0.2 mg/L, biotin 1 µg/L, vitamin B_{12} 1 µg/L, Folic acid 2 µg/L, Pabs 10 µg/L, Nicotinic acid 0.1 mg/L, Inisotol 1.0 mg/L, Calcium panthothenate 0.2 mg/L, Pyradoxine HCl 0.1 mg/L. [(b)] 10 g sponge host tissue were homogenised with sterilised mortar and pestle. Homogenate was extracted overnight in 50 mL ddH_2O and filtered sterilised using a 0.22-µm filter. Cake remaining on filter was suspended in 50 mL ddH_2O, centrifuged at 138 x g for 10 min and pellet re-suspended in 20 mL ddH_2O to make SSE (Sipkema et al. 2011). 24 h enrichment

Table S2 – Genbank accession numbers for strains reported in this study

#Accession	Sequence ID	Release Date
MZ723441	Bacillus_pumilus_strain_EE112_P4	"Aug 13, 2021"
MZ723442	Methylobacterium_goesingense_strain_PAMC_29342	"Aug 13, 2021"
MZ723443	Pseudomonas_sp_JHX-241_1	"Aug 13, 2021"
MZ723444	Pseudomonas_sp_JHX-241_2	"Aug 13, 2021"
MZ723445	Brevibacterium_frigoritolerans_strain_ER52	"Aug 13, 2021"
MZ723446	Psychrobacter_piscatorii_strain_EnD-2	"Aug 13, 2021"
MZ723447	Psychrobacter_sp_4-Z18	"Aug 13, 2021"
MZ723448	Uncultured_bacterium_clone_7A_11-051	"Aug 13, 2021"
MZ723449	Rhodococcus_sp_SS51_7	"Aug 13, 2021"
MZ723450	Psychrobacter_sp_JXH-75_1	"Aug 13, 2021"
MZ723451	Rhodococcus_yunnanensis_strain_YIM_70056	"Aug 13, 2021"
MZ723452	Micromonospora_tulbaghiae_strain_Pw20-195	"Aug 13, 2021"
MZ723453	Micrococcus_antarcticus_strain_XH180	"Aug 13, 2021"
MZ723454	Bacillus_algicola_strain_HMF_4132	"Aug 13, 2021"
MZ723455	Psychrobacter_sp_strain_AHE_PA_1	"Aug 13, 2021"
MZ723456	Psychrobacter_sp_JXH-75_2	"Aug 13, 2021"
MZ723457	Pseudomonas_sp_JHX-241_3	"Aug 13, 2021"
MZ723458	Psychrobacter_sp_strain_CJKOP-63_1	"Aug 13, 2021"
MZ723459	Kocuria_indica_strain_MS51	"Aug 13, 2021"
MZ723460	Erythrobacter_sp_strain_LA324	"Aug 13, 2021"
MZ723461	Psychrobacter_sp_strain_CJKOP-63_2	"Aug 13, 2021"
MZ723462	Dermacoccus_nishinomiyaensis_strain_BCX_20	"Aug 13, 2021"
MZ723463	Bacillus_sp_ITP29	"Aug 13, 2021"
MZ723464	Psychrobacter_sp_strain_AHE_PA_2	"Aug 13, 2021"
MZ723465	Pseudomonas_sp_JHX-241_4	"Aug 13, 2021"
MZ723466	Brevibacterium_frigoritolerans_strain_F124	"Aug 13, 2021"
MZ723467	Uncultured_bacterium_clone_Md-9	"Aug 13, 2021"
MZ723468	Pseudomonas_sp_strain_IMBM09_1	"Aug 13, 2021"
MZ723469	Erythrobacter_sp_strain_A6_0	"Aug 13, 2021"
MZ723470	Dietzia_sp_strain_H0B	"Aug 13, 2021"
MZ723471	Psychrobacter_sp_strain_CKJOP-63	"Aug 13, 2021"
MZ723472	Pseudomonas_stutzeri_strain_2Dphe2	"Aug 13, 2021"
MZ723473	Psychrobacter_sp_strain_AHE_PA_3	"Aug 13, 2021"
MZ723474	Microbacterium_maritypicum_strain_P-BL63	"Aug 13, 2021"
MZ723475	Bacillus_sp_strain_MJS-AB-C4	"Aug 13, 2021"
MZ723476	Bacillus_toyonensis_strain_WS1-2	"Aug 13, 2021"
MZ723477	Dietzia_psychralcaliphila_strain_Y96	"Aug 13, 2021"
MZ723478	Rhodococcus_sp_HLSB305_2	"Aug 13, 2021"
MZ723479	Pseudomonas_sp_strain_IMBM09_2	"Aug 13, 2021"

Table S3 – Top 3 BLASTn hits for each A11 assemby

Assembly	Identity	Max Score	Total Score	Query Cover	E-Score	Identity	Accession No.
Minion	Streptomyces sp. Sge12, complete genome	9581	472000	88.00%	0	98.13%	CP020555.1
	Streptomyces sp. 3211, complete sequence	9509	474300	91.00%	0	97.90%	CP020039.1
	Streptomyces subrutilus strain ATCC 27467 chromosome, complete genome	9430	456500	88.00%	0	97.52%	CP023701.1
Illumina	Streptomyces venezuelae strain ATCC 21018 chromosome, complete genome	34479	8.61E+06	61%	0	91.01%	NZ_CP029189.1
	Streptomyces sp. 3211 isolate 3 chromosome, complete genome	33826	9.31E+06	65%	0	95.45%	NZ_CP020039.1
	Streptomyces sp. Sge12 chromosome, complete genome	31986	9.25E+06	64%	0	92.10%	NZ_CP020555.1
Hybrid Assembly	Streptomyces sp. 3211 isolate 3 chromosome, complete genome	69549	9.66E+06	75%	0	92.38%	NZ_CP020039.1
	Streptomyces sp. Sge12 chromosome, complete genome	50122	9.62E+06	75%	0	91.91%	NZ_CP020555.1
	Streptomyces venezuelae strain ATCC 21018 chromosome, complete genome	46928	8.93E+06	71%	0	93.85%	NZ_CP029189.1

Table S4 – Core Sponge OTUs. RT refers to 'replicate threshold'.

Sponge Core OTUs (100% RT)	**Sponge Core OTUs (80% RT)**	**Sponge-Specific OTUs**
Acidimicrobiia_unclassified	Acidimicrobiia_unclassified	Candidatus_Actinomarina
Actinobacteriota_unclassified	Actinomarinales_unclassified	Corynebacteriaceae_unclassified
Bacteria_unclassified	uncultured_ge	Turicella
Bacteroidia_unclassified	Sva0996_marine_group	Corynebacteriales_unclassified
Babeliales_unclassified	Microtrichales_unclassified	Cutibacterium
Pirellulaceae_unclassified	Actinobacteria_unclassified	Propionibacteriaceae_unclassified
uncultured	Actinobacteriota_unclassified	Marinoscillum
Planctomycetota_unclassified	Bacteria_unclassified	Jejudonia
Alphaproteobacteria_unclassified	Bacteroidia_unclassified	NS5_marine_group
Arenicellaceae_ge	Cyclobacteriaceae_unclassified	Synechococcales_unclassified
Arenicellaceae_unclassified	Babeliales_unclassified	Isobaculum
Coxiella	Vermiphilaceae_ge	Lactobacillus
Gammaproteobacteria_unclassified	Blastopirellula	Lactobacillales_ge
Legionellaceae_unclassified	Pirellulaceae_ge	Lactococcus
uncultured	Pirellulaceae_unclassified	uncultured_ge
UBA10353_marine_group_ge	uncultured	Clostridium_sensu_stricto_2
Proteobacteria_unclassified	Planctomycetota_unclassified	uncultured_ge
	Alphaproteobacteria_unclassified	JL-ETNP-F27
	Rhizobiales_unclassified	OCS116_clade_ge
	Rhodobacteraceae_unclassified	Candidatus_Tokpelaia
	SAR11_clade_ge	Pseudaestuariivita
	SAR11_clade_unclassified	AEGEAN-169_marine_group_ge
	Arenicellaceae_ge	Candidatus_Hepatincola_ge
	Arenicellaceae_unclassified	Rickettsiales_ge

	Burkholderiales_unclassified	S25-593_ge
	Coxiella	Clade_Ia
	Gammaproteobacteria_unclassified	Clade_Ib
	Legionellaceae_unclassified	uncultured
	uncultured	Clade_II_ge
	UBA10353_marine_group_ge	uncultured_ge
	sediment-surface35_ge	Parablastomonas
	Proteobacteria_unclassified	Stakelama
		EC94_ge
		Methylophilaceae_unclassified
		Bergeriella
		Neisseria
		Neisseriaceae_ge
		Neisseriaceae_unclassified
		Atlantibacter
		Enterobacteriaceae_unclassified
		Escherichia-Shigella
		Yokenella
		Erwiniaceae_unclassified
		Legionella
		Actinobacillus
		Frederiksenia
		Azorhizophilus
		Pseudomonadales_unclassified
		JL-ETNP-Z34
		SUP05_cluster
		Luteolibacter